1865

Geochemical Survey of the Cordova and Middleton Island 1° × 3° Quadrangles, South-Central Alaska

U.S. GEOLOGICAL SURVEY BULLETIN 1865

ailable

Geochemical Survey of the Cordova and Middleton Island 1° × 3° Quadrangles, South-Central Alaska

By RICHARD J. GOLDFARB, RICHARD M. O'LEARY, STEPHEN J. SUTLEY, and RICHARD B. TRIPP

Results from a reconnaissance geochemical survey within a portion of the Chugach Mountains, of south-central Alaska

U.S. GEOLOGICAL SURVEY BULLETIN 1865

DEPARTMENT OF THE INTERIOR
MANUEL LUJAN, JR., Secretary

U.S. GEOLOGICAL SURVEY
Dallas L. Peck, Director

Any use of trade, product, or firm names in this publication is for descriptive purposes only and does not imply endorsement by the U.S. Government.

UNITED STATES GOVERNMENT PRINTING OFFICE: 1989

For sale by the
Books and Open-File Reports Section
U.S. Geological Survey
Federal Center
Box 25425
Denver, CO 80225

Library of Congress Cataloging-in-Publication Data

Geochemical survey of the Cordova and Middleton Island 1° × 3° quadrangles, south-central Alaska.

(U.S. Geological Survey bulletin ; 1865)
Bibliography: p.
Supt. of Docs. no.: I 19.3:1865
1. Geochemical prospecting—Alaska—Prince William Sound Region. 2. Valdez Group (Alaska) 3. Orca Group (Alaska) I. Goldfarb, R. J. II. Series.
QE75.B9 no. 1865 [TN25.P73] 557.3 s 88-600348
[553'.09798'3]

CONTENTS

Abstract 1
Introduction 1
Geology 2
Known mineral resources 3
Geochemical methods 4
Statistical summary 4
Sediment-sample factor-analysis associations 7
Concentrate-sample factor-analysis associations 14
Description of geochemical anomalies 17
1. Widespread anomalous gold and silver 17
2. Widespread anomalous tungsten 19
3. Central sulfide belt 21
4. Dead Creek area 22
5. Ellamar 23
6. Southern Port Fidalgo 23
7. Snyder Mountain–Heney Range–Hinchinbrook Island 24
8. Central Hawkins Island 24
9. Sheridan Glacier 24
10. Ragged Mountain 25
11. Gravina Peninsula 25
12. Younger Tertiary sediments 25
13. Van Cleve Glacier 26
14. Martin River Glacier 26
15. McPherson Glacier–Goat Mountain 26
16. Northeastern Port Fidalgo 26
17. Gravina River watershed 27
18. South Fork of the Bremner River 27
NURE geochemical survey 27
Conclusions 30
References cited 30

PLATES

[Plates are in pocket]

1. Map showing generalized geology and sample localities for gold-bearing concentrate samples, sediment samples with elevated zinc values, and concentrate samples of central sulfide belt, Cordova and Middleton Island 1°×3° quadrangles, Alaska.
2. Maps and tabulations of areas with geochemically anomalous samples (figures 10–18), Cordova and Middleton Island 1°×3° quadrangles, Alaska.
3. Maps and tabulations of areas with geochemically anomalous samples (figures 19–29), Cordova and Middleton Island 1°×3° quadrangles, Alaska.

FIGURES

1. Map showing geologic framework of the Cordova and Middleton Island 1°×3° quadrangles 2
2. Histograms showing frequency distribution for element concentrations in sediment samples 9
3. Histograms showing frequency distribution for element concentrations in nonmagnetic heavy-mineral-concentrate samples 11

4–9. Maps showing:

4. Distribution of factor scores for sediment factor 3 13
5. Distribution of factor scores for sediment factor 4 14
6. Distribution of factor scores for heavy-mineral-concentrate factor 1 15
7. Distribution of factor scores for heavy-mineral-concentrate factor 2 16
8. Distribution of factor scores for heavy-mineral-concentrate factor 5 18
9. Distribution of scheelite 20

10–29. Maps showing sample sites and tabulations of element concentrations greater than or equal to the 90th percentile (figures 10–18 are grouped on plate 2; figures 19–29 are grouped on plate 3):

10. Between Solomon Gulch and Wortmanns Glacier
11. Between Heney and Childs Glaciers
12. Within the upper Rude River watershed
13. Within the Woodworth Glacier and Schwan Glacier watersheds
14. Within the Scott Glacier and Sheridan Glacier watersheds
15. Between Shephard Glacier and the Heney Range
16. Within the Dead Creek and Gravina River watersheds
17. Between Ellamar and Galena Bay
18. From southern Port Fidalgo
19. From eastern Hinchinbrook Island
20. From central Hawkins Island
21. From the Gravina Peninsula area
22. From the younger Tertiary sedimentary rocks on the mainland
23. From the younger Tertiary sedimentary rocks on Kayak Island
24. From the Van Cleve Glacier area
25. North of the Martin River Glacier
26. From McPherson Glacier to Goat Mountain
27. In northeastern Port Fidalgo
28. Within the Bremner River watershed
29. In the McKinley Lake region

TABLES

1. Univariate statistical estimates for elements in 844 sediment samples 5
2. Univariate statistical estimates for elements in 749 nonmagnetic heavy-mineral-concentrate samples 6
3. Factor loadings for the first five factors after Varimax rotation of the log-transformed sediment database 12
4. Factor loadings for the first five factors after Varimax rotation of the log-transformed concentrate database 12
5. Statistical summary for 499 NURE sediment samples 28

CONVERSION FACTORS

For readers who wish to convert measurements from U.S. customary units to the metric system of units, the conversion factors are listed below.

U.S. customary unit	Multiply by	To obtain metric unit
foot (ft)	0.3048	meter
mile (mi)	1.609	kilometer
square mile (mi^2)	2.59	square kilometer
ounce (oz)	28.35	gram
ton	0.9072	metric ton

Geochemical Survey of the Cordova and Middleton Island 1° × 3° Quadrangles, South-Central Alaska

By Richard J. Goldfarb, Richard M. O'Leary, Stephen J. Sutley, *and* Richard B. Tripp

Abstract

A reconnaissance geochemical survey was conducted over the metasedimentary and mafic metavolcanic rocks of the Valdez and Orca Groups and a series of younger, dominantly marine sedimentary formations on the Cordova and Middleton Island 1°×3° quadrangles in south-central Alaska. A total of 844 sediment samples and 749 nonmagnetic heavy-mineral-concentrate samples were analyzed by semiquantitative emission spectrography and atomic absorption spectrophotometry. The spatial distribution of the data was examined using both individual-element concentration plots and R-mode factor-analysis score plots. Additionally, geochemical data were interpreted for 499 sediment samples that were collected during the U.S. Department of Energy's National Uranium Resource Evaluation survey of the quadrangles and analyzed by neutron activation analysis and X-ray fluorescence.

Concentrate samples with detectable gold values (≥ 20 parts per million) are present over much of the northern quarter of the Cordova quadrangle in streams that drain the metasedimentary and metavolcanic units of the Upper Cretaceous Valdez Group. The largest clusters of anomalous samples are found near Mt. Denson, in the Dead Creek–Brown Basin–Meteorite Mountain region, and on Wortmanns, Schwan, and Allen Glaciers. Concentrates enriched in iron, cobalt, copper, and nickel, and less consistently in silver, arsenic, and lead, delineate an extensive base-metal–sulfide-rich belt that stretches across the higher elevations of the Cordova quadrangle to the west of the Copper River; this area is underlain by both Valdez Group and early Tertiary Orca Group rocks. Anomalous concentrations of zinc in sediments on central Hawkins Island, between Ellamar and Galena Bay, to the south of Port Fidalgo, in the northern Heney Range, and on Sheridan Glacier indicate that the most geochemically favorable ground for volcanogenic massive sulfide occurrences is within Orca Group rocks. Highly anomalous values for manganese in both sample media from the Gravina River and upper Dead Creek watersheds may indicate an additional region of base-metal mineralization within Valdez Group rocks. Barium and zinc values for concentrates derived from the younger Tertiary sedimentary rocks in the southeastern part of the study area are consistently highly anomalous and may define bedded or disseminated accumulations of these metals.

INTRODUCTION

A reconnaissance geochemical survey was conducted across the Cordova and Middleton Island 1°×3° quadrangles in south-central Alaska from 1979 through 1984. The survey represents a portion of the Level III Alaska Mineral Resource Assessment Program studies which were conducted using 1:250,000-scale maps. Samples of stream or moraine sediment and heavy-mineral concentrate were collected during this survey. All the samples were analyzed by semiquantitative emission spectrography, and selected elements in the sediments were determined by atomic absorption spectrophotometry. The data, which have been tabulated in Sutley and others (1986), are statistically evaluated in this report. Additionally, stream-sediment data that were collected by the Los Alamos National Laboratory for the NURE (National Uranium Resource Evaluation) program (U.S. Department of Energy, 1981) have been evaluated.

The northern portion of the Cordova quadrangle is characterized by the rugged and glaciated Chugach Mountains; Cordova Peak, at 7,730 ft, is the highest elevation (pl. 1). Further south, the mountains give way to narrow peninsulas, broad outwash plains, and the Copper River delta within the Gulf of Alaska Coastal physiographic province (Wahrhaftig, 1965). Most of the

area is accessible only by helicopter, though the extensive coastline can be reached by boat.

GEOLOGY

The Cordova and Middleton Island quadrangles consist of portions of three fault-bounded accreted terranes (fig. 1) that become progressively younger and less deformed to the south (Plafker, 1969, 1971). From north to south the terranes are composed of the Upper Cretaceous Valdez Group of the Chugach terrane, the Paleocene to Eocene(?) Orca Group of the Prince William terrane, and the Tertiary marine and terrestrial sediments of the Yakutat terrane. The geology of the quadrangles is summarized in figure 1 and on plate 1 from the work of Winkler and Plafker (1981) and Nelson and others (1985).

The northern third of the Cordova quadrangle, which is the area north of the Contact (Landlock-Gravina-Bagley) fault system, is largely underlain by graywacke, siltstone, minor mudstone, and rare pebble conglomerate of the Valdez Group. These flysch deposits contain subordinate, interbedded tholeiitic metavolcanic rocks that are dominantly pillow basalts and bedded tuffs. The Valdez Group rocks have been complexly folded and faulted and, to the west of the Copper River, metamorphosed to grades ranging from zeolite to amphibolite facies. High-grade schist and gneiss of the informally termed Chugach metamorphic complex (Hudson and Plafker, 1982), with a probable Valdez protolith, crop out east of the Copper River.

Most of the remainder of the Cordova quadrangle is underlain by the flysch facies of the Orca Group, which was underthrusted and accreted to the Valdez Group rocks along the Contact fault system by Paleogene time (Winkler and Plafker, 1981). This accretionary sequence also contains lesser amounts of tholeiitic basalt pillows and massive flows. The intensely deformed, exposed units of the Orca Group have been metamorphosed to grades ranging from zeolite to the chlorite zone of the greenschist facies. Eocene biotite granodiorite, granite, and minor tonalite plutons have intruded the Orca Group on the Gravina Peninsula, in the vicinity of Shephard, Scott, Sheridan, Sherman, McPherson, Johnson, and Miles Glaciers, at McKinley Peak, and at Ragged Mountain.

The Tertiary neritic to bathyal sediments of the Yakataga, Redwood, Poul Creek, Tokun, and Stillwater Formations and the Eocene regressive Kulthieth

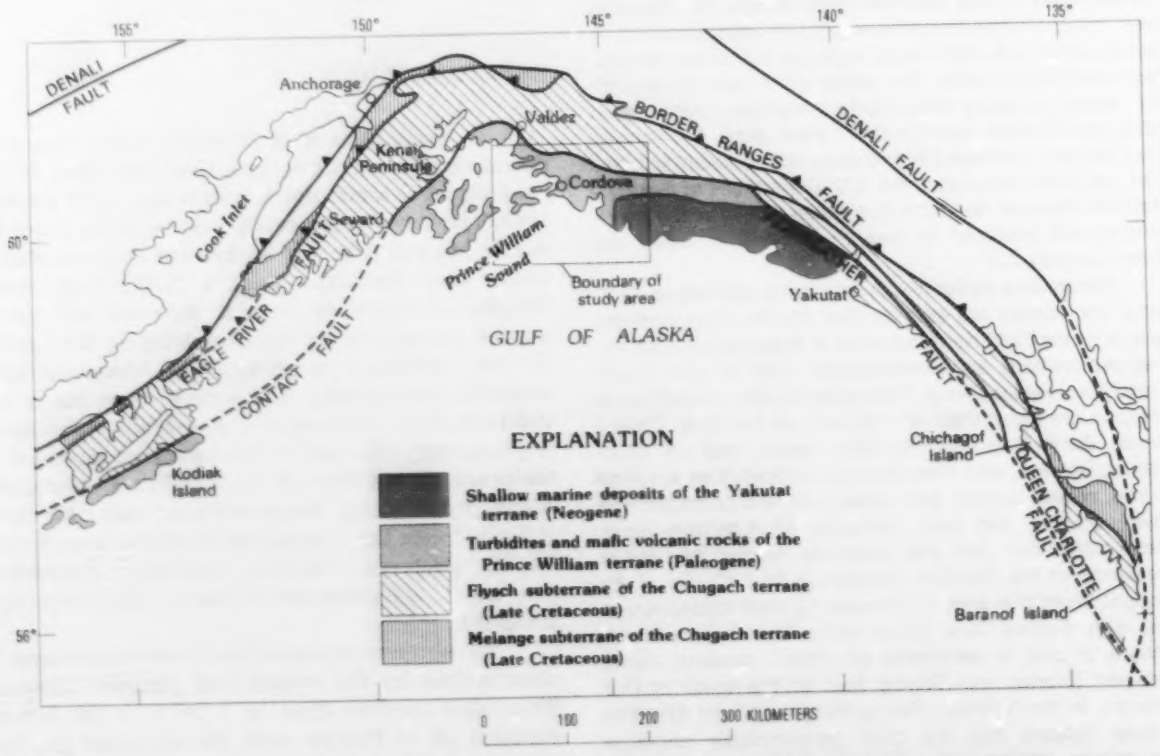

Figure 1. Geologic framework of the Cordova and Middleton Island 1° × 3° quadrangles. Geology modified from Plafker and others (1977) and Winkler and others (1984).

Formation crop out in the southeastern corner of the Cordova quadrangle and extend southward over Kayak Island onto the Middleton Island quadrangle. The Chugach and Ragged Mountain faults separate these unmetamorphosed sedimentary rocks from Orca Group rocks to the north and west. Oligocene(?) mafic dikes, sills, and plugs intrude sedimentary beds on the northern side of Kayak Island, to the south of the Nichawak River, and east of Ragged Mountain (Winkler and Plafker, 1981). A Miocene dacite plug intrudes the Yakataga and upper Poul Creek Formations at Cape St. Elias on the southern end of Kayak Island (Plafker, 1974).

KNOWN MINERAL RESOURCES

Massive Fe- and Cu-sulfide lenses and pods have historically attracted the most widespread prospecting activity on the Cordova quadrangle. These volcanogenic occurrences, which are hosted in both Orca Group metavolcanic rocks and stratigraphically lower Orca Group metasedimentary rocks (Nelson and others, 1984), commonly also contain economically significant concentrations of Ag, Au, and Zn. Coeval submarine mafic volcanism and development of a thick wedge of terrigeneous flysch indicate that ore genesis occurred near a continental margin rather than at a mid-oceanic spreading center or at an island arc (Winkler and others, 1977). Many of the massive sulfides have been remobilized along with silica into shear zones, probably during accretion and (or) regional metamorphism.

The majority of the known massive sulfide occurrences are situated in the area bounded by Galena Bay, Tatitlek Narrows, and Landlocked Bay in the northwestern corner of the Cordova quadrangle. Dozens of workings are concentrated on widespread massive sulfide lenses and disseminated sulfides within the mafic volcanic rocks immediately southwest of the Landlock fault (Cobb, 1979; Jansons and others, 1984). However, the Ellamar mine and and a few small prospects occur in stratigraphically lower metasedimentary rocks. Chalcopyrite and pyrrhotite are the most abundant sulfide phases, commonly occurring with pyrite and sphalerite. Galena is much less common, and arsenopyrite is only recognized in a few of the occurrences. Silver and Au values are quite variable.

The Ellamar orebody, which is located within interbedded slates and graywackes, was the second largest copper producer within the Prince William Sound district and the most productive mine on the Cordova quadrangle. It produced an estimated total of 7,151 tons of Cu, 191,615 oz of Ag, and 51,305 oz of Au from 301,835 tons of ore (Jansons and others, 1984). Most of the gold and silver is believed to have occurred within sphalerite (Moffit, 1954), though we have also observed disseminated gold blebs hosted by chalcopyrite stringers within massive pyrrhotite. The 1.9 million tons of 1.0 percent Cu ore at the volcanic-hosted Threeman mine to the southeast of Ellamar (Nelson and others, 1984) represents the largest identified copper resource presently known on the Cordova quadrangle.

A number of Fe- and Cu-rich massive sulfide occurrences are situated along the southern shore of Port Fidalgo, mostly near Irish Cove. Lenses, stringers, and disseminations of chalcopyrite, pyrite, pyrrhotite, and sphalerite occur within Orca Group graywackes, slates, and mafic volcanic rocks. The sediment-hosted Schlosser mine, which is the largest mine in this area, produced just over 4 million pounds of Cu plus minor Ag (Jansons and others, 1984).

Two other areas with massive sulfide occurrences are known to be located within Orca Group rocks. A number of lenses of massive pyrrhotite, chalcopyrite, and sphalerite occur within the metasedimentary rocks along the southeastern side of Scott Glacier (Jansons and others, 1984). Mineralized bodies are also enriched in Ag and Co (R. Goldfarb, unpub. data, 1985). Lenses and disseminations of Fe- and Cu-sulfide minerals are also scattered throughout the belt of greenstone bodies that extends to the northeast from the town of Cordova (Cobb, 1972; Jansons and others, 1984).

The occurrence of mafic volcanic rocks within the Valdez Group also may identify favorable areas for massive sulfide occurrences. The Midas mine, which is located in T. 10 S., R. 6 W., just 1.5 km to the north of the Cordova quadrangle, is the fourth largest copper producer in the Prince William Sound region (Nelson and others, 1984). Ore lenses contain massive pyrrhotite, pyrite, sphalerite, and chalcopyrite in Valdez Group slates that are spatially associated with mafic volcanic bodies. The Midas mine orebodies also yielded substantial Ag and Au. Additionally, shear zones within the Valdez Group metasedimentary rocks near metavolcanic rocks contain gossans and quartz veinlets with Fe-, Cu-, and Zn-sulfides within the Dead Creek watershed on the Cordova quadrangle (Jansons and others, 1984). Many of the outcrops of Valdez Group greenstone occur within the high, glaciated peaks of the quadrangle, and this relative inaccessibility has probably discouraged extensive prospecting activity.

Goodfellow and others (1984) described a newly discovered manganese deposit within an orange-weathered mudstone intercalated with Orca Group metavolcanic rocks on Hinchinbrook Island. Bementite ($Mn_7Si_6O_{15}(OH)_8$) is the principal Mn mineral, and grab samples from the deposit average about 30 percent Mn. Goodfellow and others (1984) believed the deposit to be

volcanogenic in origin, possibly originating from the seafloor alteration of tholeiitic basalt. However, no sulfide deposits are yet known to crop out in the vicinity of this manganese deposit.

Whereas gold has historically been an economically important commodity in the western part of Prince William Sound, known lode-gold occurrences are relatively rare to the east on the Cordova quadrangle. The only recorded gold production on the quadrangle, excluding by-product gold from the massive sulfide deposits, is a very minor amount from the McKinley Lake area located to the northwest of the Copper River delta. A number of small adits are scattered near McKinley Lake where discordant quartz veins that contain gold, pyrite, and arsenopyrite are hosted by slates and graywackes of the Orca Group. Small gold-bearing quartz veins also cut Valdez Group greenstone on Bligh Island (Capps and Johnson, 1913) and Valdez Group metasedimentary rocks in the Jack Bay region (Johnson, 1915).

GEOCHEMICAL METHODS

The geochemical reconnaissance survey of the Cordova and Middleton Island quadrangles consisted of the collection and analysis of 844 sediment samples and 749 heavy-mineral-concentrate samples. Much of the sampling occurred between 1980 and 1982, as part of the Chugach National Forest mineral resource appraisal (Nelson and others, 1984). Additional sampling was done in 1983 and 1984 to provide a higher sampling density within the National Forest boundaries and to cover the northeastern and northwestern portions of the Cordova quadrangle which lie outside of the National Forest boundaries.

Sediment samples were taken from first- or second-order drainages, at an approximate density of one site per 4 mi^2. In areas of extensive glacier cover, sediment was collected from active medial or lateral moraines. At least five grab samples were collected at each site along a 30-ft stretch of the active stream channel or moraine using a polyethylene or aluminum scoop. The grab samples were composited into a single sample and then air-dried. The composited sample was sieved using a stainless-steel 80-mesh screen and pulverized in the laboratory prior to analysis. The discussion that follows uses stream or moraine "sediment" as synonymous with the minus-80-mesh fraction.

Heavy-mineral-concentrate samples were collected at all sediment sites using a 14-in.-diameter gold pan. Commonly 3–4 kg of composited sediment were collected to yield the desired 30–60 g of concentrate. Concentrate samples were air-dried in the laboratory, and the highly magnetic material (magnetite, ilmenite) was removed with an electromagnet. Lightweight material was separated by flotation in bromoform (specific gravity 2.86), and the resulting heavy-mineral fraction was then separated into nonmagnetic and magnetic fractions using a Frantz Isodynamic Separator 1 at a setting of 0.6 ampere and slope settings of 5° forward and 10° side.

Both the sediment and the nonmagnetic concentrate samples were analyzed semiquantitatively for 31 elements using an optical emission spectrograph according to the method outlined by Grimes and Marranzino (1968). Additionally, atomic absorption analyses of sediment samples were performed for As, Au, Cd, Sb, and Zn using the method of Thompson and others (1968) and a modification of the method of Viets (1978). Resulting analytical data are tabulated in Sutley and others (1986). A split of each nonmagnetic concentrate was saved for microscopic examination.

STATISTICAL SUMMARY

The basic statistics for the analytical data for the sediments and heavy-mineral concentrates are given in tables 1 and 2. Many of the elements analyzed were singularly censored, with concentrations for some samples either below or in excess of analytical determination limits. Detection ratios, which are calculated as the number of noncensored values divided by the total number of samples analyzed for a given element, describe the degree to which the data is censored. Univariate statistics were computed for those elements with detection ratios greater than 0.15. Minimum, median, and maximum values are tabulated to present the range in the geochemical data.

Because the data are in some cases positively skewed (figs. 2, 3) and the emission spectrography results are reported in six-step geometric intervals, logarithmic transformations were carried out on both data sets prior to statistical interpretation. In order to better approximate the geometric mean and geometric deviation for the censored-element distributions, Cohen's (1959) maximum-likelihood method was applied. Such a method shows minimum variance, or in other words "maximum" efficiency, of the data when additional data is included (Fisher, 1959). Using Cohen's method the geometric mean $\bar{x}$ is simply the antilog of x:

$$\bar{x} = \bar{x}' - \lambda (x' - x_o)$$

where,

$\bar{x}'$ = the mean log of the unqualified values,

x_o = the censoring point, and

λ = a factor determined from a series of curves by Cohen (1959).

Table 1. Univariate statistical estimates for elements in 844 sediment samples

[N, not detected at the given concentration; L, detectable, but less than the given concentration; G, greater than given concentration; leaders (--), not determined]

Element[1]	Detection ratio[2]	N[3]	L[4]	G[5]	B[6]	Minimum	Median	90th percentile	95th percentile	98th percentile	Maximum	Geometric mean[7]	Geometric deviation[7]	Expected range[8]
Fe.....	1.0	0	0	0	0	1	5	7	10	10	20	4.5	1.6	1.8-12
Mg.....	1.0	0	0	0	0	.15	1.5	3	3	5	10	1.5	1.7	.5-4.3
Ca.....	1.0	0	0	0	0	.10	1	2	3	5	7	.9	2.3	.2-4.8
Ti.....	1.0	0	0	0	0	.07	.5	.7	.7	.7	1	.4	1.6	.2-1.0
Mn.....	.99	0	0	8	0	200	1,000	2,000	3,000	5,000	5,000G	1,097	1.7	380-3,170
Ag.....	.02	802	29	0	0	.5N	.5N	.5N	.5L	.5L	10	--	--	--
As.....	.01	837	3	0	0	200N	200N	200N	200N	200N	500	--	--	--
B	.96	2	31	0	0	10N	50	100	130	100	200	37	2.1	8.4-163
Ba.....	.99	3	6	0	0	20N	700	1,000	1,500	1,500	5,000	690	1.9	191-2,491
Be.....	.87	27	79	0	0	1N	1.5	2	2	3	7	1.4	1.5	.6-3.2
Co.....	.99	0	2	0	0	5L	30	50	70	70	100	26	1.7	9.0-75
Cr.....	.99	1	1	0	0	10N	100	200	200	500	1,500	105	1.9	29-379
Cu.....	1.0	0	0	0	0	5	50	100	150	200	1,000	49	2.1	11-216
La.....	.83	88	55	0	0	20N	50	50	100	100	200	34	1.8	10-110
Mo.....	.04	796	12	0	0	5N	5N	5N	5L	7	20	--	--	--
Nb.....	.12	441	304	0	0	20N	20N	20	20	20	20	--	--	--
Ni.....	1.0	0	0	0	0	5	50	70	100	100	200	44	1.7	15-127
Pb.....	.97	5	23	0	0	10N	30	50	70	70	700	27	1.8	8.3-97
Sc.....	1.0	0	0	0	0	5	20	30	50	50	70	21	1.5	9.3-47
Sr.....	.98	3	11	0	0	100N	300	500	700	700	1,000	290	1.7	100-838
V	1.0	0	0	0	0	10	200	300	300	300	500	169	1.5	75-380
W	.01	837	5	0	0	50N	50N	50N	50N	50N	300	--	--	--
Y	.99	0	1	0	0	10L	30	50	70	70	500	31	1.6	12-79
Zn.....	.12	335	407	0	0	200N	200L	200	200	200	500	--	--	--
Zr.....	.99	0	1	1	0	10L	150	300	300	500	1,000G	144	1.9	40-520
Au (AA)...	.06	249	1	0	577	.02N	.02N	.02N	.05	.16	1.5	--	--	--
Zn (AA)...	1.0	0	0	0	7	5	85	140	160	190	330	82	1.7	28-237
Sb (AA)...	.01	671	8	0	161	1N	1N	1N	1N	1N	2	--	--	--
Cd (AA)...	.78	21	128	0	161	.05N	.1	.3	.4	.5	1	.10	2.2	.02-.48
As (AA)...	.61	69	195	0	161	5N	5	25	30	50	190	6.1	2.7	.8-44

[1]All values in parts per million, except minimum, median, percentiles, maximum, geometric mean, geometric deviation, and expected range for Fe, Mg, Ca, and Ti are in percent. All elements were determined by semiquantitative emission spectrography except for where (AA) analysis is noted following the specific element.

[2]Detection ratio is the number of uncensored concentrations divided by the total number of samples analyzed for a given element.

[3]N is the number of samples in which concentrations could not be detected at the lower determination limit.

[4]L is the number of samples in which concentrations were reported as observable but were less than the lower determination limit.

[5]G is the number of samples in which concentrations were reported as observable but were greater than the upper determination limit.

[6]B is the number of samples in which the element was not analyzed.

[7]Geometric mean and geometric deviation were calculated using Cohen's maximum-likelihood method for censored distributions.

[8]Expected range is the distribution of 95 percent of all data expected for lognormal data.

Table 2. Univariate statistical estimates for elements in 749 nonmagnetic heavy-mineral-concentrate samples

[N, not detected at the given concentration; L, detectable, but less than the given concentration; G, greater than given concentration; leaders (--), not determined]

Element[1]	Detection ratio[2]	N[3]	L[4]	G[5]	B[6]	Minimum	Median	90th percentile	95th percentile	98th percentile	Maximum	Geometric mean[7]	Geometric deviation[7]	Expected range[8]
Fe	1.00	0	0	0	0	.5	5	20	30	50	50	4.2	2.7	0.6-31
Mg	.99	0	1	0	1	.05L	.5	1.5	2	2	7	.5	2.1	.11-2.2
Ca	.99	0	1	0	22	.05L	5	10	15	15	20	3.5	2.8	.45-27
Ti	.67	9	0	239	0	.005L	1	2G	2G	2G	2G	1.1	3.1	.11-11
Mn	.99	0	0	2	0	50	700	1,500	2,000	2,000	10,000G	734	2.1	166-3,237
Ag	.19	591	12	0	0	1N	.5N	7	20	100	1,000	.04	40	0-64
As	.18	601	5	8	0	500N	500N	1,500	7,000	15,000	20,000G	43	17	.1-12,427
Au	.05	697	7	4	0	20N	20N	20N	20	200	1,000G	—	—	--
B	.96	1	27	4	0	20N	70	300	500	1,500	5,000G	77	2.9	9.2-648
Ba	.93	5	9	39	0	50N	500	3,000	10,000G	10,000G	10,000G	624	3.5	51-7,644
Be	.36	345	133	0	0	1N	1L	3	5	7	500	1.4	2.1	.3-6.2
Bi	.10	607	69	0	1	20N	20N	20L	30	70	500	—	—	--
Cd	.01	731	4	0	4	50N	50N	50N	50L	50	700	—	—	--
Co	.89	31	54	0	0	10N	20	200	200	500	2,000	24	3.7	1.8-329
Cr	.85	17	92	0	0	20N	70	200	300	700	10,000	56	3.0	6.2-504
Cu	.95	8	28	1	0	10N	70	700	1,000	2,000	50,000G	75	4.6	3.5-1,587
La	.68	191	45	0	0	50N	50	300	700	1,000	2,000	69	3.0	7.7-621
Mo	.03	714	14	0	0	10N	10N	10N	10L	10	200	—	—	--
Nb	.42	240	192	0	0	50N	50L	100	150	200	1,000	41	2.0	10-164
Ni	.90	69	9	0	0	10N	50	150	200	500	1,000	35	3.3	3.2-381
Pb	.66	85	167	0	0	20N	20	300	700	1,500	10,000	34	5.6	1.1-1,066
Sb	.01	745	0	0	2	200N	200N	200N	200N	200N	500	—	—	--
Sc	.54	259	73	0	28	10N	10	30	50	70	200	11	2.4	1.8-60
Sn	.08	658	28	2	0	20N	20N	20L	30	100	2,000G	—	—	--
Sr	.74	118	76	0	0	200N	200	1,000	1,000	2,000	10,000	291	2.4	51-1,676
Th	.13	611	43	1	0	200N	200N	200L	500	700	5,000G	—	—	—
V	1.00	0	0	0	0	20	150	300	500	500	1,000	159	1.9	44-574
W	.27	511	34	0	0	100N	100N	500	1,000	2,000	5,000	29	7.7	.5-1,719
Y	.97	6	16	0	0	20N	100	500	700	1,000	2,000	111	2.8	14-870
Zn	.05	663	44	2	0	500N	500N	500L	500	2,000	20,000G	—	—	--
Zr	.19	0	0	603	0	30	2,000G	2,000G	2,000G	2,000G	2,000G	10,960	7.0	224-540,000

[1] All values in parts per million, except minimum, median, percentiles, maximum, geometric mean, geometric deviation, and expected range for Fe, Mg, Ca, and Ti are in percent. All elements were determined by semiquantitative emission spectrography.

[2] Detection ratio is the number of uncensored concentrations divided by the total number of samples analyzed for a given element.

[3] N is the number of samples in which concentrations could not be detected at the lower determination limit.

[4] L is the number of samples in which concentrations were reported as observable but were less than the lower determination limit.

[5] G is the number of samples in which concentrations were reported as observable but were greater than the upper determination limit.

[6] B is the number of samples in which the element was not analyzed.

[7] Geometric mean and geometric deviation were calculated using Cohen's maximum-likelihood method for censored distributions.

[8] Expected range is the distribution of 95 percent of all data expected for lognormal data.

The geometric deviation is calculated by Cohen's method in a similar manner.

According to Miesch (1976), 95 percent of all values for a lognormal distribution fall within an expected range from:

(Geometric mean)/ (Geometric deviation)^2 to

(Geometric mean) × (Geometric deviation)^2.

Expected ranges for sediment and concentrate data from the Cordova and Middleton Island quadrangles are listed in tables 1 and 2.

Anomalous element values are those that deviate from the norm or stand out above some geochemical background. Commonly the 95th percentile for a given geochemical distribution has been chosen as a geochemical threshold, with all values greater than that threshold being considered anomalous. The 95th-percentile values for all analyzed elements are listed in tables 1 and 2. However, for many elements the reader may wish to adjust geochemical thresholds upward or downward from the 95th percentile to accommodate distinct breaks in the frequency distribution of the data. Therefore, we have included histograms for most of the studied elemental distributions (figs. 2, 3).

R-mode factor analysis with Varimax rotation was used to identify the dominant geochemical association in both log-transformed data sets. Prior to log-transformation, the more highly censored elements were removed from each database. All elements with detection ratios less than 0.60 were removed from the sediment data matrix. For the concentrate data, some relatively highly censored elements that are common pathfinders for various mineral resource types (in other words, *e.g.*, As, W) were kept in the data matrix for R-mode factor analysis. A series of analyses, both with and without these highly censored element distributions, showed that inclusion of these few censored elements caused virtually no change in the other variable interrelationships. At the same time, their inclusion provides a quick means for identifying correlations within the upper ends of their distributions. All remaining censored data in each matrix were treated as follows:

N—All values of an element qualified with an "N" were changed to 0.5 of the lower limit of detection for that element.

L—All values of an element qualified with an "L" were changed to 0.7 of the lower limit of detection for that element.

G—All values of an element qualified with a "G" were changed to 1.3 times the maximum detected value.

Factor analysis places similarly behaving experimental variables (elements) into groups termed "factors." Specific lithologies or ore deposit types may be defined by a distinct suite of trace elements, and therefore certain factors might be used to define the more common geochemical signatures in the study area. Factor loadings for the sediment and concentrate data sets are listed in tables 3 and 4. The factor loadings, which depict the influence of each variable on a factor, may be interpreted similarly to correlation coefficients. The optimal number of factors that were chosen from each data matrix, and discussed below, were based on the breaks in slope on plots of factor number versus total variance. Factor scores, described below, for each sample on each factor measure the contribution of that factor to each individual sample.

Sediment-Sample Factor-Analysis Associations

A five-factor model that explains 73 percent of the total variance was selected as most appropriate for summarizing the sediment data. The first factor shows high loadings for all the mafic elements; samples with highest scores onto this factor delineate areas throughout the Cordova and Middleton Island quadrangles that are underlain by mafic volcanic rocks. These areas include Ellamar, southern Port Fidalgo, northeastern Hinchinbrook Island, the lower Rude River east to Scott Glacier, Ragged Mountain, upper Solomon Gulch, Meteorite Mountain, Wortmanns Glacier, Cordova Glacier–Rude Lake, Mt. O'Neel–Childs Glacier–upper Allen Glacier, and Heney Glacier. Suprisingly though, anomalous factor-1 scores do not occur within the Woodworth and Schwan Glacier systems which are also partially underlain by mafic volcanic rocks. Minor geochemical differences between these latter two areas and the group of the former areas led to the Woodworth and Schwan Glacier systems being better delineated by anomalous factor-5 scores (see below). Additionally, samples from streams that drain the younger Tertiary sediments in the Don Miller Hills and on Kayak Island are relatively enriched in this mafic factor.

Factor 2, with high positive loadings (>0.50) for Ba, Be, La, Pb, Sr, Y, and Zr, reflects a geochemical association characteristic of the Tertiary granitic bodies that intrude both flysch sequences on the Cordova quadrangle and of the high-grade gneissic rocks of the Valdez Group east of the Copper River. Samples with anomalous factor-2 scores are found in drainages or on glaciers underlain by the Eocene intrusive rocks of the Sheep Bay pluton, around lower Sherman Glacier, and from lower Martin River Glacier northwest to Miles Lake. Additional anomalous accumulations of this felsic element suite cluster on both branches of Scott Glacier south to the Siamese Lakes and from the area east of Whalen Bay east to the area north of Beartrap Bay. These high positive factor-2 scores identify either local felsic component enrichments in Orca Group flysch or

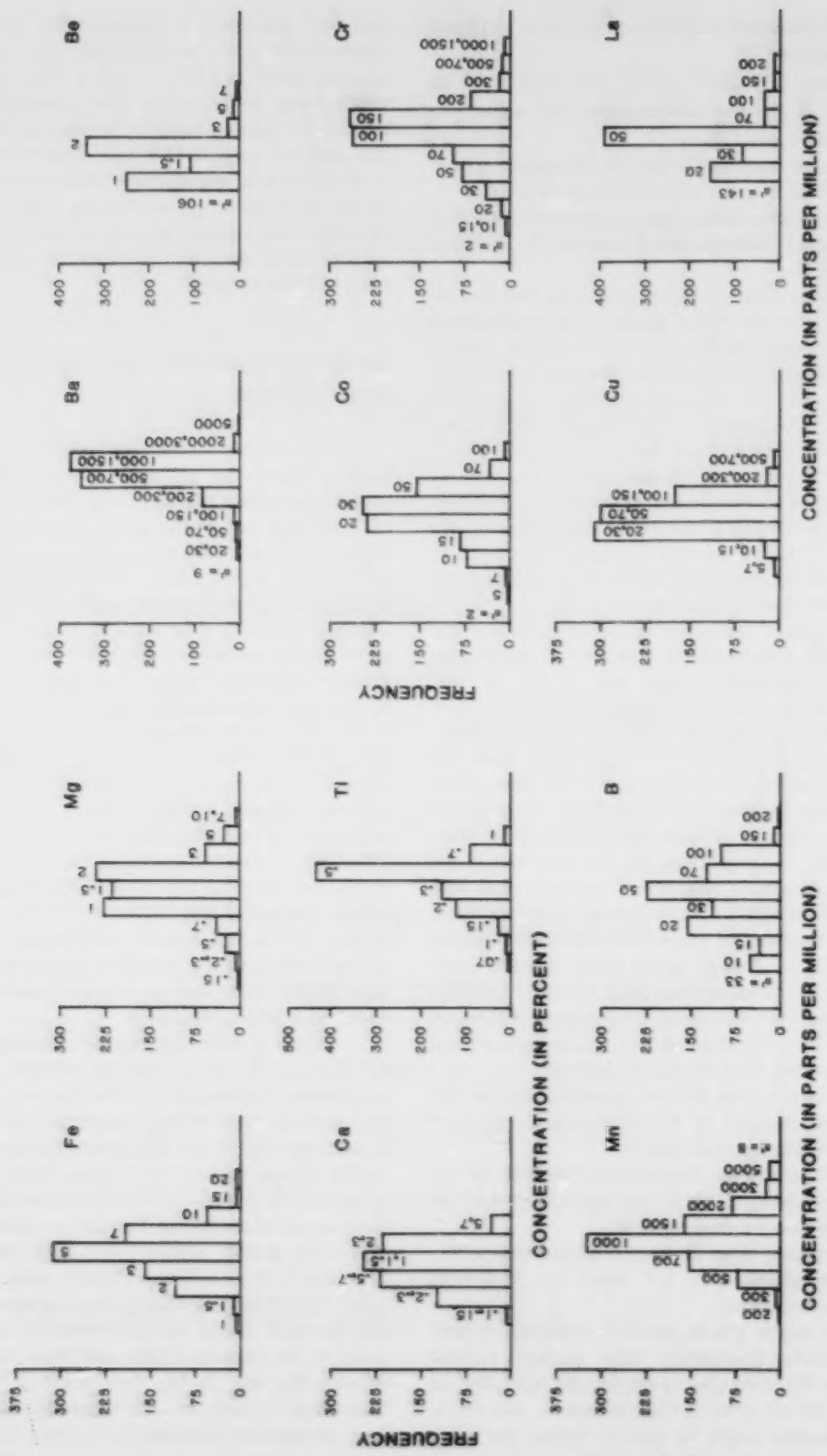
Be
Cr
La
Ba
Co
Cu
Mg
Ti
B
Fe
Ca
Mn
FREQUENCY
CONCENTRATION (IN PARTS PER MILLION)
CONCENTRATION (IN PERCENT)

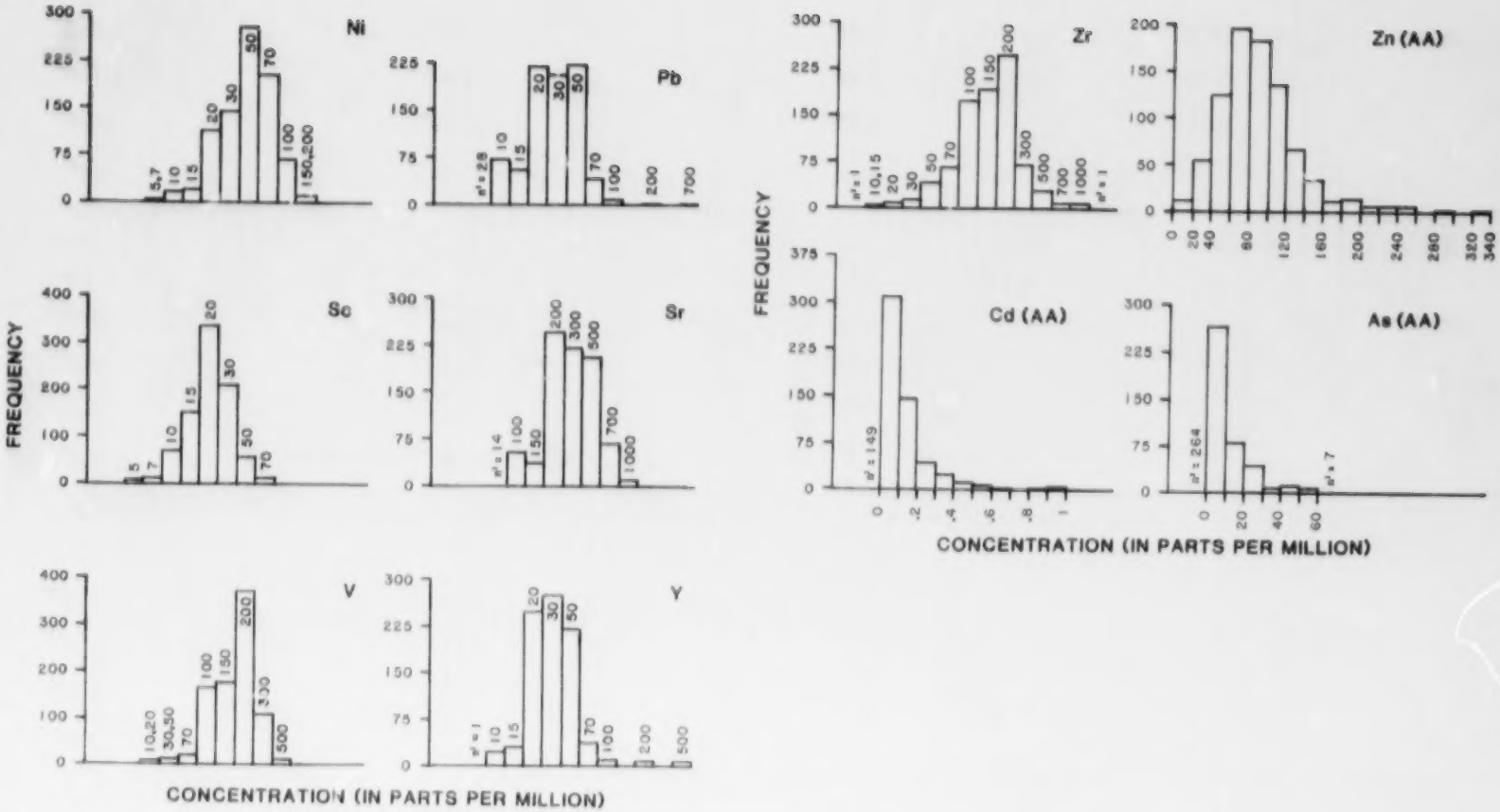

Figure 2. Histograms showing frequency distribution for element concentrations in sediment samples.

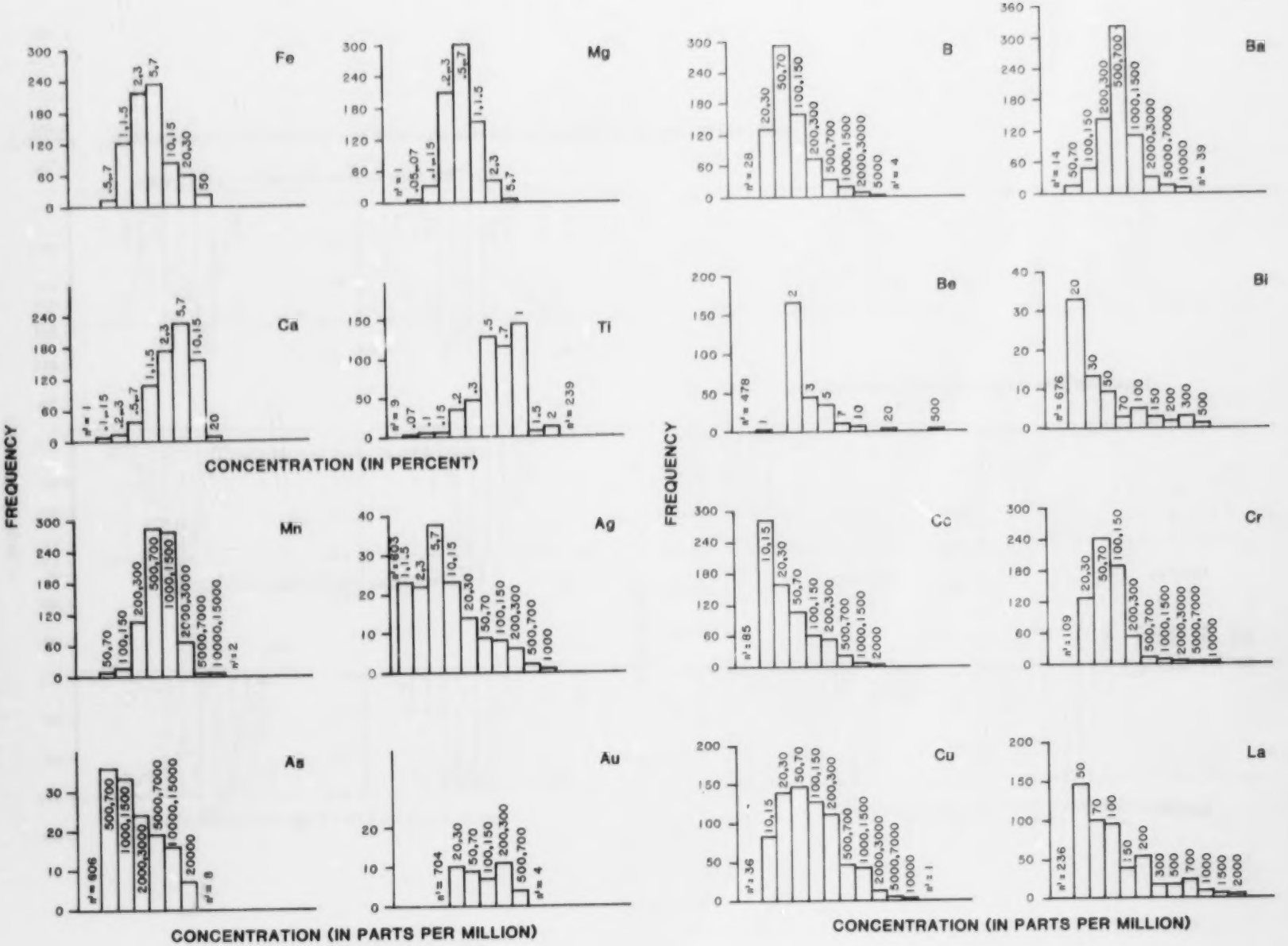
Fe
Mg
B
Ba
Ca
Ti
Be
Bi
Mn
Ag
Co
Cr
As
Au
Cu
La
FREQUENCY
CONCENTRATION (IN PERCENT)
CONCENTRATION (IN PARTS PER MILLION)

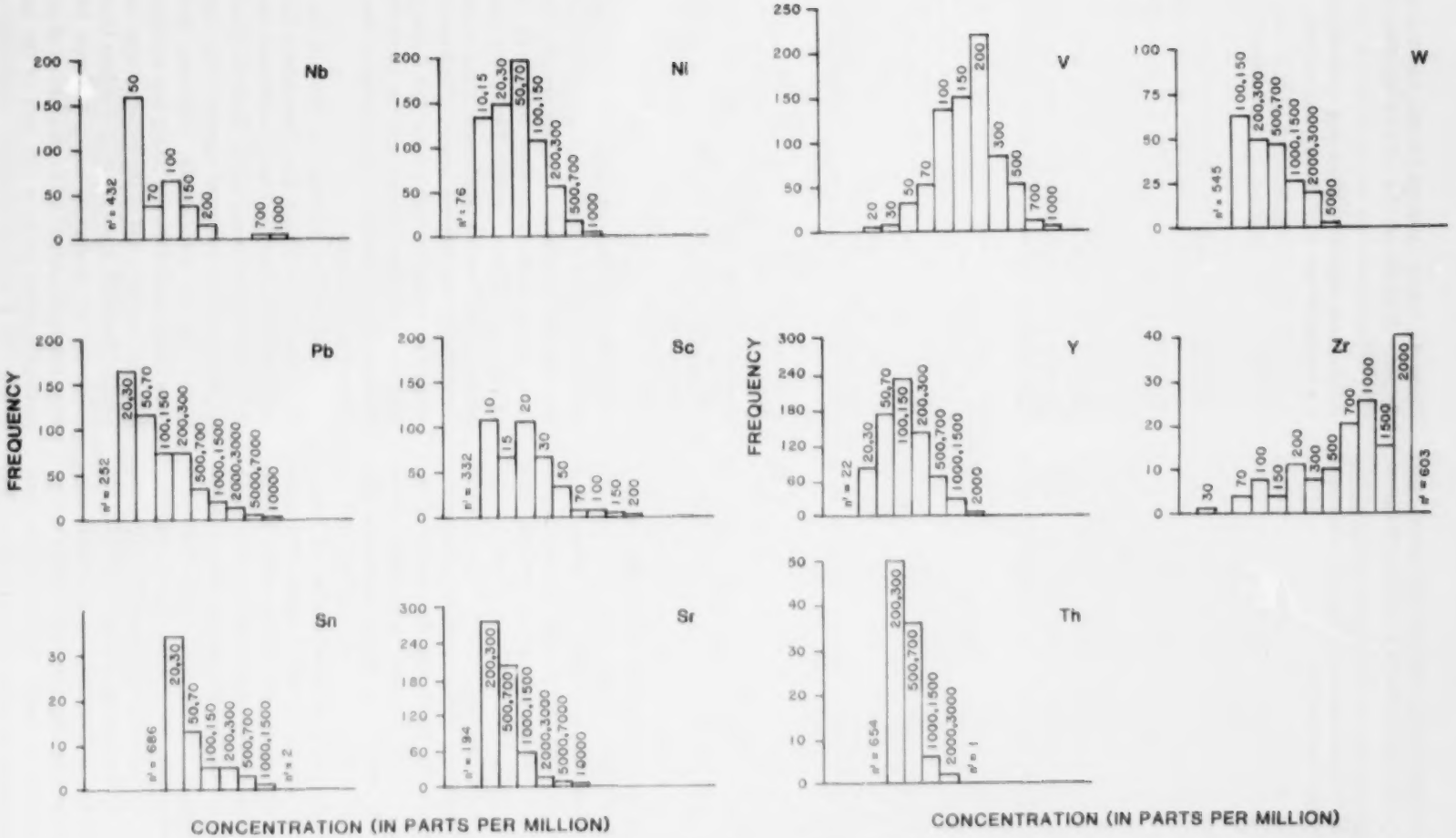

Figure 3. Histograms showing frequency distribution for element concentrations in nonmagnetic heavy-mineral-concentrate samples.

Table 3. Factor loadings for the first five factors after Varimax rotation of the log-transformed sediment database

[Total variance explained by five factors equals 73 percent. Leaders (--), loadings less than |0.30| that have been omitted. AA, determined by atomic absorption spectrophotometry]

Element	Factor				
	1	2	3	4	5
Fe	0.78	--	--	--	--
Mg	.86	--	--	--	--
Ca	.35	--	-0.76	--	--
Ti	.73	0.40	--	--	--
Mn	--	--	--	0.81	--
B	--	.44	.64	--	--
Ba	--	.81	--	--	-0.31
Be	--	.72	--	--	.39
Co	.68	--	--	.54	--
Cr	.83	--	--	--	--
Cu	.68	--	--	--	.39
La	--	.61	--	--	.43
Ni	.83	--	--	--	--
Pb	--	.70	--	--	--
Sc	.83	--	--	--	--
Sr	--	.72	.42	--	--
V	.83	--	--	--	--
Y	--	.53	-0.33	.32	--
Zr	--	.83	--	--	--
Zn (AA)	--	--	.69	.34	--
As (AA)	--	--	.36	--	-0.71
Percent of total variance explained by factor.	29	19	10	8	7

Table 4. Factor loadings for the first five factors after Varimax rotation of the log-transformed concentrate database

[Total variance explained by five factors equals 61 percent. Leaders (--), loadings less than |0.30| that have been omitted]

Element	Factor				
	1	2	3	4	5
Fe	0.88	--	--	--	--
Mg	--	0.69	--	0.35	--
Ca	--	.79	--	--	--
Ti	--	--	0.53	--	--
Mn	--	.77	--	--	--
Ag	.39	--	--	--	0.57
As	--	--	--	--	.72
B	--	.40	--	-0.31	--
Ba	--	--	.46	-0.30	-0.45
Be	--	--	--	-0.75	--
Co	.80	--	--	--	.35
Cr	--	--	--	.62	--
Cu	.79	--	--	--	--
La	--	--	.64	--	--
Nb	--	--	.68	--	--
Ni	.88	--	--	--	--
Pb	.52	--	--	--	.37
Sc	--	--	.38	.65	--
V	--	.68	--	--	--
W	--	--	--	--	.52
Y	--	--	.80	--	--
Zr	--	--	.64	--	--
Percent of total variance explained by factor.	16	13	13	9	9

small, unexposed igneous bodies. All Valdez Group rocks east of the Copper River, plus those around McCune and Shiels Glaciers south to lower Allen Glacier, yield samples with high positive factor-2 scores, which most likely reflect widespread granite melt injections in the high-grade metamorphic rocks.

Samples with anomalously positive factor-3 scores cluster from Hinchinbrook Island northeast through the headwaters of the Rude River and over much of the southeastern corner of the Cordova quadrangle and on Kayak Island on the Middleton Island quadrangle (fig. 4). Enrichments of B and Zn and relatively low Ca concentrations characterize sediments from all watersheds underlain by younger Tertiary sediments except those to the east of Bering Lake and the lower Bering River. Similar geochemical signatures occur over much of Hinchinbrook and Hawkins Islands, the Heney Range and Eyak Lake region, and the upper Rude River and Raging Creek watersheds. Most likely, the anomalously high B and low Ca reflect lithogeochemical differences between this belt of Orca Group flyschoid rocks and the rest of the Orca Group and Valdez Group metasedimentary rocks. The anomalous Zn, especially considering the scattering of outcrops of mafic volcanic rocks and massive sulfide prospects along this belt, may indicate the widespread presence of sphalerite. Four samples with anomalous factor-3 scores that group over Bligh Island and onto the mainland at Tatitlek are also derived from Orca Group metasedimentary rocks with subordinate amounts of volcanic units. The entire northeastern corner of the Cordova quadrangle contains samples with anomalously low factor-3 scores. The location of sediments with relatively high Ca and low B and Zn content between Van Cleve Glacier and the South Fork of the Bremner River correlates with outcrops of the paragneiss of the Valdez Group.

High positive loadings for Mn and Co, and to a lesser extent for Y and Zn, characterize factor 4. All areas underlain by Orca Group rocks from Sheep Bay to the northwestern corner of the Cordova quadrangle are characterized by sediment samples with high factor-4 scores (fig. 5). Additionally, sediments derived from Orca Group rocks between Sheep Bay and Simpson Bay, from the northern half of the Heney Range northeast to Snyder Mountain, and on central Hawkins Island are also delineated by anomalous factor-4 scores. Most likely, these anomalies reflect a Mn enrichment of Orca Group metasedimentary rocks in this part of the accretionary terrane that is perhaps related to widespread submarine

exhalative activity suggested by the common occurrence of interbedded mafic volcanic rocks. The less strongly loaded Co and Zn might reflect an abundance of disseminated sulfides throughout the flysch as a result of the exhalative activity. Alternatively, Co and Zn show a relatively high affinity for adsorption by Mn-oxides which could be abundant in a region with a high-Mn background.

Three areas underlain by Valdez Group metasedimentary rocks also are distinguished by large clusters of samples with high positive factor-4 scores (fig. 5). Samples with high factor-4 scores continue north and east across the Landlock fault (Contact fault system) to Silver Lake and Silver Glacier. The similar geochemical signatures on both sides of the Landlock fault support the hypothesis of Dumoulin (1987) that the Contact fault system in this area may actually lie further to the north. A second cluster of high scores occurs throughout the Gravina River watershed and extends into upper Dead Creek and onto Wortmanns Glacier. These anomalies, which are discussed in more detail later (fig. 16 on pl. 2), identify a geochemically favorable area for bedded Mn occurrences and (or) base-metal mineralization. A third group of samples with anomalous factor-4 scores that are associated with the high-grade metasedimentary rocks of the Valdez Group along the southern side of the South Fork of the Bremner River reflect a minor enrichment of Mn and Co in this part of the Valdez Group.

A strong negative loading for As dominates factor 5. Samples with the most positive factor-5 scores tend to cluster on Woodworth, Schwan, Heney, Childs, and Grinnell Glaciers. The relative paucity of As in sediments

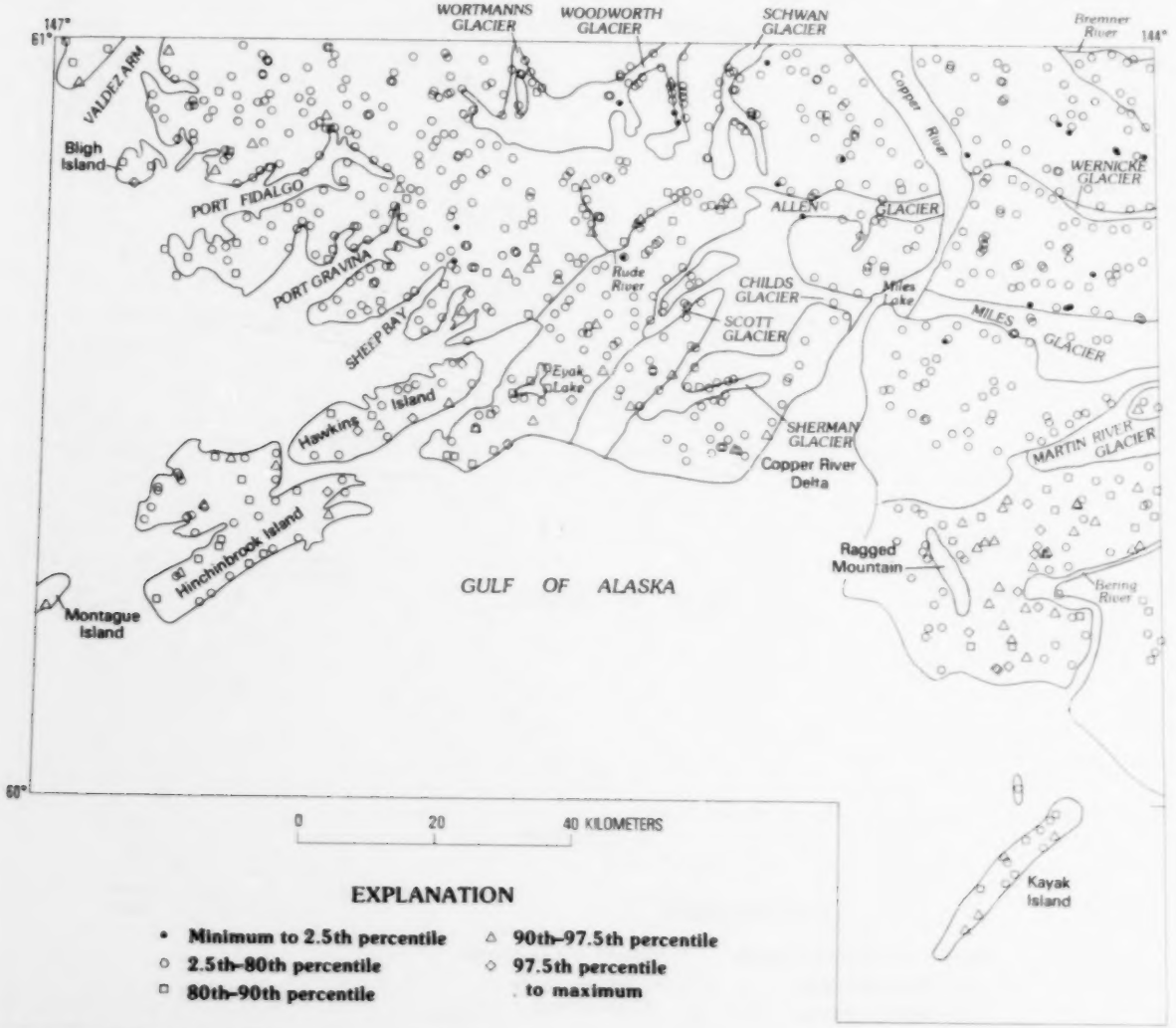

EXPLANATION

- • Minimum to 2.5th percentile
- ○ 2.5th–80th percentile
- □ 80th–90th percentile
- △ 90th–97.5th percentile
- ◇ 97.5th percentile to maximum

Figure 4. Distribution of factor scores for sediment factor 3.

derived from these areas may reflect the high proportion of mafic volcanic rocks within each glacier basin and the relatively low background As content of these rocks. Alternatively, the interbedded flysch in these regions may simply contain fewer arsenopyrite-bearing quartz veins relative to other areas underlain by Valdez Group and Orca Group flyschoid units.

Concentrate-Sample Factor-Analysis Associations

A five-factor model was also chosen to reduce the concentrate data, and it explains only 60 percent of the total variance. Eigenvalues represent the fraction of the data variance that is correlated with each factor. Eigenvalues for all factors beyond the fifth factor were less than one, and thus the inclusion of additional factors would not have been advantageous. Exclusion of the few highly censored elements included in table 4, as well as principal component and oblique rotation solutions rather than a Varimax rotation solution, did little to increase the amount of the variance explained by factors chosen as significant. Thus, whereas the results of the analysis described below point out the major correlations and regional trends in the data matrix, observation of individual element distributions contributes to a more thorough understanding of local anomalies.

Factor 1 shows high loadings for Fe, Co, Cu, and Ni, and reflects the abundance of pyrite and chalcopyrite in the concentrate samples. Samples with the highest

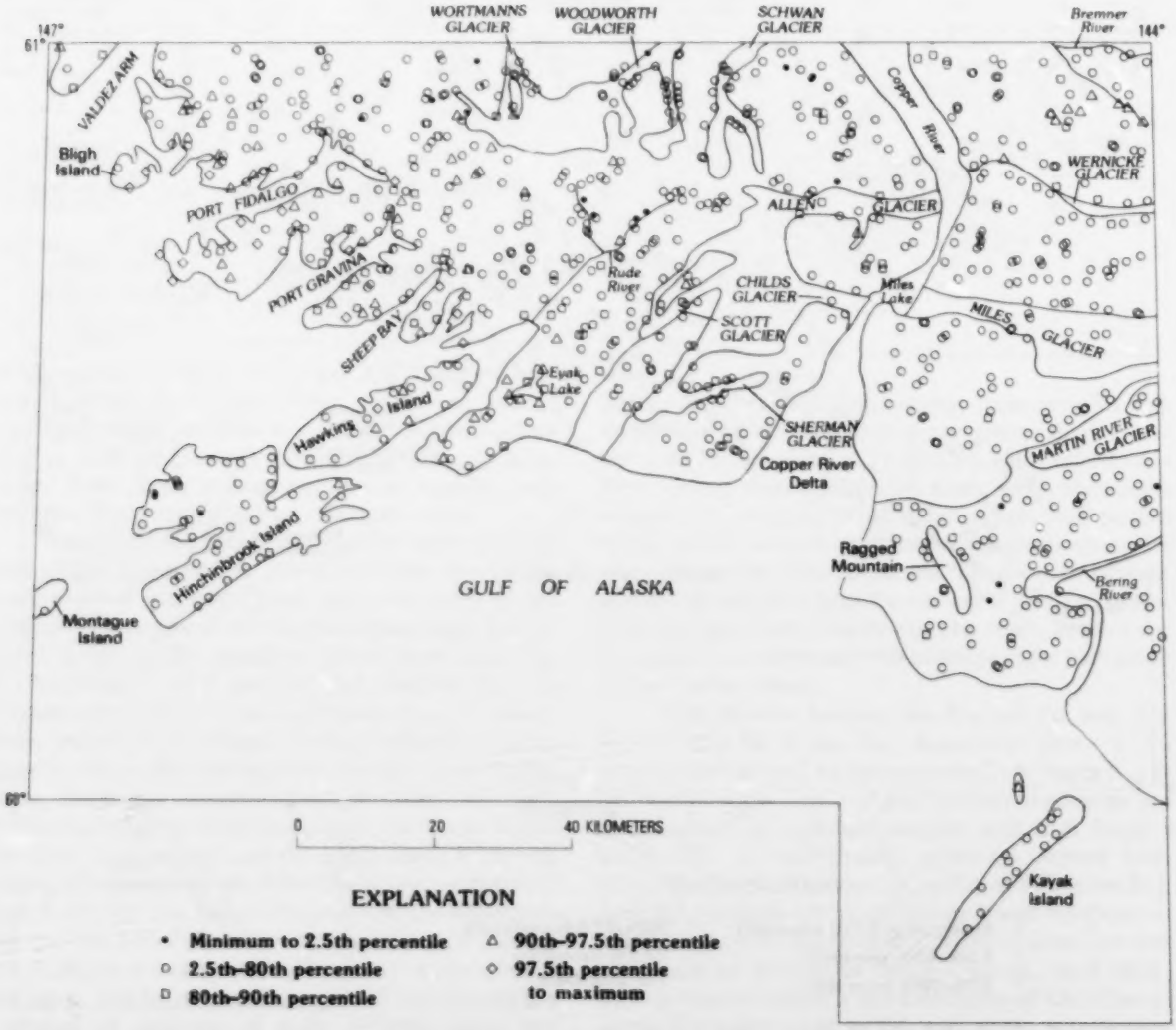

Figure 5. Distribution of factor scores for sediment factor 4.

positive factor-1 scores occur over one large area of the Cordova quadrangle as is explained in more detail below as the "central sulfide belt" (see pl. 1). Weaker positive loadings for Pb and Ag indicate the presence of galena in many of the sulfide-rich samples. Most of the samples within this belt are located at the higher elevations of the Chugach Mountains and in drainages on both sides of the Contact fault system (fig. 6). High scores do not continue east of the Copper River, which indicates that there is very little geochemical favorability for any similar sulfide occurrences in the high-grade rocks of the Chugach metamorphic complex.

High loadings for Mg, Ca, Mn, and V characterize factor 2. High factor-2 scores cluster in the headwaters of the Sheep River, Koppen Creek, Gravina River, and Dead Creek (fig. 7) and define the Mn-rich area discussed below (fig. 16 on pl. 2). Anomalous scores that are also scattered over areas underlain by mafic volcanic rocks of both the Orca and Valdez Groups, perhaps reflect some mafic silicate minerals within the nonmagnetic heavy-mineral-concentrate fractions. Unfortunately, the approximately 100 samples with the most negative scores represent those collected in a single field season and for which background concentrations of Mg, Ca, Mn, and V were consistently determined at lower spectrographic steps than in other field seasons. Hence, the Mg-Ca-Mn-V association dominantly reflects analytical variance.

Samples with high factor-3 scores and with the strongest loadings for Y, Nb, La, and Zr, are dominantly derived from the Tertiary Stillwater, Kulthieth, Tokun, and Poul Creek Formations in the southeastern corner of

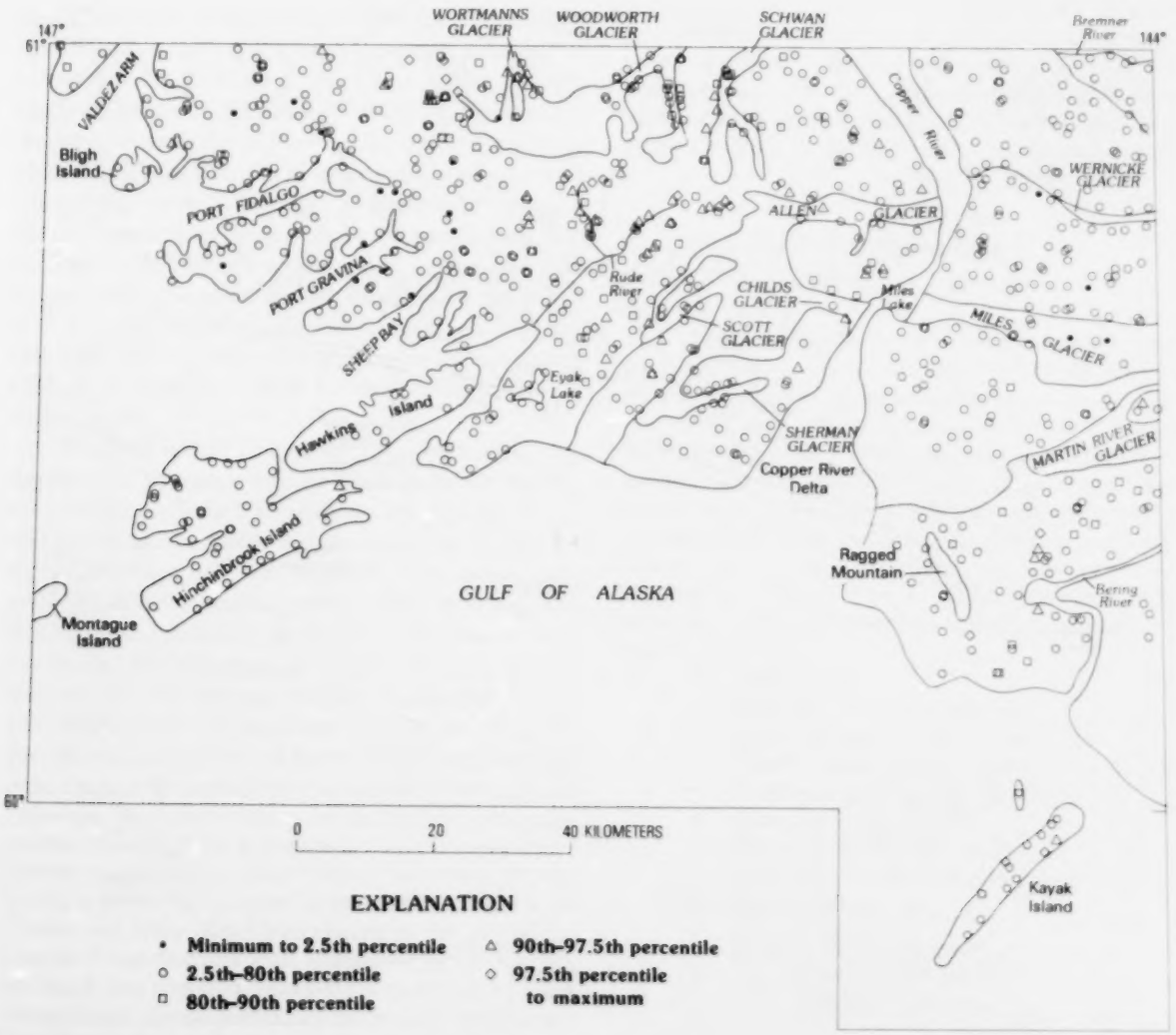

Figure 6. Distribution of factor scores for heavy-mineral-concentrate factor 1.

the Cordova quadrangle. However, concentrate samples derived from the younger Yakataga Formation, which underlies most of Kayak Island on the Middleton Island quadrangle, show no such lithophile element enrichment. The relative abundance of La, Nb, Y, and Zr in the four former formations is likely due to the high proportion of accessory minerals, including microscopically visible apatite and zircon, within these units. The Yakataga Formation is predominantly ice-rafted debris deposited during pronounced uplift along the Gulf of Alaska (Plafker, 1974); thus, concentrate samples of detritus weathered from this formation would be expected to have chemistries similar to those of the older Orca Group rocks. The fairly high Ba loading of factor 3 reflects the abundance of barite in the concentrates from this region (figs. 22 and 23 on pl. 3).

A number of other areas contain clusters of slightly less anomalous factor-3 scores. Some sample sites with high scores are underlain by the high-grade gneissic rocks of the central Chugach metamorphic complex in the vicinity of Wernicke Glacier. Other sample sites with high scores stretch across the northern border of the Cordova quadrangle from the Bremner River and South Fork of the Bremner River to the eastern edge of Schwan Glacier, which is an area largely underlain by transitional high-grade schist. The anomalous scores probably reflect a concentration of Y, Nb, La, and Zr in certain metamorphic minerals specific to a higher grade metamorphic facies or in some of the local anatectic stringers, dikes, and sills described by Hudson and Plafker (1982). Clusters of samples with high factor-3 scores also are located northeast, northwest, and southeast of Mt. Den-

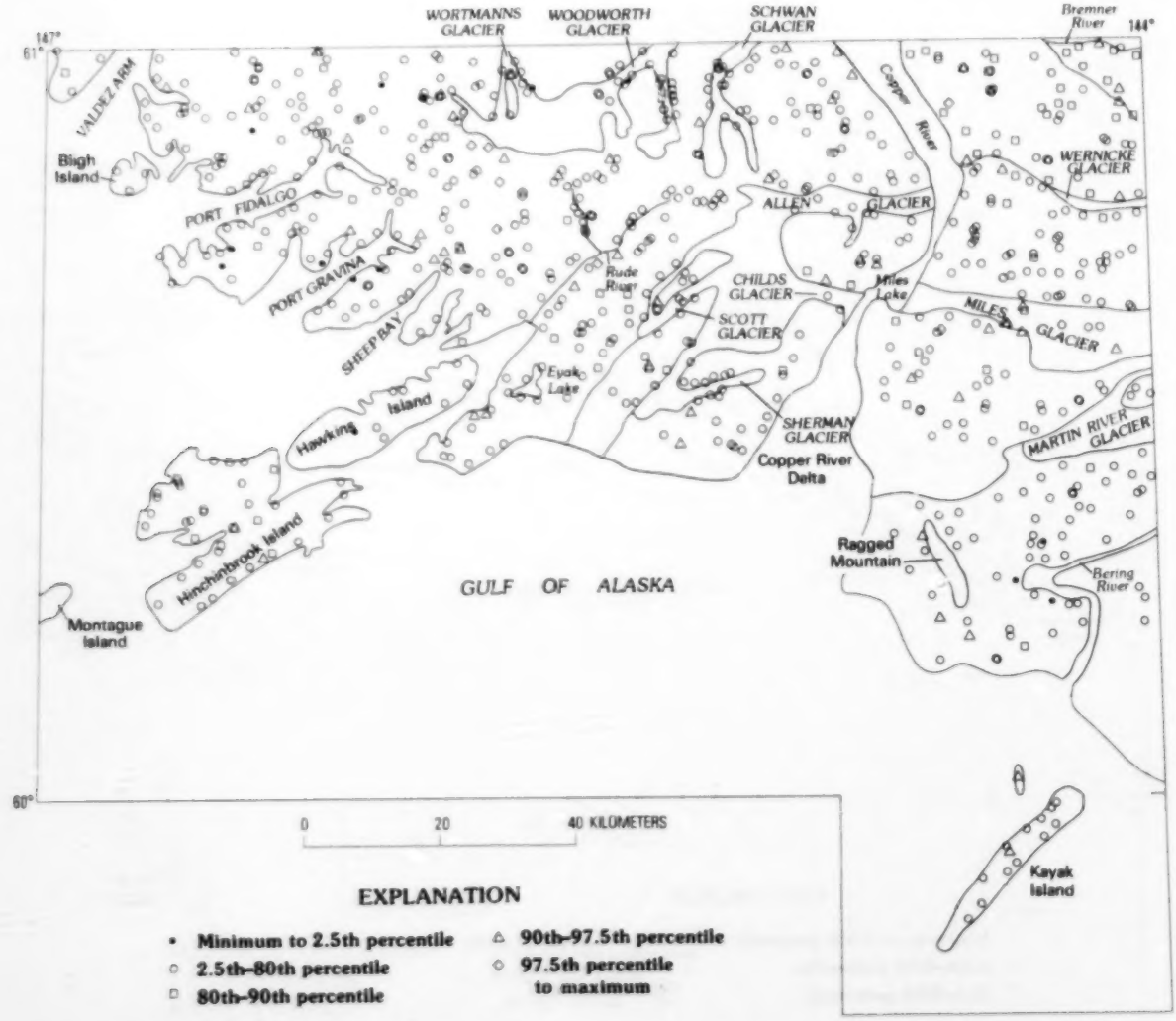

Figure 7. Distribution of factor scores for heavy-mineral-concentrate factor 2.

son and in Brown Basin. These anomalies may reflect Y, Nb, La, and Zr enrichments associated with a relatively higher grade metamorphic mineral assemblage in Valdez Group rocks. Geologic studies in this part of the Chugach Mountains have identified upper-greenschist- and amphibolite-facies metamorphic assemblages (Marti Miller, written commun., 1985). The cause of a final anomalous group of samples from drainages on Mt. Eyak and in the northwestern Heney Range near Cordova is unknown.

Factor 4 shows strong positive loadings for Cr and Sc and a strong negative loading for Be. Samples with high factor-4 scores appear to be largely derived from mafic volcanic rocks. Samples with the highest scores from areas south of the Contact fault system are derived from Orca Group volcanic rocks in the northwestern Heney Range, on central Hinchinbrook Island, south of Port Fidalgo, and from Billygoat Mountain northwest to Galena Bay. North of the Contact fault system, anomalous samples are associated with Valdez Group volcanic rocks in Brown Basin, on Wortmanns Glacier, on Woodworth Glacier, and between lower Schwan Glacier and the Copper River. A string of anomalous samples extends downstream from a small ultramafic body that intrudes Valdez Group rocks to the northeast of Port Fidalgo and is discussed in more detail below (fig. 27 on pl. 3). Samples with anomalous factor-4 scores to the east and west of Mt. Denson suggest other poorly exposed or unexposed mafic or ultramafic units lie in these regions.

Factor 5 is defined by strong positive loadings for Ag, As, and W; weaker positive loadings for Co and Pb; and a weaker negative loading for Ba. Clusters of anomalous concentrate samples (fig. 8) define areas with the highest densities of precious-metal-, base-metal-, and probably scheelite-bearing quartz veins. The negative loading for Ba indicates the absence of barite in these systems and the lack of any such vein systems within the relatively Ba rich younger Tertiary sedimentary rocks. The largest group of anomalous samples are from the Wortmanns Glacier–Brown Basin–Dead Creek area and from areas as far west as Mt. Denson and Silver Lake, all underlain by Valdez Group rocks. Highly anomalous samples also are from drainages in Valdez Group rocks between northwestern Allen Glacier and Shiels Glacier to the west of the Copper River and near LaGorce Glacier and lower Van Cleve Glacier to the east of the Copper River. Samples with anomalous factor-5 scores are much less common within areas underlain by Orca Group rocks. Small clusters of anomalous samples are located over the southern end of the Gravina Peninsula, south of the lower portion of Scott Glacier, and in the McPherson Glacier–Goat Mountain region. All samples from streams that drain the younger Tertiary sedimentary units are characterized by anomalous negative factor scores.

DESCRIPTION OF GEOCHEMICAL ANOMALIES

Interpretation of distribution plots for factor scores and individual element concentrations, especially for the highly censored populations, identify a number of geochemically anomalous areas that are not solely related to lithologic variation. Many of these anomalies are geochemically favorable areas for the presence of syngenetic and (or) epigenetic metallic mineral resources and are discussed in detail below. In addition, we discuss the widespread distributions of Au (pl. 1), Ag, and W (fig. 9) which appear to delineate the extent of much of the epigenetic quartz veining. Maps showing sample sites and tabulations of data for specific areas are in figures 10–18 (grouped on pl. 2) and figures 19–29 (grouped on pl. 3).

1. Widespread Anomalous Gold and Silver

Concentrate samples with microscopically visible gold, and corresponding analytical values for Au of at least 20 ppm, generally occur in clusters across the upper quarter of the Cordova quadrangle (pl. 1). The areas delineated by these clusters are underlain by both the metasedimentary and metavolcanic rocks of the Valdez Group; there is no obvious spatial relationship between the gold distribution and the major faults in the Valdez Group. These areas include [the number in parentheses is equal to the total number of samples with microscopically visible gold and (or) analytically detected Au within each area]:

1. Fish Bay (1).
2. Northeast of Silver Lake (1).
3. North and east of Mt. Denson (5).
4. Dead Creek–Brown Basin to the area southwest of Meteorite Mountain (8).
5. Wortmanns Glacier (5).
6. West side of Woodworth Glacier (1).
7. East branch of Woodworth Glacier (2).
8. Schwan Glacier (8).
9. Heney Glacier (1).
10. McCune and Shiels Glaciers (3).
11. Allen Glacier (5).
12. Headwaters of the Rude River, just to the west of the divide with Allen Glacier (1).
13. Watershed west of Eagle Creek (3).

14. North of Wernicke Glacier (2).
15. Southwest of Wernicke Glacier (3).

Only four areas that are underlain by Orca Group metavolcanic and metasedimentary rocks contained Au:

1. Both sides of St. Matthews Bay (2).
2. McKinley Lake (1).
3. Southwest Ragged Mountain (1).
4. Upper Rude River, to the north of Scott Glacier (3).

Silver values of at least 1 ppm in heavy-mineral concentrates are associated with all Au-bearing concentrate samples except those at St. Matthews Bay and Ragged Mountain. Most likely, many of the Au grains are actually electrum. Mitchell (1979) reported that gold in mineralized quartz veins in the Hope-Sunrise district, further to the west on the Seward 1° × 3° quadrangle but also within the Valdez Group, commonly contains greater than 50 percent Ag.

Concentrate samples with anomalous Ag values commonly form relatively broad halos surrounding, and inclusive of, drainages with many of the Au-bearing samples. This is especially true for Mt. Denson, Dead Creek–Brown Basin–Meteorite Mountain, western Wortmanns Glacier, Woodworth Glacier, Schwan Glacier, and the area west of Eagle Creek. The analytically detected Ag probably reflects Ag substitution in arsenopyrite, galena, and (or) chalcopyrite; one or more of these sulfide phases are consistently present in each of the six areas. The more widespread Ag anomalies rela-

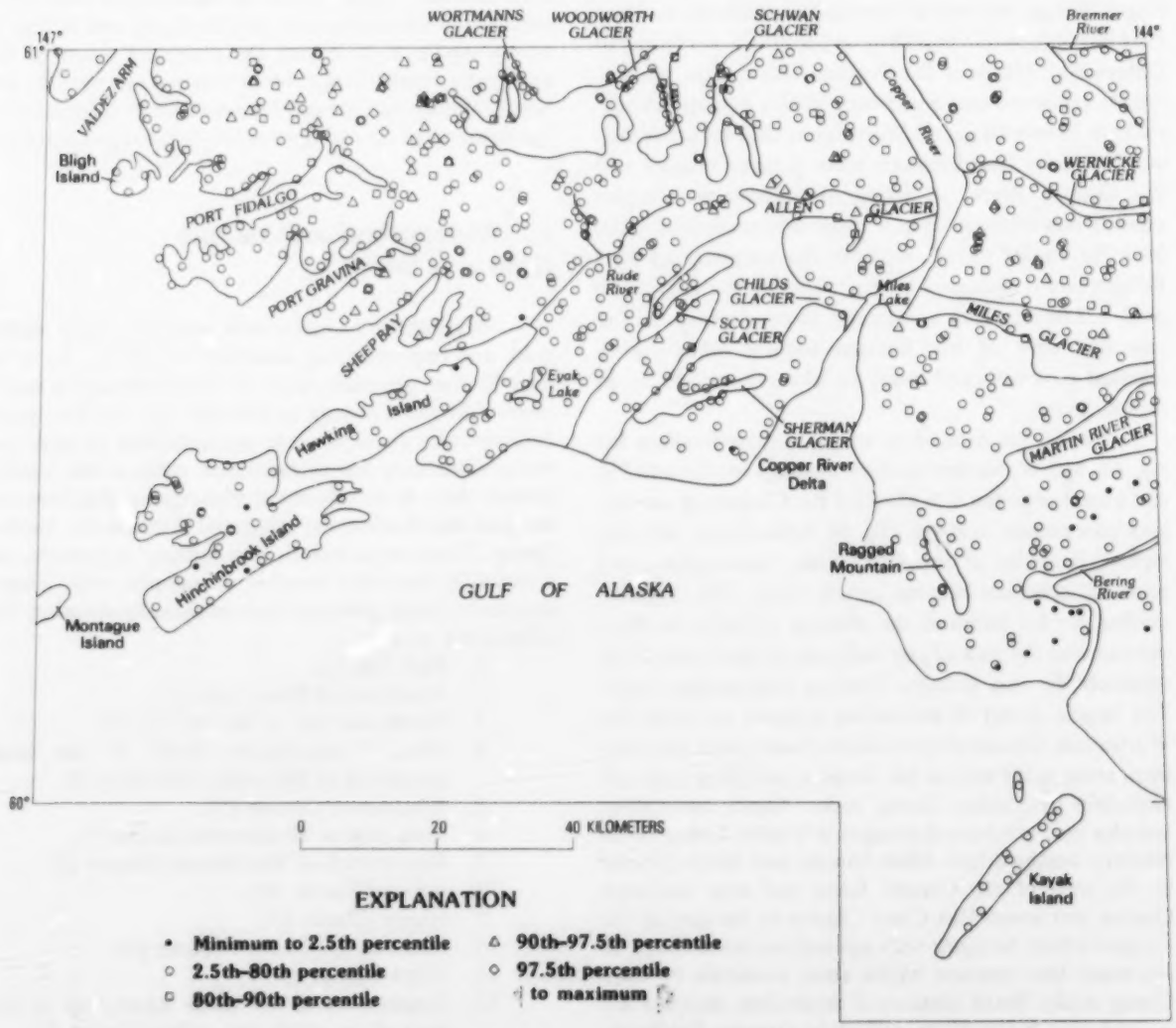

Figure 8. Distribution of factor scores for heavy-mineral-concentrate factor 5.

tive to anomalous Au, suggest a wider distribution of sulfide-bearing quartz veins than sulfide- and Au-bearing quartz veins in these areas.

Other regions of relatively limited areal extent also contain anomalous Ag in concentrate samples but lack any anomalous Au. Concentrate samples with anomalous Ag cluster at Tatitlek Narrows and Landlocked Bay, near Scott Glacier, and in the vicinity of Rude Lake, in association with arsenopyrite-, chalcopyrite-, and galena-rich samples. Point anomalies for Ag are scattered throughout the Cordova quadrangle and are usually associated with an abundance of one or more sulfide phases. Anomalous Bi and Sn values, both usually between 20 ppm and 100 ppm, are commonly associated with many of the anomalous Ag values and also represent elemental substitutions within sulfide minerals.

Arsenopyrite and, to a lesser extent, galena, sphalerite, and chalcopyrite are commonly found with pyrite in many of the Au-bearing quartz veins known throughout the western portion of the Valdez Group (Goldfarb and others, 1986). The common association of Au with anomalous As, Cu, and Pb in concentrates (and with microscopically visible arsenopyrite, chalcopyrite, and galena) within the northern part of the Cordova quadrangle suggests a similar quartz vein–Au–sulfide assemblage. Arsenopyrite is abundant in all Au-rich areas except west of Eagle Creek, north of Wernicke Glacier, Ragged Mountain, Heney Glacier, McCune Glacier, Woodworth Glacier, and Schwan Glacier. Chalcopyrite is commonly abundant in Au-bearing concentrate samples from the Brown Basin–Dead Creek–Meteorite Mountain, Wortmanns Glacier, Woodworth Glacier, Schwan Glacier, upper Rude River, headwaters of the Rude River, and McCune Glacier regions. Galena is found in Au-bearing concentrate samples from the Silver Glacier, Mt. Denson, Brown Basin–Dead Creek–Meteorite Mountain, Wortmanns Glacier, Woodworth Glacier, McKinley Lake, upper Rude River, and St. Matthews Bay regions. The lack of anomalous Zn and microscopically visible sphalerite in all Au-bearing concentrate samples may suggest that any sphalerite present in the source lodes is relatively Fe-rich; this Fe-rich sphalerite would be removed by magnetic separation during sample preparation work, and consequently Zn would not be reported in the analysis. Alternatively, Zn is relatively mobile in the weathering environment and may be transported hydromorphically, whereas the other metals are dominantly transported as detrital grains.

From interpretation of the concentrate data it is apparent that most detrital gold is being weathered from Au-bearing fissure veins that are widely distributed in both metasedimentary and metavolcanic rocks of the Valdez Group. Gold was a common by-product from many of the copper mines within the Prince William Sound region; disseminated gold grains were observed in polished sections (R. Goldfarb, unpub. data, 1986) of a massive pyrrhotite-chalcopyrite lens from Ellamar. However, no Au was analytically detected or microscopically visible in concentrates from the Solomon Gulch, Ellamar, Irish Cove, Snyder Mountain–Heney Range–Hinchinbrook Island, or Scott Glacier regions. Any Au contained within concentrated sulfide minerals weathered from massive sulfide bodies at these localities also was too scarce to be analytically detected. Therefore, even for the relatively high proportion of Au-bearing samples within the central sulfide belt (see anomalous area 3 below), the placer Au is believed to have been derived solely from quartz-vein sources.

The distributions of anomalous Ag, As, Cu, Pb, and Zn, which are much more widespread than that of anomalous Au and commonly show no spatial association with Au-bearing concentrates, indicate that Au is the only suitable geochemical pathfinder for auriferous veins on the Cordova quadrangle. Corresponding stream-sediment samples were essentially useless in identifying areas that are geochemically favorable for Au. A few sediments with anomalous spectrographic Ag values, determined by semiquantitative techniques, cluster on Wortmanns and Woodworth Glaciers and near McKinley Lake. Generally though, the Ag anomalies provide little help in identifying Au-rich areas. Similarly, even with the greater sensitivity of atomic absorption spectrophotometry, Au concentrations in sediment samples were usually below the analytical detection limits needed to identify Au-rich regions. Gold was detected in only one-third of the sediment samples that not only were analyzed by atomic absorption but also corresponded with concentrate samples that showed gold. Rarely was gold detected in sediment samples if it was not found in corresponding concentrate samples. Geochemical identification of Au-rich areas was thus only possible through the concentration of the heavy-mineral fraction of the sediments.

2. Widespread Anomalous Tungsten

The distribution of analytically detected W (≥ 100 ppm) in concentrate samples shows a strong correlation with the presence of microscopically visible scheelite on the Cordova quadrangle. The only exceptions occur south of Port Fidalgo, south of the Midas mine, from Meteorite Mountain west to the Copper River, and to the east of the lower half of the Rude River. These areas, all underlain by relatively high proportions of metavolcanic rocks, yield concentrates with microscopically visible scheelite but with analytical values almost everywhere less than 100 ppm W. The scheelite in these areas is believed to be weathering from veins within interbedded metasedimentary rocks and is diluted in concentrate

samples by the abundant pyrite, and perhaps some magnesian silicates, weathered from the metavolcanic units.

The spatial distribution of the scheelite (fig. 9), and to a lesser extent anomalous W, roughly correlates with the distribution of Valdez Group rocks. Almost all concentrate samples collected from watersheds underlain by Valdez Group rocks contain microscopically visible scheelite. Only the Heney Glacier and Rude Lake areas, where metavolcanic rocks are extensively exposed, lack scheelite.

The source of the scheelite is still uncertain. Traces of scheelite may occur as disseminated grains within Valdez Group metasedimentary rocks . The correlation of the anomalous W with the spatial distribution of metasedimentary rocks supports such an idea. Spectrophotometric values for W concentrations in 30 Valdez Group graywackes, slates, and argillites nowhere exceed 2.5 ppm (R. Goldfarb, unpub. data, 1985) and thus are well within normal background levels. However, the possiblity of an uneven distribution of weakly disseminated scheelite grains within the Valdez Group rocks can not be conclusively eliminated.

A more plausible source for the detrital scheelite grains may be the ubiquitous quartz fissure veins. Gold-bearing quartz veins in metamorphosed turbidite (Henley and others, 1976) and greenstone (Fyfe and Kerrich, 1984) terrains commonly are enriched in W. Whereas semiquantitative emission spectrographic analyses showed most Au-bearing quartz veins from the Valdez Group on the Seward 1°×3° quadrangle to the west of the study area to contain less than 50 ppm W (lower analytical detection limit for rock samples), a few veins

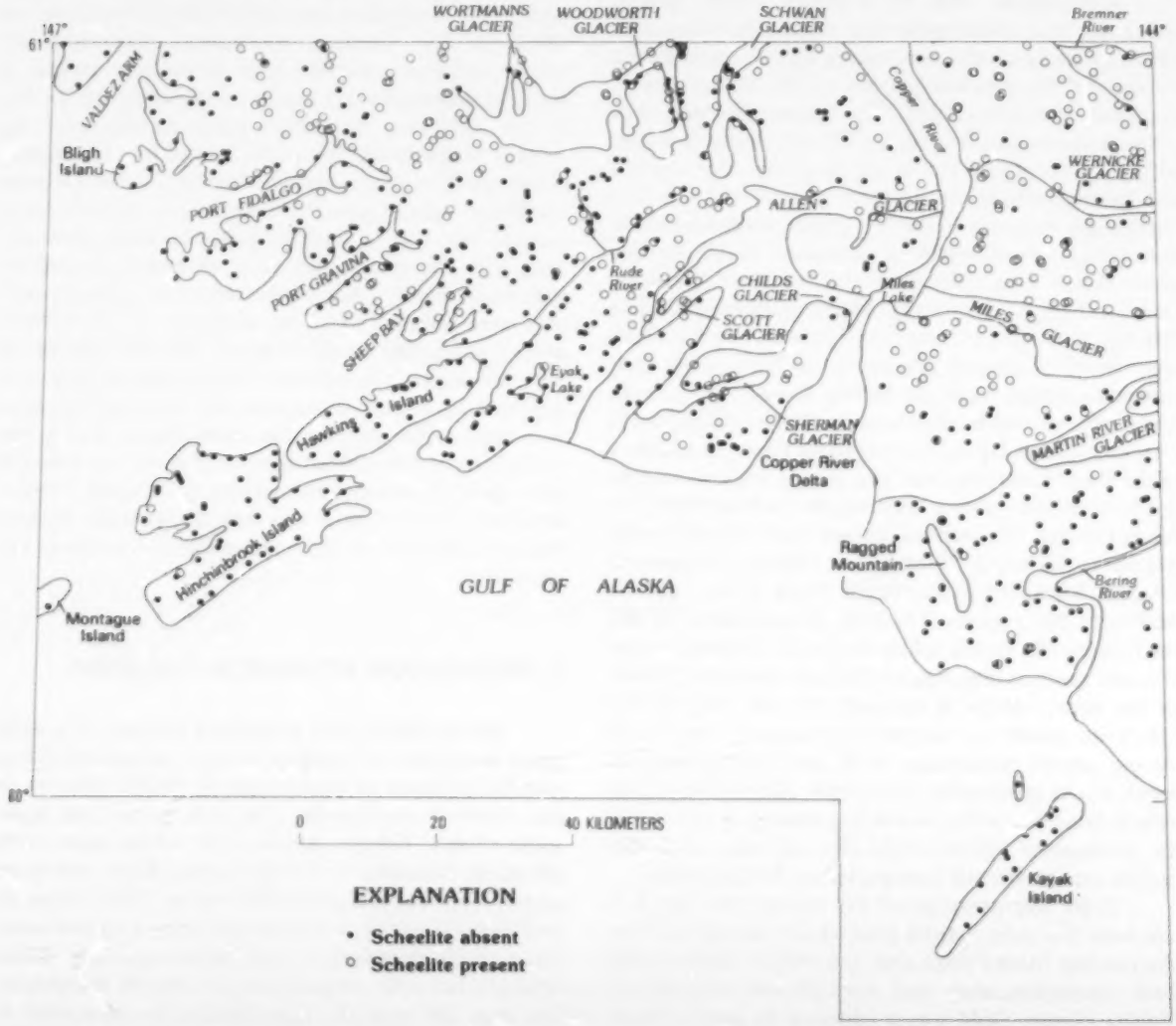

Figure 9. Distribution of scheelite.

contained as much as 1,000 ppm W, probably as scheelite (R. Goldfarb, unpub. data, 1985). Therefore, we believe that W, along with Si and less commonly with Au and base metals, probably was leached from Valdez Group rocks by fluids produced during regional greenschist and amphibolite metamorphic reactions and was deposited in widely scattered joint sets and shear zones.

Such a hypothesis for the source of the scheelite is further supported by the distribution of W within samples from drainages underlain by Orca Group rocks. Scheelite, plus anomalous W, occurs in a significant number of samples only in three areas south of the Contact fault system. Two of these areas are rather limited in extent. The first of the two areas is that underlain by Tertiary granitic rocks on the peninsula southeast of Port Gravina. Continuation of the W anomalies to the adjacent peninsulas across Sheep Bay and Parshas Bay suggests other, poorly exposed, granitic rocks and (or) a contact aureole at these localities. The second small area runs from Whalen Bay and the Schlosser mine across to the shores of St. Matthews Bay. The source of the anomalous W is unknown in this area which is underlain by both Orca Group metasedimentary and metavolcanic rocks.

Almost all concentrate samples derived from the Orca Group rocks between the Martin fault and the Bagley fault (Contact fault system) to the east of the Copper River contain anomalous W. These anomalies continue west across Sherman, Sheridan, Scott, and Shephard Glaciers, and up into the Rude River watershed to the southeast of Rude Lake. The southern extent of the anomalous W distribution corresponds fairly closely to the southern boundary of the low pressure-high temperature metamorphic mineral assemblage (categories D and E) of Miller and others (1984) just south of the Chugach metamorphic complex. The Orca Group rocks within this portion of the Prince William terrane are the most highly metamorphosed units within the accreted terrane. Because scheelite solubility begins to become significant at temperatures of about 300–350° C (Foster, 1977), this is the one part of the Orca Group where widespread W migration into scheelite-bearing quartz veins is likely. Much of the remainder of the Orca Group has only been regionally metamorphosed to subgreenschist facies, and therefore a metamorphic fluid phase capable of leaching significant W from the sedimentary pile did not develop.

3. Central Sulfide Belt

The higher elevations of the Cordova quadrangle, to the west of the Copper River, define an extensive region that contains anomalous amounts of base metals in concentrate samples (fig. 6, pl. 1). Samples with elevated concentrations of Fe (≥ 10 percent), Co (≥ 100 ppm), Cu (≥ 200 ppm), and Ni (≥ 150 ppm) are derived from both metavolcanic and interbedded metasedimentary rocks on both sides of the Contact fault system. Pyrite and chalcopyrite are abundant in most samples, and slates and metavolcanic rocks with lenses and disseminations of Fe- and Cu-sulfides are common throughout much of the region. Also, quartz veins within shear zones commonly contain the same sulfide minerals. Whereas none of the known sulfide occurrences within this large belt have any recorded production, the previously discussed Midas mine lies on the Valdez quadrangle, about 1.5 km northwest of the edge of this belt.

Concentrate samples within this large sulfide-rich belt are also commonly anomalous in Ag, As, and Pb. Samples with elevated Pb values (≥ 300 ppm), which reflect observed concentrations of galena, cluster throughout the western and central portions of the belt. Only samples from the upper reaches of Simpson Creek and the Gravina River lack anomalous Pb contents. Galena has been observed in outcrop in pyrite-bearing quartz fissure veins in the headwaters of the Rude River drainage system, north of the Gravina fault. Further to the east, concentrate samples that contain anomalous amounts of Fe, Co, Cu, and Ni, near Woodworth, Schwan, Heney, Allen, Childs, and Grinnell Glaciers, show only background Pb values.

Concentrate samples with anomalous As concentrations (≥ 500 ppm) within the sulfide-rich belt are associated with metasedimentary and metavolcanic rocks between Wortmanns Glacier and upper Solomon Gulch (just south of the Midas mine), near Rude Lake and Cordova Glacier, throughout the upper Rude River watershed, from lower Scott Glacier south to the Siamese Lakes, and near Shiels and McCune Glaciers. None of the volcanogenic massive sulfides within the Prince William Sound region have been recognized to contain arsenopyrite; the arsenopyrite is thus believed to have been weathered from the widespread quartz fissure veins. Within the more heavily prospected regions of Prince William Sound such epigenetic veins have commonly been noted to contain arsenopyrite.

This extensive central sulfide belt, distinguished by its abundance of Fe- and (or) Cu-sulfide minerals, is best delineated using the concentrate-sample medium. However, absolute concentration values from the concentrate samples are often difficult to evaluate on a comparative basis. For example, there may be little meaningful difference between a concentrate sample with 10 percent Fe and 50 percent Fe. The latter may simply indicate that relatively fewer accessory heavy minerals occur within a given sampled watershed and therefore the sulfide minerals will make up a larger portion of the heavy-mineral fraction. This does not necessarily imply the presence of a greater concentration of pyrite within the

latter watershed. Thus, whereas the concentrate samples delineate this entire sulfide-rich region, absolute stream-sediment concentration values within the region may better target the strongest anomalies.

Between Solomon Gulch and Wortmanns Glacier (fig. 10 on pl. 2), Mg, Cr, and Ni anomalies in sediments cluster in three areas. Three samples (169, 196, 198) at the head of Solomon Gulch contain anomalous Mg (3–10 percent), Ca (5 ppm), Cr (300–1,000 ppm), and Ni (100–150 ppm). Similarly, four samples (163, 164, 165, 167) along Brown Creek contain anomalous Mg (10 percent), Cr (500–1,500 ppm), and (or) Ni (100–150 ppm), and three samples (173, 174, 781) in the center of Wortmanns Glacier contain anomalous Mg (3–5 percent), Cr (200–500 ppm), and Ni (100 ppm). These anomalies most likely define areas underlain by the more mafic phases of the volcanic rocks within this portion of the Valdez Group. However, two sites indicate a high geochemical favorability for the concentration of base-metal sulfides. Sediment sample 781, taken near the head of Wortmanns Glacier, contains 180 ppm Zn, in addition to 3,000 ppm Mn, 500 ppm Cr, 100 ppm Ni, and detected, but <0.5 ppm, Ag. Sediment sample 161, taken below the furthest west glacier at the head of Brown Basin contains 200 ppm Pb, and the corresponding concentrate sample contains 0.7 percent Pb.

A number of sediment samples on the eastern side of the central sulfide belt are highly anomalous in Ca, Co, Cu, Cr, and Ni, and are derived from both metasedimentary and metavolcanic rocks within the Valdez Group. Moraine sediments eroded off Mt. Williams and Mt. O'Neel (fig. 11 on pl. 2) consistently contain 3–5 percent Ca, 200 ppm Cr, 150–1,000 ppm Cu, and 100 ppm Ni. The relative abundance of chalcopyrite in corresponding concentrate samples, abundant float with disseminated pyrite and chalcopyrite, and a few known sulfide occurrences in the area (C10–C12; Jansons and others, 1984) indicate a high geochemical favorability for additional Fe- and Cu-sulfide occurrences. Anomalous Cu (150–300 ppm), Mg (3–5 percent), Ca (3–5 percent), and Ni (100 ppm) within sediments throughout the Heney Glacier system (fig. 11 on pl. 2) may simply reflect high background values for mafic volcanic rocks; none of the anomalous sediment samples have corresponding concentrate samples with microscopically visible chalcopyrite. Similarly, anomalous Mg (5–7 percent), Ca (5–7 percent), Co (100 ppm), Cr (200–700 ppm), and Ni (100–150 ppm) in sediments from moraines across Allen Glacier (fig. 11 on pl. 2) reflect local lithogeochemical background. Further west however, across the drainage divide and within the upper Rude River watershed (fig. 12 on pl. 2), two sediment samples (461, 462) contain 3 percent Mg, 70–100 ppm Co, 200–500 ppm Cu, 100 ppm Ni, and 70–100 ppm Pb. Corresponding and surrounding concentrate samples are enriched in Fe, Ag, As, Ba, Bi, Cu, and Pb, and thus these two sediment samples may define an area that is rich in base-metal sulfides.

A number of other small base-metal anomalies stand out in the central sulfide belt. One sediment sample (547), which contains 200 ppm Cu, 100 ppm Ni, and 250 ppm Zn, with 2,000 ppm Cu in the corresponding concentrate sample, is derived from mixed metavolcanic and metasedimentary rocks on the western side of the easternmost branch of Woodworth Glacier (fig. 13 on pl. 2). The sample site lies 2 km east of shear zones in metavolcanic rocks that are known to contain thin veins of chalcopyrite (C13; Jansons and others, 1984). Two samples with Zn concentrations of 200 and 210 ppm (461 and 832, respectively) were collected from localities to the southwest and southeast of Cordova Peak (fig. 12 on pl. 2). One of these samples (461) and two nearby concentrate samples (511, 512) with sphalerite are from streams that drain moraines derived from the divide on the northern side of the northwestern branch of Scott Glacier. Metasedimentary nunataks on the glacier host Fe-Cu-Zn massive sulfide pods. Within the Scott Glacier basin itself, and continuing south to creeks entering into Scott Lake, Cu and Zn values are anomalous in many of the sediment samples. Corresponding concentrates contain sphalerite and show anomalous values for Ag, As, Cu, Co, Fe, and Ni, and locally for Pb (438, 448, 600, 609, 610; fig. 14 on pl. 2). Sediment-sample sites with 3–5 percent Ca encircle the Shephard Glacier–upper Power Creek–Snyder Mountain region, to the northeast of the town of Cordova. This obviously reflects the high percentage of volcanic rocks with various Ca-bearing minerals in this area. However, in addition to anomalous contents of Fe, Co, Cr, Cu, and Ni in both sediment and concentrate samples in this area, Ag, Pb, and Zn contents are also anomalous in both media (fig. 15 on pl. 2). Stream-sediment samples 429 and 430, near the headwaters of Power Creek, both contain 0.5 ppm Ag.

4. Dead Creek Area

Eight concentrate samples to the south and southwest of the Brown Basin drainage divide (fig. 16 on pl. 2) are highly anomalous in As (as much as 15,000 ppm) and W (500–5,000 ppm) and less consistently in Ag and Bi. The lack of consistently anomalous values for Fe, Cu, and Ni distinguish these samples from those within the adjacent central sulfide belt which also contains samples with highly anomalous Ag, As, and Co values. It is believed that the anomalous concentrations of metals reflect disseminated and (or) quartz-vein-hosted arsenopyrite and scheelite within the Valdez Group metasedimentary rocks.

5. Ellamar

The entire Ellamar region, from Galena Bay and Silver Lake south to Landlocked Bay and Bligh Island, is delineated by the strongest Zn anomaly for sediments on the Cordova and Middleton Island quadrangles (pl. 1; fig. 17 on pl. 2). Additionally, corresponding concentrate samples from the northern half of this group of samples (793, 796–799) contain microscopically visible barite. Only two other localities on the Cordova and Middleton Island quadrangles, in drainages underlain by the younger Tertiary sediments and in the Hinchinbrook Island–Heney Range–Snyder Mountain area, contain numerous barite-rich samples. Twelve sediment samples in the Ellamar region contain 150–330 ppm Zn. Extensive occurrences of disseminated and massive base-metal sulfides are common throughout the area. Some of the anomalies are from drainages on Ellamar Mountain and southern Bligh Island, both of which lack any known mineral occurrences. At the former, however, subsequent follow-up studies (R. Goldfarb and S. Nelson, unpub. data, 1986) have identified sulfide-rich quartz veins near a large shear zone that cuts both argillite and greenstone. Selected samples contain as much as 10 percent Fe, 2 percent Pb, 2.3 percent Zn, 50 ppm Ag, 0.10 ppm Au, 61 ppm Bi, 3,000 ppm Cu, 1.1 ppm Hg, and 12 ppm Sb.

Most of the sediment samples that contain anomalous Zn values are derived from interbedded Orca Group metasedimentary and metavolcanic rocks west of the Landlock fault. These samples are also anomalous in Co (70–100 ppm), Cr, except on Bligh Island, (300–500 ppm), and Ni (100 ppm) and are less consistently enriched in Fe, Mg, Mn, and Cu. Three of the Zn anomalies however are from drainages underlain by metasedimentary Valdez Group rocks to the southeast of The Lagoon and east of the Landlock fault. No known mineral occurrences exist in this area, and sediments contain only background amounts of Co, Cr, and Ni. Whether this anomalous Zn reflects remobilization from some of the volcanogenic massive-sulfide-related mineralization across the Contact fault system is presently uncertain.

Surprisingly, the Ellamar region is only weakly delineated by base metals in the concentrate samples. Anomalous values for Fe, Cr, Ni, and Pb occur quite irregularly in the area delineated by anomalous Zn values in sediments. Chalcopyrite, locally associated with anomalous Cu and Ag values, was noted in six concentrate samples near Landlocked Bay and Billygoat Mountain, in one sample from Boulder Bay, and in one sample from Cloudman Bay on Bligh Island. The presence of neither sphalerite nor anomalous Zn characterized any of the concentrate samples, although there was anomalous Zn in corresponding sediment samples. As discussed earlier, sphalerite collected in the heavy-mineral concentrates may have been removed from the nonmagnetic fraction during magnetic separation prior to analysis or the Zn may be transported in solution and not as detrital sphalerite. Thus, Zn concentrations within sediment samples appear to best delineate the Ellamar-type base-metal resources.

The elevated Zn concentration of sediments at Ellamar, near Irish Cove, on central Hawkins Island, and in the northern part of the Heney Range, seems to indicate the presence of base-metal sulfides rather than just a high lithogeochemical background. The same mafic volcanic rocks as those which host known mines and prospects in all the above areas do not yield Zn in anomalous amounts near Mt. Freemantle, north of Galena Bay, on Hinchinbrook Island, to the south of the Heney Range, north of Eyak Mountain, and at Ragged Mountain. Thus, in the former four regions, anomalous Zn values in some of the watersheds that lack any known mineral occurrences are believed to indicate geochemical favorability for additional base-metal-sulfide occurrences.

6. Southern Port Fidalgo

The metasedimentary and metavolcanic Orca Group rocks along the southern shore of Port Fidalgo host a number of volcanogenic massive sulfide occurrences (C63, C65, C66; Jansons and others, 1984), including the relatively large Schlosser (C66) deposit. As in the Ellamar region, stream sediments with anomalous contents of Zn (150–240 ppm) best delineate geochemically favorable areas for mineral occurrences (fig. 18 on pl. 2). Samples with Zn enrichments extend from Irish Cove northeast to Whalen Bay. The most anomalous sample, on the southwestern shore of St. Matthews Bay from a drainage in metavolcanic rocks that contains no known ore mineral occurrences, also contains 500 ppm Cr. A few sediments in this area also contain anomalous As contents.

This area is also delineated by regionally anomalous Cr (200–1,000 ppm) and locally anomalous Ni (70 ppm) in most concentrates from Irish Cove to the eastern side of St. Matthews Bay. These anomalous samples are centered slightly south and east of the Zn-rich sediment samples. The Cr-Ni enrichments may reflect pyroxene and garnet grains that have made it into the nonmagnetic heavy-mineral-concentrate fraction. A few concentrate samples contain chalcopyrite and galena.

Sediment samples collected immediately southwest of the Zn anomalies and on the far end of the peninsula contain at least 5,000 ppm Mn (fig. 18 on pl. 2). Some of these samples also contain anomalous As, and corresponding concentrates contain 150–500 ppm Pb but no

microscopically visible galena. It is uncertain whether these anomalies represent man-made contamination, an accumulation of Mn-oxides, or distal, bedded Mn occurrences.

7. Snyder Mountain–Heney Range–Hinchinbrook Island

Concentrate samples that contain anomalous contents of Ba (3,000 to >10,000 ppm) extend in a belt from lower Power and Ibeck Creeks (to the south of Snyder Mountain) southwest through the entire Heney Range (fig. 15 on pl. 2) and across the eastern half of Hinchinbrook Island (fig. 19 on pl. 3). The belt continues to the southwest across Montague Island within the Seward 1°×3° quadrangle (Goldfarb and others, 1985). The elevated Ba concentrations most likely reflect abundant detrital barite (barite is microscopically visible in many of the samples) that is disseminated throughout this portion of the Orca Group metasedimentary rocks. Concentrate samples from streams that drain Orca Group rocks to the northwest and the east of this area lack any anomalous Ba. The restriction of the Ba to this portion of the Orca Group may reflect: (1) a more oxidizing environment, and (or) (2) Ba-rich fumarolic discharges associated with the more proximal volcanic sequence of this portion of the flysch section.

Sites with sediment samples that contain 10 percent Fe and 150 ppm Cu stretch continuously from the northwestern corner of the Heney Range northeast to Snyder Mountain and along lower Power and Ibeck Creeks (fig. 15 on pl. 2). Many of the corresponding concentrate samples are enriched in chalcopyrite and pyrite. The lack of anomalous Ca, Co, and Ni in either sample type, along with the widespread anomalous Ba in concentrates, distinguishes these samples from those further northeast in upper Power and Ibeck Creeks. Small copper prospects (C22, C23, C30–C37; Jansons and others, 1984) are abundant in this area. Mineralization occurs as disseminations and pods of Fe- and Cu-sulfides. Additionally, all sediment samples from streams that drain the southeastern side of Mt. Eyak and the northern and northeastern sides of the Heney Range contain 150–190 ppm Zn. Similar Zn-dominant sediment anomalies characterize the more heavily prospected Ellamar and southern Port Fidalgo regions. A number of concentrate samples throughout the Heney Range are anomalous in Pb, including sample 205 with 5,000 ppm Pb and sample 208 with 10,000 ppm Pb (fig. 15 on pl. 2). However, the lack of galena or any other microscopically visible Pb-rich mineral, plus the proximity to the town of Cordova, suggest that the anomalous Pb may be man-made contamination.

One sediment sample (584) on Nuchek Creek on Hinchinbrook Island (fig. 19 on pl. 3) is highly anomalous in Fe (20 percent), Co (100 ppm), Cr (1,000 ppm), Ni (200) ppm, and V (500 ppm) and is from a stream that partially drains a bedded Mn occurrence (C98, fig. 19 on pl. 3). The occurrence is hosted within a mudstone but is fairly close to a thick sequence of mafic volcanic rocks. Manganese is not anomalous in the sediment or in the corresponding concentrate sample; however, concentrate sample 136 from the drainage basin south of Nuchek Creek contains 3,000 ppm Mn. A broad Cr anomaly in sediments is present to the north, east, and west of sample 584, with five surrounding samples that contain 200 ppm Cr. Because no Cr-rich mineral phases are specifically associated with the Mn body, the anomalous Cr most likely reflects a local lithogeochemical enrichment of the metavolcanic host rocks. Three concentrate samples to the south of site 584 from drainages in both metasedimentary and metavolcanic units contain the only chalcopyrite noted in concentrates from the entire island. Concentrate sample 519 on the northeastern corner of the island contains 30 percent Fe, 5,000 ppm Ba, 200 ppm Co, 200 ppm Cu, 300 ppm Ni, and 700 ppm Zn, plus microscopically visible barite, sphalerite, and approximately 90 percent pyrite. The sample is derived from an area underlain by metavolcanic rocks.

8. Central Hawkins Island

The central portion of Hawkins Island, which is underlain by interbedded Orca Group metasedimentary and metavolcanic rocks, yielded a cluster of sediment samples with anomalous contents of Zn (fig. 20 on pl. 3), similar to those in the Ellamar, southern Port Fidalgo, and Mt. Eyak–northern Heney Range regions. Four samples near Canoe Passage contain 150–220 ppm Zn, and two of these contain 5,000 ppm and >5,000 ppm Mn. Three small copper prospects (C47–C49; Jansons and others, 1984) are reported in this area.

9. Sheridan Glacier

Three sediment samples (572–574) taken along the western side of Sheridan Glacier contain 1,000 ppm Cu (fig. 14 on pl. 2). This region, including the western side of Sheridan Glacier and the eastern side of Sheridan Glacier to the north of Sherman Glacier, also is strongly anomalous in Zn, with values in sediments ranging as high as 260 ppm (sample 558). Boron, Cu, and As values in concentrates within this area are in some cases anomalous. Pyrite, which is fairly ubiquitous throughout much of the Cordova and Middleton Island quadrangles, is noticeably sparse in this region; it was only detected in one-third of the concentrate samples.

The Sheridan Glacier region is underlain by both Orca Group metasedimentary rocks and Eocene felsic intrusive bodies. A small area of sediment-hosted massive sulfide occurrences between Sheridan and Scott Glaciers is known to contain massive chalcopyrite, pyrrhotite, bornite, and sphalerite (C16; Jansons and others, 1984). In addition to high Fe, Cu, and Zn values, spectrographic analyses of the ore pods show as much as 200 ppm Ag, 500 ppm Co, and 1,000 ppm Pb (R. Goldfarb, unpub. data, 1985). The highly anomalous Cu and Zn values indicate other similar zones of massive sulfide mineralization may occur to the south and east of the one known mineralized locality.

10. Ragged Mountain

Elevated Fe, Mg, Ca, Co, Cr, Cu, Ni, and V values in sediment samples form a strong anomaly surrounding Ragged Mountain in the southeastern corner of the Cordova quadrangle. Anomalous Fe values (7–15 percent) form the broadest halo, which extends to the south and east of Martin Lake. Concentrate samples lack anomalous metal values and microscopically visible sulfide minerals, except for some pyrite grains. The regional sediment anomalies are therefore believed to reflect a high, local geochemical background for the Orca Group metavolcanic rocks at Ragged Mountain.

11. Gravina Peninsula

Almost the entire Gravina Peninsula, plus the area between Parshas Bay and the mouth of Port Fidalgo, contains sediments with anomalous contents of As (fig. 21 on pl. 3). Anomalous values range from 35 ppm to as high as 190 ppm (sample 689), 200 ppm (sample 105), and 500 ppm (sample 106) As. Samples are from streams that drain both Eocene granite and Orca Group metasedimentary rocks. About half of the corresponding concentrate samples in the area contain detectable As (usually less than 1,500 ppm) and microscopically visible arsenopyrite. However, the concentrates usually contain less arsenopyrite, and therefore have lower As contents, than the concentrates from other areas in the Cordova quadrangle (Silver Glacier to Wortmanns Glacier, Sheridan and Scott Glaciers, and upper Rude River) which generally exhibit much weaker sediment anomalies. The relatively low As content of many of the concentrates on and adjacent to the Gravina Peninsula suggests that if arsenopyrite is widespread in quartz fissures, as is most probable especially along granite-sediment contacts, then it is relatively fine grained and much of it may be lost during panning.

Sediment samples from streams that drain the Tertiary granite of the Gravina Peninsula, to the south of Beartrap Bay, are also anomalous in Be (3–5 ppm), La (70–200 ppm), Mo (5–7 ppm), Pb (70–100 ppm), and Y (70 ppm). Corresponding concentrate samples, in addition to local arsenopyrite, contain abundant scheelite and rare monazite, thorite, and cassiterite, and as much as 300 ppm Bi, 2,000 ppm La, 150 ppm Nb, 2,000 ppm Sn, 1,000 ppm W, 2,000 ppm Y, and >5,000 ppm Th. These data reflect the relatively high degree of differentiation of the Sheep Bay pluton.

Additionally, five sediment samples with 25–35 ppm As and detectable Ag (<0.5 ppm), come from the area between Beartrap Bay and the East Fork of Olsen Bay Creek. Most of the sediment samples lack corresponding concentrate samples, but it is believed that the anomalous Ag and As reflect minor arsenopyrite- and perhaps Au-bearing quartz veinlets within the Orca Group metasedimentary rocks.

12. Younger Tertiary Sediments

The entire southeastern corner of the Cordova quadrangle and Kayak Island on the Middleton Island Quadrangle are underlain by the unmetamorphosed, Tertiary, neritic to bathyal Yakataga, Redwood, Poul Creek, Tokun, and Stillwater Formations and the regressive Kulthieth Formation. Sediment samples weathered from all these lithologies have high regional background contents of B (70–150 ppm) and Fe (7–10 percent) with the exception of the area to the east of Shephard Creek and Bering River where Fe concentrations range from 3 to 5 percent.

On the mainland, locally anomalous metal values mainly stretch from Dick Creek south through the Don Miller Hills. Sediments along this belt (fig. 22 on pl. 3) generally contain enrichments of Cr (200 ppm), Cu (100 ppm), Ni (70 ppm), and Zn (150–220 ppm). These may reflect local enrichment of base metals within the black shales of many of the formations, local concentrations of interbedded mafic volcanic rocks, and (or) perhaps metal enrichment due to proximity to the Redwood fault. The one sediment sample that was collected on Wingham Island (395) contains 500 ppm Cu, along with 10 percent Fe and 70 ppm Ni, and most likely characterizes a high background in the mafic volcanic source region. Sediment samples along the northeastern coast of Kayak Island (fig. 23 on pl. 3) show local Cr, Cu, Ni, and Zn anomalies similar to those along Dick Creek and in the Don Miller Hills. However, sediment samples from drainages on the eastern side of the central portion of Kayak Island also contain anomalous Mo and Ba, with one sample (021) containing 5,000 ppm Ba.

Almost the entire area underlain by the younger Tertiary sedimentary rocks weathers abundant barite into concentrate samples, with most Ba concentrations exceeding the 1 percent upper analytical detection limit (figs. 22, 23 on pl. 3). Only samples from Clear Creek (T. 17 S., R. 8 E.), lower Trout Creek, and streams that drain the Shockum Mountains lack barite, which suggests that the Stillwater and Kulthieth Formations are not the source of any of the anomalies. The barite is associated with sphalerite in concentrate samples over all parts of Kayak Island, the northern and western Don Miller Hills west to Clear Creek, near Gandil Mountain, and in the Dick Creek watershed. Analytical concentrations commonly reach or exceed 2 percent Zn. The samples that are anomalous in Zn show a good spatial correlation with the pyritic and glauconitic Poul Creek Formation. A detailed geochemical soil survey on Kayak Island suggests that much of the anomalous Zn may be associated with interbedded basaltic pyroclastic and flow rocks within the marine sedimentary rocks (Pickthorn and others, 1985).

Most concentrate samples with anomalous Zn also contain 10–30 percent Fe, 150–700 ppm Ni, and less commonly anomalous Ag, Cu, and Mo, with the anomalous Cu tied up in microscopically visible chalcopyrite. The most highly anomalous cluster of these samples drain the Poul Creek Formation on northern Kayak Island, where the samples also contain anomalous Pb and microscopically visible galena. Concentrate samples within the region north and northeast of Kushtaka Lake on the mainland, which is largely underlain by the Tokun Formation, contain 10–20 percent Fe and 150–200 ppm Ni, along with anomalous Ba, but lack any Ag, Cu, Mo, or Zn enrichments.

13. Van Cleve Glacier

Three concentrate samples (379, 617, 637) taken between Van Cleve Glacier and Van Cleve Lake contain 100–500 ppm Co (fig. 24 on pl. 3). Sample 617 also contains 700 ppm As, 2,000 ppm B, 1,500 ppm Cu, and 1,000 ppm Th. Sample 637 also contains 5,000 ppm As and 300 ppm Ni. Pyrite, arsenopyrite, scheelite, and chalcopyrite were noted in sample 617. Concentrate samples 605 and 615, which are from sites located slightly up glacier, do not contain microscopically visible chalcopyrite but do contain 2,000 ppm and 1,000 ppm Cu, respectively. Samples in this region are derived from both Valdez Group metasedimentary rocks and Tertiary granitic rocks.

14. Martin River Glacier

One concentrate sample (400) collected from a stream that drains a ridge underlain by Orca Group metavolcanic rocks on the northern side of the Martin River Glacier contains 20 percent Fe, 1.5 ppm Ag, 500 ppm Co, 500 ppm Ni, and 500 ppm Zn, with microscopically visible scheelite, chalcopyrite, sphalerite, and about 90 percent pyrite (fig. 25 on pl. 3). The origin of the anomaly is uncertain.

15. McPherson Glacier–Goat Mountain

Seven concentrate samples from McPherson Glacier northwest to Goat Mountain and north to Miles Glacier that were derived from Orca Group metasedimentary rocks contain 500–5,000 ppm As and abundant arsenopyrite (fig. 26 on pl. 3). Like many samples throughout the Cordova and Middleton Island quadrangles, they also contain abundant pyrite and scheelite. One concentrate sample (350) contains 500 ppm Cr and another (349) contains 100 ppm Sn, but otherwise no other anomalous element values accompany the As enrichments. Corresponding sediment samples show background concentrations for all elements, although one adjacent sample to the north of Goat Mountain does contain 500 ppm Cr. The source of the arsenopyrite is unknown but most likely is quartz fissure veins within the flyschoid units.

16. Northeastern Port Fidalgo

The most anomalous concentrate samples in Cr are from sites that stretch from Silver Lake and Fish Bay east for about 10 km and are dominantly derived from Valdez Group metasedimentary rocks cut by numerous splays of the Contact fault system (fig. 27 on pl. 3). Chromium concentrations for 15 samples range from 200 ppm to 10,000 ppm at sites 727 and 730. Many of these samples are also anomalous in Ag, As, Au, and to a lesser extent, in Pb and Sn. The two samples (732, 783) with the lowest anomalous Cr values of 200 ppm contain 500 ppm and >2,000 ppm Sn, respectively. However, the proximity of these latter two sites to popular recreational anchorages suggests that the extreme Sn anomalies reflect man-made contamination.

Some corresponding sediment samples are anomalous in As, and three samples also contain 200 ppm Cr (086), 300 ppm Cr (088), and 500 ppm Cr (727) (fig. 27 on pl. 3). The former two samples are from streams that drain, in part, an exposure of serpentinized dunite and peridotite to the northeast (Nelson and others, 1985). The latter, and most anomalous, sediment sample, which was taken below a small ridge north of Port Fidalgo, suggests the presence of additional ultramafic rocks in this region. The additional anomalous Cr

values for concentrates further west suggest the existence of other small mafic and (or) ultramafic Cr-silicate-bearing bodies in the vicinity of Mt. Denson.

17. Gravina River Watershed

The entire Gravina River watershed is strongly anomalous in Mn for both sediment and concentrate samples (fig. 16 on pl. 2). Six sediment samples, which were collected from sites along the entire river, contain at least 5,000 ppm Mn. Ten concentrate samples throughout the upper reaches of the watershed and part of the Dead Creek basin contain at least 1,500 ppm Mn, which is well above a regional background of 500–1,000 ppm Mn. Concentrate samples 108, 631, and 652 each contain at least 1 percent Mn. No other elements in either sample media are consistently anomalous along with the Mn. Lithophile elements in both sample types, plus As, B, Bi, Co, Cr, Cu, and W in concentrates, are locally present in anomalous amounts.

The Gravina River mainly drains Valdez Group metasedimentary rocks, but minor intercalated metavolcanic units also crop out in the watershed. Jansons and others (1984) reported the presence of altered, silicified felsic intrusive float that contains pyrite, chalcopyrite, and scheelite within the Gravina River system (C55). They also identified base-metal-bearing shear zones along Dead Creek (C56, C57), immediately to the northwest. Whether either of these occurrence types, or perhaps bedded Mn occurrences, are the source of the extensive anomalies is presently unknown.

18. South Fork of the Bremner River

Two sediment samples (219, 220) that were taken on opposite sides of the South Fork of the Bremner River and derived from hornblende schist of the Valdez Group contain 1,500 ppm Cr. No other highly anomalous element values occur in the sediments or in corresponding concentrates. The most likely source for the anomalous Cr contents is garnet or cordierite in the sediments derived from the relatively high grade metamorphic rocks.

NURE GEOCHEMICAL SURVEY

A regional geochemical survey was conducted over most quadrangles in Alaska by the U.S. Department of Energy as part of the HSSR (Hydrogeochemical and Stream Sediment Reconnaissance) portion of the NURE program. A total of 499 composited stream-sediment samples were collected from the Cordova quadrangle and 14 were collected from the Middleton Island quadrangle. Each sample was dried, sieved to minus-100 mesh, and analyzed by delayed neutron counting for U; energy dispersive X-ray fluorescence for Ag, As, Bi, Cd, Cu, Nb, Ni, Pb, Se, Sn, W, and Zr; and instrumental neutron activation analysis for Al, Au, Ba, Ca, Ce, Cl, Co, Cr, Cs, Dy, Eu, Fe, Hf, K, La, Lu, Mg, Mn, Na, Rb, Sb, Sc, Sm, Sr, Ta, Tb, Th, Ti, V, Yb, and Zn. The resultant analytical data are tabulated in a report by the U.S. Department of Energy (1981).

The distribution of the NURE samples was strongly biased towards sites along the Copper River and the Gulf of Alaska coastline. No samples were taken within the more inaccessible regions of the Cordova quadrangle, especially from Meteorite Mountain east to Heney Glacier and south up to the high elevations of the Chugach Range, within the Allen, Scott, Sheridan, and Childs Glacier systems, and to the east of the Copper River from Wernicke Glacier south to McPherson, Johnson, and Martin River Glaciers. Samples were apparently collected only at the more accessible locations, with little attempt to avoid possible man-made contamination. For example, sample 444067, with the highest Cu (297 ppm) and Zn (540 ppm) concentrations in the NURE database, appears to have been collected just across the road from the Cordova airport and below a large garbage dump. Additionally, many of the coastal sample sites were within sloughs in the Copper River delta muds and therefore provide no information specific to individual watersheds within the study area.

Table 5 lists the number of qualified samples and minimum, median, 90th, 95th, and 97.5th percentile, and maximum values for each element determined in the NURE survey of the Cordova and Middleton Island quadrangles. The U and U/Th data provide the most useful information not readily apparent from our survey. The Sheep Bay pluton represents the most uraniferous intrusive body on the studied quadrangles. NURE sediment samples from streams that drain the granite usually contain U concentrations of 6–35 ppm (fig. 21 on pl. 3), and U/Th ratios locally exceed 1.0. A radiometric survey of the Cordova quadrangle (U.S. Department of Energy, 1978) indicated a preferred equivalent uranium anomaly just north of Sheep Bay. As stated earlier, our survey identified monazite and thorite in concentrate samples from the Gravina Peninsula that obviously contributed to the anomalous U concentrations. Scintillometer readings as high as 375 cps identified some of the more radioactive granitic outcrops. Delayed neutron activation analysis of four sampled outcrops showed Th values of 20–29 ppm and U values of 5.9–8.0 ppm (R. Goldfarb, unpub. data, 1984).

Table 5. Statistical summary for 499 NURE sediment samples

[All values in parts per million]

Element	L[1]	Minimum	Median	90th percentile	95th percentile	97.5th percentile	Maximum
U	0	0.52	2.74	4.45	5.69	8.33	48.12
Ag.....	494	5L	5L	5L	5L	5L	6
Bi.....	491	5L	5L	5L	5L	5L	11
Cd.....	492	5L	5L	5L	5L	5L	9
Cu.....	1	10L	41	74	84	113	297
Ni.....	72	15L	26	44	50	58	217
Pb.....	221	5L	5	11	12	14	60
Sn.....	485	10L	10L	10L	10L	10L	48
W	473	15L	15L	15L	15L	17	46
As.....	60	5L	12	31	46	60	492
Se.....	494	5L	5L	5L	5L	5L	5
Zr.....	0	36	152	281	412	568	5,503
Al.....	1	20,130	68,080	79,000	81,960	84,420	94,640
Au.....	499	.05L	.09L	.12L	.15L	.13	6.0
Ba.....	52	171L	636	945	1,027	1,185	9,134
Ca.....	9	1,187L	18,790	40,280	49,070	55,210	78,050
Ce.....	9	9L	56	83	93	107	501
Cl.....	396	98L	141L	732	1,504	2,661	18,730
Co.....	14	0.1L	15	26	30	34	103
Cr.....	17	9L	81	131	154	189	1,004
Cs.....	360	1.1L	2.3L	3.8	4.4	5.2	13
Dy.....	16	2.0L	4.0	5.0	6.0	8.0	53
Eu.....	18	0.3L	1.3	1.6	1.8	1.9	4.6
Fe.....	0	13,040	41,810	60,640	68,960	87,040	223,300
Hf.....	19	1.8L	5.5	12	18	20	256
K.....	53	3,737L	12,960	18,020	20,080	23,190	30,260
La.....	31	4L	27	38	47	54	254
Lu.....	38	0.1L	0.3	0.5	0.6	0.7	4.6
Mg.....	22	2,187L	10,890	16,660	18,350	20,500	47,280
Mn.....	0	125	818	1,524	2,059	2,715	60,080
Na.....	0	5,435	20,710	28,420	31,330	35,070	50,070
Rb.....	419	24L	48L	73	84	88	147
Sb.....	508	1L	2L	3L	4L	4L	5
Sc.....	0	4.9	17	23	25	29	53
Sm.....	12	0.6L	4.5	6.5	7.3	9.0	50
Sr.....	470	203L	344L	515L	594	630	964
Ta.....	506	1L	1L	2L	3L	3L	3
Tb.....	487	1L	1L	2L	2	2	7
Th.....	13	1.7L	6.8	11	14	19	89
Ti.....	13	823L	4,009	5,207	5,712	6,171	33,550
V	3	29	127	172	189	218	983
Yb.....	118	1.3L	3.1	4.6	5.4	6.2	44
Zn.....	334	10L	64L	163	189	212	540

[1]Number of samples qualified with a "less than."

Two other areas with smaller clusters of U anomalies were identified from the NURE data. Four sediment samples along the South Fork of the Bremner River contain 6–30 ppm U, as much as 89 ppm Th (sample 444197), and anomalous concentrations of many of the rare-earth elements (fig. 28 on pl. 3). Enrichments of these elements most likely indicate the presence of monazite, apatite, allanite, and other accessory minerals

common to the silicic, felsic igneous rocks within the high-grade metasedimentary rocks of the Valdez Group to the east of the Copper River. On the northern side of Galena Bay in the northwestern corner of the Cordova quadrangle, three samples (444003, 444004, 444008) contain 4–9 ppm U (fig. 17 on pl. 2) with background Th values of 4.5 ppm or less. The source of the anomalous U in this area, which is underlain by metavolcanic and metasedimentary rocks of both accretionary flysch sequences, is presently unknown.

Thirteen of the NURE samples contain 0.13–6.04 ppm Au. The majority of these samples with anomalous Au also contain anomalous Th which is known to interfer with Au during neutron activation analysis (D. Broxton, oral commun., 1982). Six of the samples, though, probably represent true anomalies. Two of these lie on Dead Creek (443886, 443888) and also contain enrichments of As, Cu, Cr, Ni, and W (fig. 16 on pl. 2). These two sediment samples, from streams that drain Valdez Group metasedimentary rocks, reflect the same anomalies as displayed by our concentrate samples from the Dead Creek area (see above, anomalous area 4). One sample (444085) on the southern side of Port Fidalgo, between Irish Cove and the Schlosser mine, contains 0.41 ppm Au, 36 ppm As, and 296 ppm Cu (fig. 18 on pl. 2). The Au is believed to be contained within sulfide grains that are being weathered from volcanogenic massive sulfide occurrences, which were discussed above in anomalous area 6. Two samples near known Au-bearing quartz veins in the McKinley Lake area contain 6.04 ppm Au and 451 ppm As (443810) and 1.71 ppm Au, 492 ppm As, and 5 ppm Bi (444150) (fig. 29 on pl. 3). Sample 443911, which was taken along the northeastern shore of Eyak Lake, contains 0.4 ppm Au (fig. 15 on pl. 2).

Widespread As anomalies cluster in two localities. Samples with values of 30–60 ppm As (though 444105 in Comfort Cove contains 308 ppm As) are characteristic of much of the Gravina Peninsula, an area described earlier (anomalous area 11; fig. 21 on pl. 3). Samples with concentrations of at least 100 ppm As stretch along both sides of the highway from Eyak to McKinley Lake. The highest As concentrations in this area are for the two Au-, and probably arsenopyrite-, bearing samples near McKinley Lake (fig. 29 on pl. 3). Arsenic enrichments in samples to the east of these two samples are more difficult to decipher. Many of these samples to the east appear to have been collected from sloughs and tidal muds and often contain high concentrations of Fe. None of the concentrate samples collected in our survey from adjacent watersheds contain any microscopically visible arsenopyrite. Therefore, the anomalous As contents may reflect coprecipitation of dissolved As with Fe-oxides.

Many of the NURE Cu and Zn anomalies occur in areas that were also delineated by our survey. However, many of the base-metal-rich areas defined by our study lack clusters of anomalous NURE samples (for example, central sulfide belt, Ellamar, southern Port Fidalgo, Sheridan Glacier, and Van Cleve Glacier). NURE samples with anomalous Cu values, usually between 100 ppm and 200 ppm and with no other anomalous elements, are associated with the greenstones northeast of the town of Cordova, especially near Mt. Eyak, Mt. Kelly, Power Creek, Scott Glacier, and Ibeck Creek. Additionally, two other samples on Power Creek (443905, 443906) both contain 30 ppm Pb, which is a highly anomalous concentration for the NURE data (fig. 15 on pl. 2). Three samples along Dead Creek (443885, 443887, 443888) contain 87–95 ppm Cu along with anomalous Au and W (fig. 16 on pl. 2), in contrast to our survey which found only background amounts of Cu in the Dead Creek area (anomalous area 4). Zinc concentrations of 200–250 ppm (fig. 15 on pl. 2, fig. 20 on pl. 3) are associated with five NURE sites in the Heney Range and two sites to the west on northern Hawkins Island (anomalous area 7).

Two samples to the south of Saddlebag Glacier (443966, 444151) contain 217 ppm and 231 ppm Zn, respectively, and might reflect unrecognized massive sulfide occurrences within Orca Group metasedimentary rocks (fig. 29 on pl. 3). Sample 443784, which was taken from a stream that drains the eastern side of the Don Miller Hills, contains 521 ppm Zn along with 217 ppm Ni and 343 ppm Cr (fig. 22 on pl. 3), which is representative of the most anomalous Zn value from either our study or the NURE survey for a sediment derived from the younger Tertiary sediments. These two Zn-dominant anomalies are the only significant base-metal enrichments identified by the NURE survey and not evident from our study.

The major Cr and Mn anomalies defined by our study were also identified, though less strongly, by the NURE samples. Two samples that were taken from streams that drain the east-central side of Hinchinbrook Island just over the divide from the bedded Mn deposit (Goodfellow and others, 1984) contain 552 ppm Cr, 3,737 ppm Mn, and 22 percent Fe (444244) and 327 ppm Cr and 11 percent Fe (444245) (fig. 19 on pl. 3). Sample 444255, which is from a site actually on Nuchek Creek and within the mineralized watershed, contains 14 percent Fe and 3.4 percent Ti (fig. 19 on pl. 3). All three of the sediments are strongly enriched in most of the rare-earth elements. Two samples (443880, 443882) on the Gravina River contain 1.89 percent Mn and 3,765 ppm Mn, respectively, and one adjacent sample (443888) on Dead Creek contains 3,154 ppm Mn (fig. 16 on pl. 2). This is within the same area (anomalous area 17) that is defined by Mn anomalies in both sediment and con-

centrate samples from our survey. Chromium values in NURE sediments of 341 ppm (444061) just below the known ultramafic outcrop and 261 ppm and 264 ppm (444059 and 444060, respectively) further down drainage occur near Cr anomalies in the northeastern Port Fidalgo region (anomalous area 16; fig. 27 on pl. 3).

A few Cr and Mn single-site anomalies in the NURE data may identify additional areas of interest that are not evident from our survey. One sample (443737) in the mudflats to the northwest of Ragged Mountain contains more than 6 percent Mn along with 102 ppm As and 48 ppm W. Another sample (444305), which was taken along the Martin River slough, contains 3,511 ppm Mn. Both of these highly anomalous samples are believed to reflect a highly reducing depositional environment rather than enrichments in source rocks. Sample 443777, along Strawberry Harbor, contains 6.1 percent Ca, 2.08 percent Ti, 1,004 ppm Cr, and 4,873 ppm Mn, along with elevated concentrations for all rare-earth elements (fig. 22 on pl. 3). These values might reflect either (1) contamination from nearby, past oil development and (or) high-tide debris; or (2) an enrichment of these elements within concretions in the Tokun Formation. Sample 444119, from a stream that drains Orca Group metasedimentary rocks on southern Hawkins Island, contains 2.06 percent Mn and 103 ppm Co and may indicate an additional region with massive sulfide-related metal enrichments in the flysch (fig. 20 on pl. 3).

Three NURE samples that were collected on Kayak Island (fig. 23 on pl. 3) indicate Ba and Zn enrichments within a region also identified by our survey (anomalous area 12). Samples 443759 and 443760 contain 9,134 ppm and 5,115 ppm Ba, respectively. The former also contains 6 ppm Ag, 46 ppm As, 319 ppm Cr, and enrichments of many of the rare-earth elements. Both sites are on streams that drain Poul Creek and Yakataga Formation rocks on the west-central side of the island and may define the most favorable area for bedded barite occurrences on the island. Sample 444767, which was collected on the opposite side of the island, contains 277 ppm Zn and probably reflects an enrichment of sphalerite.

CONCLUSIONS

The U.S. Geological Survey's geochemical survey of the Cordova and Middleton Island quadrangles has identified regions of geochemically favorable ground for the presence of metallic mineral occurrences. Anomalous Au contents of concentrate samples indicate that Au-bearing quartz veins are probably widespread throughout the medium-grade metamorphic rocks of the Valdez Group; the size, density, and therefore economic significance of such veins are uncertain. Iron, Co, Cu, and Ni anomalies in concentrates show that sulfide minerals are widespread within Valdez Group and Orca Group rocks over much of the central portion of the Cordova quadrangle. Whether these all occur as uneconomic disseminations or whether massive sulfide bodies similar to the nearby Midas mine orebody are present in the area is also uncertain. Elevated Zn concentrations in sediment samples provide the broadest haloes for identification of massive sulfide bodies in the Ellamar, southern Port Fidalgo, northern Heney Range, central Hawkins Island, and Sheridan Glacier regions. Many of the samples were collected from watersheds that are near known volcanogenic massive sulfide occurrences even though the watersheds themselves lack any such known mineral occurrences. Widespread Ba and Zn anomalies in concentrates derived from the younger Tertiary sedimentary formations indicate the possibility for sediment-hosted base-metal mineralization within the southeastern corner of the study area.

Interpretation of the geochemical data clearly indicates the necessity for collecting heavy-mineral-concentrate samples during geochemical surveys of this region. Even where the lower determination limits and greater accuracy of atomic absorption spectrophotometry were used for sediment samples, most of the areas identified as anomalous by emission spectrography of concentrate samples were still not apparent for the sediment medium. This was especially true for Au-rich concentrate samples; very few corresponding sediment samples contained anomalous Au or As as determined by atomic absorption spectrophotometry. A biased sample distribution, analytical interference problems, and the above stated need for concentrating a large sediment volume prior to analysis severely limit the usefulness of the NURE geochemical data. Whereas most anomalies identified from the NURE survey were also apparent from our survey, most of the anomalies delineated by our survey would not have been found by the NURE study. Hence, we believe the NURE geochemical surveys should be used only to supplement Alaska Mineral Resource Assessment Program or similar surveys, rather than in lieu of such surveys.

REFERENCES CITED

Capps, S.R., and Johnson, B.L., 1913, Mineral deposits of the Ellamar district: U.S. Geological Survey Bulletin 542–D, p. 86–124.

Cobb, E.H., 1972, Metallic mineral resources map of the Cordova quadrangle: U.S. Geological Survey Miscellaneous Field Studies Map MF–392, scale 1:250,000.

Cobb, E.H., 1979, Summary of references to mineral occurrences (other than mineral fuels and construction materials) in the Cordova quadrangle: U.S. Geological Survey Open-File Report 79–973, 74 p.

Cohen, A.C., 1959, Simplified estimates for the normal distribution when samples are singly censored or truncated: Technometric, v. 1, no. 3, p. 217–237.

Dumoulin, J.A., 1987, Sandstone composition of the Valdez and Orca Groups, Prince William Sound, Alaska: U.S. Geological Survey Bulletin 1774, 37 p.

Fisher, R.A., 1959, Statistical methods for research workers: New York, Hafner Publishing Co., 356 p.

Foster, R.P., 1977, Solubility of scheelite in hydrothermal chloride solutions: Chemical Geology, v. 20, p. 27–43.

Fyfe, W.S., and Kerrich, R., 1984, Gold—Natural concentration processes, *in* Foster, R.P., ed., Gold '82—The geology, geochemistry, and genesis of gold deposits: Geological Society of Zimbabwe Special Publication No. 1, p. 99–128.

Goldfarb, R.J., Leach, D.L., Miller, M.L., and Pickthorn, W.J., 1986, Geology, metamorphic setting, and genetic constraints of epigenetic lode-gold mineralization within the Cretaceous Valdez Group, south-central Alaska, *in* Keppie, J.D., Boyle, R.W., and Haynes, S.J., eds., Turbidite-hosted gold deposits: Geological Association of Canada Special Paper 32, p. 87–105.

Goldfarb, R.J., Tripp, R.B., and Smaglik, S.M., 1985, Geochemical map showing distribution of barite, galena, and sphalerite within the Chugach National Forest, Alaska: U.S. Geological Survey Miscellaneous Field Studies Map MF–1645–C, scale 1:250,000.

Goodfellow, Robert, Nelson, S.W., Bouse, R.M., and Koski, R.A., 1984, The geologic setting and composition of a newly discovered manganese deposit on Hinchinbrook Island, Alaska: U.S. Geological Survey Open-File Report 84–671, 9 p.

Grimes, D.J., and Marranzino, A.P., 1968, Direct current arc and alternating current spark emission spectrographic field methods for semiquantitative analysis of geologic materials: U.S. Geological Survey Circular 591, 6 p.

Henley, R.W., Norris, R.J., and Paterson, C.J., 1976, Multistage ore genesis in the New Zealand geosyncline—A history of post-metamorphic lode emplacement: Mineralium Deposita, v. 11, p. 180–196.

Hudson, Travis, and Plafker, George, 1982, Paleogene metamorphism of an accretionary flysch terrane, eastern Gulf of Alaska: Geological Society of America Bulletin, v. 93, p. 1280–1290.

Jansons, Uldis, Hoekzema, R.B., Kurtak, J.M., and Fechner, S.A., 1984, Mineral occurrences in the Chugach National Forest, southcentral Alaska: U.S. Bureau of Mines, Mineral Land Assessment Report 5–84, 43 p., 2 map sheets.

Johnson, B.L., 1915, The gold and copper deposits of the Port Valdez district: U.S. Geological Survey Bulletin 622, p. 140–188.

Miesch, A.T., 1976, Geochemical survey of Missouri—Methods of sampling, laboratory analysis, and statistical reduction of data: U.S. Geological Survey Professonal Paper 954–A, 39 p.

Miller, M.L., Dumoulin, J.A., and Nelson, S.W., 1984, A transect of metamorphic rocks along the Copper River, Cordova and Valdez quadrangles, Alaska, *in* Reed, K.M., and Bartsch-Winkler, Susan, eds., The U.S. Geological Survey in Alaska—Accomplishments during 1982: U.S. Geological Survey Circular 939, p. 52–57.

Mitchell, P.A., 1979, Geology of the Hope-Sunrise (gold) mining district, north-central Kenai Peninsula, Alaska: Stanford, Calif., Stanford University, M.S. thesis, 123 p.

Moffit, F.H., 1954, Geology of the Prince William Sound region, Alaska: U.S. Geological Survey Bulletin 989–E, p. 225–310.

Nelson, S.W., Dumoulin, J.A., and Miller, M.L., 1985, Geologic map of the Chugach National Forest, Alaska: U.S. Geological Survey Miscellaneous Field Studies Map MF–1645–B, scale 1:250,000.

Nelson, S.W., Miller, M.L., Barnes, D.F., Dumoulin, J.A., Goldfarb, R.J., Koski, R.A., Mull, C.G., Pickthorn, W.J., Jansons, Uldis, Hoekzema, R.B., Kurtak, J.M., and Fechner, S.A., 1984, Mineral resource potential map of the Chugach National Forest, Alaska: U.S. Geological Survey Miscellaneous Field Studies Map MF–1645–A, scale 1:250,000.

Pickthorn, W.J., Goldfarb, R.J., O'Leary, R.M., Sutley, S.J., and Weaver, S.C., 1985, Kayak Island—Analysis of a geochemical anomaly, *in* Bartsch-Winkler, Susan, and Reed, K.M., eds., The U.S. Geological Survey in Alaska—Accomplishments during 1983: U.S. Geological Survey Circular 945, p. 82–83.

Plafker, George, 1969, Tectonics of the March 27, 1964 Alaska earthquake, U.S. Geological Survey Professional Paper 543–I, p. I1–I74.

_____ 1971, Possible future petroleum resources of Pacific-margin Tertiary basins, Alaska, *in* Future petroleum provinces of North America: American Association of Petroleum Geologists Memoir 15, p. 120–135.

_____ 1974, Geologic map of Kayak and Wingham Islands, Alaska: U.S. Geological Survey Open-File Report 74–82, scale 1:31,680.

Plafker, George, Jones, D.L., and Pessagno, E.A., Jr., 1977, A Cretaceous accretionary flysch along the Gulf of Alaska margin, *in* Blean, K.M., ed., U.S. Geological Survey in Alaska—Accomplishments during 1976: U.S. Geological Survey Circular 751–B, p. B41–B43.

Sutley, S.J., O'Leary, R.M., and Goldfarb, R.J., 1986, Analytical results and sample locality map of moraine-sediment, stream-sediment, and heavy-mineral-concentrate samples from the Cordova and Middleton Island 1° × 3° quadrangles, Alaska: U.S. Geological Survey Open-File Report 86–381, 115 p.

Thompson, C.E., Nakagawa, H.M., and Van Sickle, G.H., 1968, Rapid analysis for gold in geologic materials, *in* Geological Survey research 1968: U.S. Geological Survey Professional Paper 600–B, p. B130–B132.

U.S. Department of Energy, 1978, NURE aerial gamma-ray and magnetic reconnaissance survey, Chugach-Yakutat area, Alaska—Bering Glacier, Icy Bay, Valdez, Cordova, Mt. Saint Elias, and Yakutat quadrangles, v. 1—Narrative report: Huntington Valley, Pa., LKB Resources, Inc., Bendix Open-File Report GJBX–127 (78).

U.S. Department of Energy, 1981, Uranium hydrogeochemical and stream sediment reconnaissance of the Cordova NTMS quadrangle, Alaska: Grand Junction, Colo., Bendix Field Engineering Corp. Report GJBX 185 (81), 65 p.

Viets, J.G., 1978, Determination of silver, bismuth, cadmium, copper, lead, and zinc in geologic materials by atomic absorption spectrometry with tricaprylylmethylammonium chloride: Analytical Chemistry, v. 50, p. 1,097–1,101.

Wahrhaftig, Clyde, 1965, The physiographic provinces of Alaska: U.S. Geological Survey Professional Paper 482, 52 p.

Winkler, G.R., MacKevett, E.M., Jr., and Nelson, S.W., 1977, Stratabound iron-copper-zinc sulfide deposits, Prince William Sound region, southern Alaska, *in* Blean, K.M., ed., The U.S. Geological Survey in Alaska—Accomplishments during 1976: U.S. Geological Survey Circular 751–B, p. B44–B45.

Winkler, G.R., Miller, M.L., Hockzema, R.B., and Dumoulin, J.A., 1984, Gudebook to the bedrock geology of a traverse of the Chugach Mountains from Anchorage to Cape Resurrection: Alaska Geological Survey Guidebook, 40 p.

Winkler, G.R., and Plafker, George, 1981, Geologic map and cross sections of the Cordova and Middleton Island quadrangles, southern Alaska: U.S. Geological Survey Open-File Report 81–1164, 26 p.

☆ U.S. GOVERNMENT PRINTING OFFICE: 1989—773-047/06,013 REGION NO. 8

U.S. DEPARTMENT OF THE INTERIOR
March 3, 1849

1865

DEPARTMENT OF THE INTERIOR
U.S. GEOLOGICAL SURVEY

BULLETIN 1865
PLATE 1

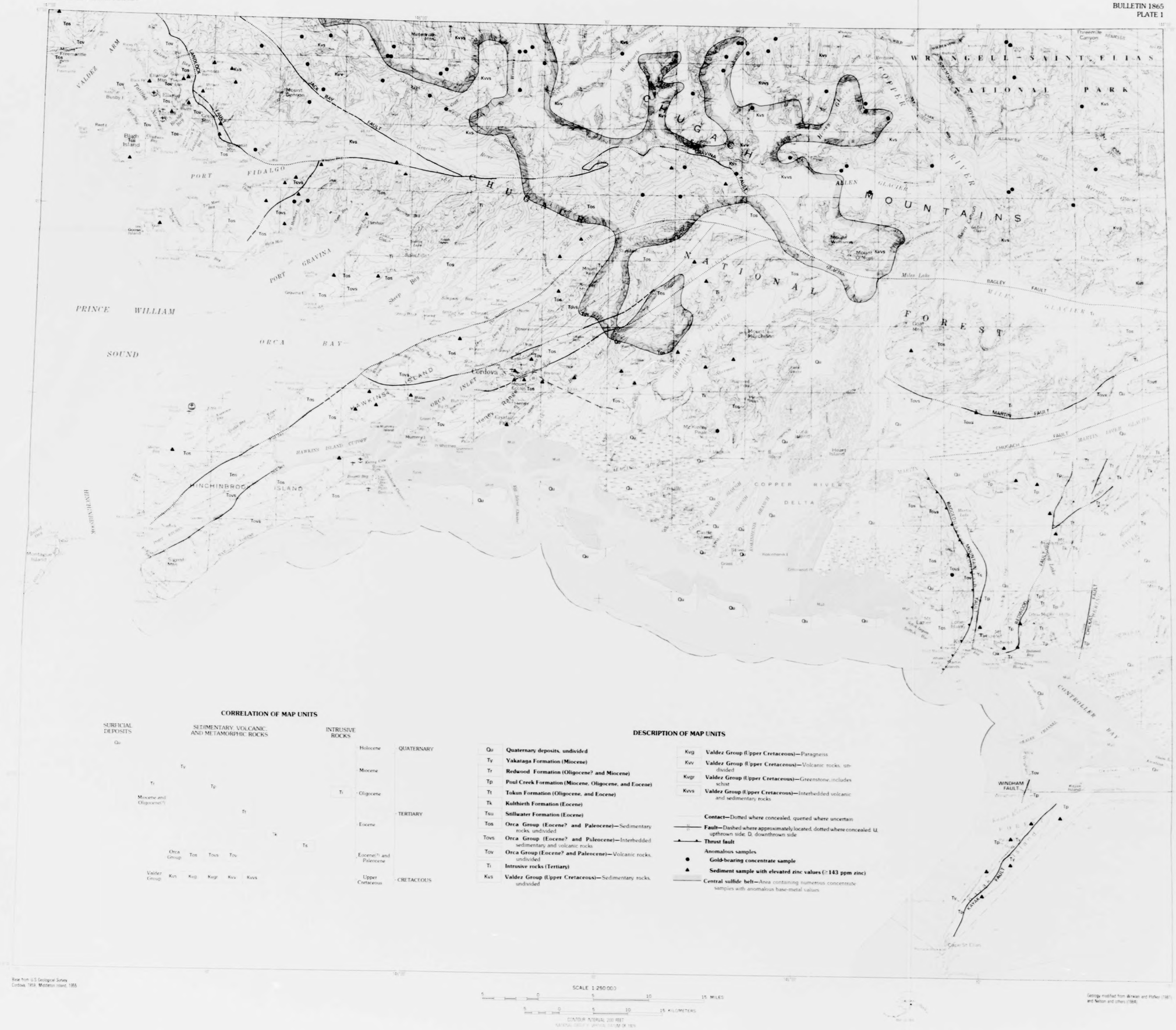

CORRELATION OF MAP UNITS

SURFICIAL DEPOSITS	SEDIMENTARY, VOLCANIC, AND METAMORPHIC ROCKS	INTRUSIVE ROCKS		
Qu			Holocene	QUATERNARY
	Ty		Miocene	TERTIARY
	Tr, Tp, Miocene and Oligocene(?)	Ti	Oligocene	
	Tt		Eocene	
	Tk, Tsu			
	Orca Group: Tos, Tovs, Tov		Eocene(?) and Paleocene	
	Valdez Group: Kvs, Kvg, Kvgr, Kvv, Kvvs		Upper Cretaceous	CRETACEOUS

DESCRIPTION OF MAP UNITS

- **Qu** Quaternary deposits, undivided
- **Ty** Yakataga Formation (Miocene)
- **Tr** Redwood Formation (Oligocene? and Miocene)
- **Tp** Poul Creek Formation (Miocene, Oligocene, and Eocene)
- **Tt** Tokun Formation (Oligocene, and Eocene)
- **Tk** Kulthieth Formation (Eocene)
- **Tsu** Stillwater Formation (Eocene)
- **Tos** Orca Group (Eocene? and Paleocene)—Sedimentary rocks, undivided
- **Tovs** Orca Group (Eocene? and Paleocene)—Interbedded sedimentary and volcanic rocks
- **Tov** Orca Group (Eocene? and Paleocene)—Volcanic rocks, undivided
- **Ti** Intrusive rocks (Tertiary)
- **Kvs** Valdez Group (Upper Cretaceous)—Sedimentary rocks, undivided
- **Kvg** Valdez Group (Upper Cretaceous)—Paragneiss
- **Kvv** Valdez Group (Upper Cretaceous)—Volcanic rocks, undivided
- **Kvgr** Valdez Group (Upper Cretaceous)—Greenstone, includes schist
- **Kvvs** Valdez Group (Upper Cretaceous)—Interbedded volcanic and sedimentary rocks

Contact—Dotted where concealed, queried where uncertain
Fault—Dashed where approximately located, dotted where concealed. U, upthrown side; D, downthrown side
Thrust fault
Anomalous samples
Gold-bearing concentrate sample
Sediment sample with elevated zinc values (≥143 ppm zinc)
Central sulfide belt—Area containing numerous concentrate samples with anomalous base-metal values

SCALE 1:250,000
0 5 10 15 MILES
0 5 10 15 KILOMETERS
CONTOUR INTERVAL 200 FEET
NATIONAL GEODETIC VERTICAL DATUM OF 1929

MAP SHOWING GENERALIZED GEOLOGY AND SAMPLE LOCALITIES FOR GOLD-BEARING CONCENTRATE SAMPLES, SEDIMENT SAMPLES WITH ELEVATED ZINC VALUES, AND CONCENTRATE SAMPLES OF CENTRAL SULFIDE BELT, CORDOVA AND MIDDLETON ISLAND 1° × 3° QUADRANGLES, ALASKA

I 19.3:

best copy available

1865

DEPARTMENT OF THE INTERIOR
U.S. GEOLOGICAL SURVEY

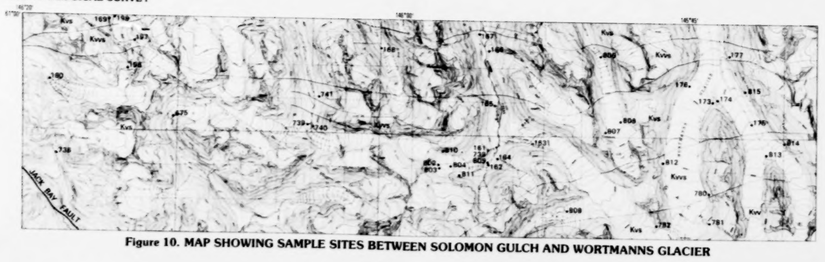

Figure 10. MAP SHOWING SAMPLE SITES BETWEEN SOLOMON GULCH AND WORTMANNS GLACIER

Tabulation for figure 10

SAMPLE SITE	SEDIMENT ANOMALIES	CONCENTRATE ANOMALIES
161	Pb(200), (Fe, Ba, Cr, V)	Fe(50), Ag(500), As(>50,000), Au(>1,000), Bi(300), Co(500), La, Nb, Ni, Pb(7,000), W(1,000), Y(1,000), Zn(2,000), (Co, Sc, V).
162	(Fe, Ba, Ni, V)	Fe(50), Ag, As(10,000), Bi(150), Co(300), La, Pb(3,000), V, Th(300), W(2,000), Y(1,500), (Ca, Sc).
163	Ni, (Fe, V)	Fe(50), Co(1,500), Nb(200), Ni(500), Zn(3,000), (Sc, V, Y).
164	Ni, (Fe, V)	Co(20), As(15,000), La(1,000), Pb, Sc, Y(700), Y(1,500), (Nb).
165	Mg(10), Cr(500), Cu(2,000), Ni, (Fe, Ca, V).	Fe(50), Co(2,000), Cu(2,000), Nb(200) Ni(1,000), Th(700).
166	(Ba, Ni, V)	Fe(50), As(10,000), B, Co(1,000), Cu(1,000), Ni(500), Pb, (Ag).
167	Mg(10), Ca(5), Cr(1,500), Cu(200) Ni(150), (Fe, Co, V).	Ca(20), Co(2,000), Cr, V, (Mg, Co).
168	Mg(5), Cr(300), Ni, (Fe, Ca, Ba, V)	Fe, As(15,000), Co(700), Cr(1,000), Pb(1,500), Zn(2,000), (Ca, Ag, V).
169	Mg(10), Ca(5), Co, Cr(1,000), Ni(150), Sc, (Fe, Mn, V).	Ca(20), (Mg, V).
173	Mg(5), Ni, (Fe, Ca, Co, Cr, Cu, V)	As(15,000), Au(50), Co(700), Cu(5,000), Ni(200), Pb(500), V, W, (Mg, Ag).
174	Mg(5), Co, Ni, As, (Fe, Ca, Cu, Cr, V).	Ag(300), As, Au(300), B, Co(500), Cu(5,000), Sn(20), Y(700), (Mo, Ni).
175	(Fe, Ni, V)	As(15,000), Pb, Th(700), (Mg, Ag, Co, Nb).
176	(Ni)	Fe, As, Co(5,000), Cu(1,500), Ni.
172	(Ni)	Co, V, (Fe, Mg, Co).
190	Ba, Sr, (Ca, Ni)	Ag, As, Au(150).
196	Ca(5), Cr(300), Ni, (Fe, Mg, Co, Cu, V).	As, Au(70), Cu(3,000), (Mn, Ag, V).
197	(Ba, Ni, V)	Nb, Sn, (Mo, La, Y).
198	Mg(10), Co(5), Cr(1,000), Ni(150), (Fe, Co, V).	Co(300), Ni, Fe, (As).
675	---	As(20,000), Nb, Th.
736	(Be)	Ag(200), As(200), Pb, Sn(50), (As, Bi, Sc).
738	As(1.5), (Be, As)	Ag(50), As(>20,000), Bi(70), Pb(2,000), Th, (Co, Sn).
739	Au, As(45)	Fe, As(20,000), Ag, Co(700), Ni, Pb,
740	As	As(50), As(>20,000), Au, Bi(100), Pb(1,500), Th, (Co).
741	---	Ag, As, Co(500), Pb, Zn(1,000), (Bi,Th).
740	Ag, Ba, (Fe, Mo)	---
781	Ca(5), Mn(3,000), Ag, Co, Cr(500), Cu, Ni, Sc, Zn(180), Cd, (Fe, Mg, Ti, V).	Ag, As(15,000), Au, Bi, Mo, Pb(1,000), Th, (Co, Nb, Sn, Y).
742	Ba, Sc, (Fe, Ti, Mn, Co)	---
802	Sr, As, (Ba)	La, Mo(10), Pb(1,000), Sc, Sn(70), Y(1,500), Th(500), (Mn, Bi, V).
803	Ba, Sr	As(15,000), Fe, Co(300), Ni, Pb(1,000), Th.
804	Ba, Sr, (Ti)	Ag, As(20,000), Ni, Pb(3,000), Fe, Bi, Co.
805	Mo(7), (Ba, As)	As, Bi, Pb, (Co, Ni, Zn, Th).
806	Ag, Mo(5), (Ba, Pb, As)	Mo, (Mg, Sc).
807	Mo(5), As(.08), (Ba)	Mg, Sc, (Cr, Sn).
808	Mo(10)	Mo(10), Sn, (Sc, Th).
809	La, Mo, As(.06), As(160)	Ag(70), As(20,000), Au(200), Bi, Mo, Pb(1,500), Th, (Co, Ni).
810	Au, As(150), (Ba)	As(20,000), (Ni).
811	(Ba)	Ag, As(100), Mo(10), Sn, (Bi, Pb, Th).
812	Co, Mo, Cd(.6), As(40), (Co, Ni, Zn)	Ag, Sc, (Mg, Sn).
813	Mo(15), As, (Ba)	(Mg, Ba, Cr, Sc).
814	Ag, Mo(7), As, (Ba, Pb)	Mo, (Co, Ni).
815	Mo(7), As(.12), (Ba)	As, Co(500), (Fe, Ag, Cu, Ni).

Figure 12. MAP SHOWING SAMPLE SITES WITHIN THE UPPER RUDE RIVER WATERSHED

Tabulation for figure 12

SAMPLE SITE	SEDIMENT ANOMALIES	CONCENTRATE ANOMALIES
481	Ag(.5), Co(100), Cu(200), Ni, Pb(100), Zn(200), Cd, (Fe, Mg, Ba).	As(15,000), B(1,000), Ba, Be(7), Bi, Cu, W(5,000), (Ca, Pb, Sb, V).
482	Ba, Co, Cu(500), Ni, Pb, (Fe, Mg, Mn, B, V).	Fe(50), Ag, Ba, Bi(50), Co(500), Cu, Ni(300), Pb(1,500).
483	(Fe, Mg, Ba, Co, Ni, V)	Insufficient sample.
481	(Cu)	Ag(50), Au(700), Ba, Bi(50), Ni, Pb(2,000), W, Th, (Fe, Mn, Cr, Cu, Nb, V).
482	(B, Cu, Ni, Pb)	Fe(50), Ag, Bi, Cu(2,000), Ni(300), Pb(2,500), (As, Co).
483	(B, Cu, Ni)	Fe(500), Ag(200), Au(700), Bi(50), Cu, Ni(500), Pb(2,000), (Co).
484	(B, Cu)	Fe(50), Bi, Ni(300), Pb, (Co).
485	(Cd)	Mg, Mn, As(>20,000), Bi, Cu, V, (Ca, Co, Cr, Pb).
486	---	As, Bi, Ni, W, (Fe, Sc, Th).
487	(Ba)	W, Th, (Bi).
488	---	Bi, Ni, Pb, (Fe).
489	(B, Ba)	Bi, Ni, Pb, (Fe).
503	---	Fe(50), Bi, Ni, Pb.
506	(Fe, Cu)	Fe(50), Bi, Ni, Pb, (Ag).
507	---	Fe(50), Ag, Au(100), Bi, Cu(2,000), Ni(300), (Co, Pb).
508	---	Fe(50), Au, Bi, Ni.
509	(Fe, Ba, Cu, Pb, Zn)	(Bi).
510	(Fe, Ba, Cu, Pb)	W, (Ni).
511	---	Ag, Cu, Ni(300), Pb, Zn(1,000) (Fe, Co, Th).
512	Pb, (Fe, B, Ba, Cu, Ni)	Zn(700).
832	Zn(210), (Ni)	Insufficient sample.

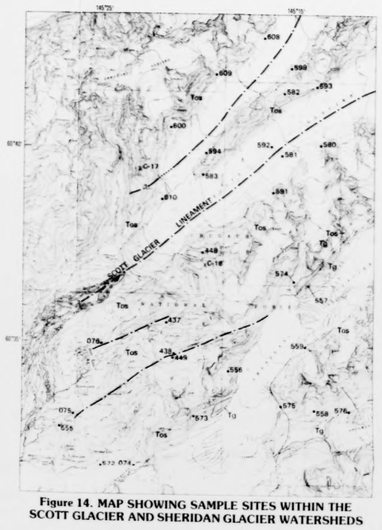

Figure 14. MAP SHOWING SAMPLE SITES WITHIN THE SCOTT GLACIER AND SHERIDAN GLACIER WATERSHEDS

Tabulation for figure 14

SAMPLE SITE	SEDIMENT ANOMALIES	CONCENTRATE ANOMALIES
674	(Ba, Pb)	Be(7).
675	Ba, (Mn, Co, Ni)	Insufficient sample.
676	Mg, (Ba)	Insufficient sample.
437	Cu, (Fe, Mg, B, Ba, Co, Ni, Pb, V)	(Ca, Be).
438	Fe, (B, Ba, Cu, Ni, Pb)	As, As(>20,000), Bi(1,000), Be, Cu(1,500), (Ca, Bi, Co, Pb, Zn).
448	Pb, (Fe, Mg, Ba, Cu, Ni)	As, As, Bi(1,000), Ni, Cu(1,000), Pb, Sb(500), Zn(700), (Fe, Co).
449	(Fe, Ba, Cu, Ni, Pb)	Be, Bi, Th, (Co, B).
555	Zn(170), (Cd, As)	---
556	Zn(190), As(45), (Co)	Bi(1,000), Be.
557	---	(Ca).
558	Zn(260), (Cu)	(Ba).
559	Co, (Fe, Cu)	W(3,000), (Nb).
572	Mn, Co, Cu(1,000), Zn(180), (Fe, Ba, Ni, Pb, Cd).	(Sb).
573	Cu(1,000), (Ba, Co, V)	---
574	Cu(1,000), (Fe, Ba, V)	Be, W.
575	(Ba)	As(10,000), Be, Bi, Th.
576	Ba, Sr, (Pb)	(Be).
580	W(300), Zn, (Ca, Ba, Co, Cu, Ni, Pb, Cd).	---
581	(Ba, Cu)	Be.
582	Ni, Pb, Zn(180), (Fe, Ba, Co, Cu, Cd, As).	---
583	(Fe, Cu)	(Fe, Ni).
591	Ba, (Fe, Cu, Ni, Pb)	W(2,000), (Be).
592	Fe, Ba, Cu, Sr, (Co, Ni, Pb)	V, (Be).
593	(Fe, Ba, Cr, Cu)	W, (Ca, Be).
596	Fe, Ba, Cu, (Mg, Ca, Co, Ni, Pb, V)	Cr(500), Ni, W(2,000), Th, (Co, Be).
599	Ba, (Fe, Ca, Mn, Co, Ni, Pb)	Be, W, (Ca).
600	Ba, (Fe, Ca, Cu, Ni, Pb)	As(>20,000), (Bi, Th).
606	(Ba, Pb)	W(2,000), (Th).
609	(Ba, Pb)	Pb, Th.
610	(Fe, Ca, Ba, Cu)	Cu(2,000), Ni(300), (Fe, Co).

KNOWN MINERAL OCCURRENCES (Jansons and others, 1984)

C16 Massive and disseminated pyrrhotite, bornite, chalcopyrite, and sphalerite.
C17 Massive and disseminated pyrrhotite, pyrite, chalcopyrite, and sphalerite.

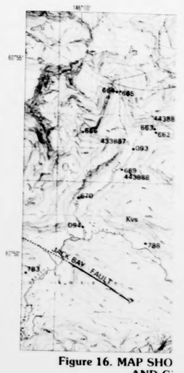

Figure 16. MAP SHO AND G

SAMPLE SITE	SEDIMENT ANOMALIES
093	(Cr)
094	(Mg, Cr)
631	(Mn, Cu, Pb)
632	(Ba, Pb)
653	La, Y, (Fe, Ca, Ba, Co, Zr
654	Fe, Co, Cu, Ni, Pb, Cd, (Mg, Ca, Mn, Ba, V).
661	---
662	W(50)
663	---
664	---
665	---
666	As(55)
667	---
668	Y, (Mn)
669	---
670	An
786	Mo(5,000), Yt(100), Zr(500)
808	Mo(10)
095	(Zr)
096	Mo(5,000)
108	Ag
109	Mo(5,000), Y
110	Mo(>5,000), Y
629	Mo, (Cu)
630	---
650	Yt(500), (Fe, B, Ba, Co, Pb
652	Fe, Yb(1), Mo(>5,000), Yt((B, Ba, Co, Pb, Zr).
783	Mo(5,000), Co(100), (Fe)

NURE SEDIMENT ANOMALIES

443885	Cu(82), W(11), As(60), (
443886	(As), Au(.19), (Bi), (M
443887	Co(90), (As),
443888	Co(45), W(40), As(53),
443889	Cd(91), W(17), Dy(11),
443882	Dy(11), Lu(.6), Mo(1,5

KNOWN MINERAL OCCURRENCES (Jans

C35	Altered felsic intrusio
C36	Shear zone containing s and acrulite.
C37	Shear zone containing p

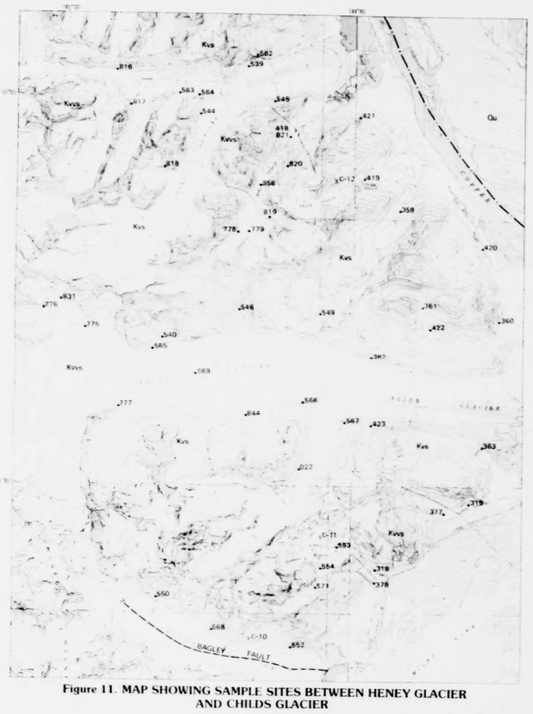

Figure 11. MAP SHOWING SAMPLE SITES BETWEEN HENEY GLACIER AND CHILDS GLACIER

Tabulation for figure 11

SAMPLE SITE	SEDIMENT ANOMALIES	CONCENTRATE ANOMALIES
022	Ag(.5), Ba, Co(100), Mo, Ni, Pb, (Ca).	Mn(1,000), Ag, (Y).
318	Ca, Co(200), Ni, Sc, (Fe, Mg, Cu, Cr, V)	Co(700), Cu(2,000), (Fe).
319	Ca	(Ca).
358	Ba, (Fe, Ca)	Insufficient sample.
359	Ba, (Fe, Pb)	As, Pb(2,000).
360	Ba, (Fe, Cu, Ni, Pb)	Ag(500), As(20,000), Au(>1,000), Bi(100), Pb(1,000), (Co).
361	(Fe, B, Ba, Pb)	Ag, Au, (Bi).
362	(Fe, B, Ba, Co, Cu, Ni, Pb)	---
363	Fe, Ca, (Co, Ni, V)	(Bi).
377	(Pb)	Ba, (Pb, Sr).
378	Fe, Mg(5), Ca(5), Cu(200), Sc, (Mn, Co, Cr, Ni, V, Zn).	Mg, Ca, Co, (Bi).
418	Ca, Ni, (Fe, Mg, Co, Cr)	Fe, Bi, Cu(3,000),
419	Au(.65), (Ca, Ba)	Ag(1,000), As(10,000), Au(>1,000), B(1,000), Bi(50), Pb(3,000), (Fe, V, Y).
420	Ca, (Mg, Cr, Cu)	B, (Y).
421	Ni, (Ba, Co, Cr, Cu)	Ag(30), Bi(50), Pb(3,000), (Be).
422	Pb, (Ba, Co, Ni, Zn)	Be, (Cr).
423	(Ba)	As, (Be).
539	---	Ca, B(2,000), (Mn, Bi, V).
540	As	Ag(100), Au(200).
544	Cu, (Mg, Ca, Co, Ni)	---
545	Cu, (Mg, Ca, Co, Ni	B(700).
546	---	---
549	---	B, (Be).
550	Cu, (Mg, Ca, Ni)	Cu, (Fe, Co, Ca, W).
552	Ca, Ni, (Fe, Mg, Co, Cu)	(Ca).
553	(Fe, Cu)	(Co, Cu).
554	Cu(200), (Ca, Ni)	(Ca, Mn, Cu).
562	Fe, Ca, Ni, (Mg, Ba, Co, Cu)	(Ca).
563	Fe, Mg(5), Ca(5), Cu(200), Ni, Sc, (Co, V).	Ag(200), Au(>1,000), V, Zn.
564	Fe, Mg(5), Ca(5), Co, Cu(500), Ni, Sc, (V).	(V).
565	(Ba, Zr, Au)	Ag, Au(50), Be(7), (Ca, Co, W).
566	Co, Cu, Ni, (Ba, B, Zn)	Ag(50), Au(200), Be(7), W, (Ca).
567	(B, Ba, Zr)	---
568	Mg(5), Ca(5), Co(300), Ni, Sc, (Fe, Co, Cr).	Mg, Mn, Cu, (Ca).
569	Fe, Mg(7), Ca(7), Co(100), Cu(300), Ni(150), Sc(70), (Cr, V).	Fe(50), Cu(1,500), Ni(500), (Be).
571	Fe, Mg(5), Ca, Co, Cu(1,000), Ni, Sc, (Cr, V).	Cu(>20,000), (Ca).
775	Ba, La, (Fe, Ca, Mn)	B, Co(1,000), Pb(1,000), (Ni, Sn, Y, Th.
776	Mg(5), Ca(7), B(150), Co, Cr(300), Ni, Sc(70), V(500), (Fe, Mn, Cu).	B(>5,000), W(2,000), (V).
777	Mg(5), Ca(5), Co(100), Cr(700), Ni, Sc(70), V(500), (Fe, Mn, Cu).	Fe(50), B(1,000), Co(1,500), Cu, Ni(500), (Zn).
778	Ag, Ba(2,000), (Ti)	B(>5,000),
779	Mg(5), Ca(7), Co, Cr(500), Ni, Sc(70), V(500), (Fe, Mn).	Fe, Co(1,500), Ni(500), (Cu).
816	Cu, Mo(7), (Co, Ni)	---
817	(Mg, Ca, Cu, Ni)	---
818	Ba, Mo(10), (Ti)	(Ba, Sc, Sn).
819	Mo(7), (Ba)	Mo(10), (Ba, Sc, Sn).
820	Mo(7), As(.16), (Cr)	Au, (B, Sc).
821	Mo	---
831	Ag, Ba(2,000), Sr, (Ca)	Mn(15,000), Ag(50), As, Au(200), B(2,000), Bi, Pb(3,000), Sn, V, Th, (Ca, Y).
844	Ba, (Ti)	Mn, (Ca, Be).

KNOWN MINERAL OCCURRENCES (Jansons and others, 1984)

C10 Disseminated pyrite and chalcopyrite in slates and greenstones.
C11 Pyrite, pyrrhotite, chalcopyrite, and malachite in shear zones.
C12 Massive pyrite and pyrrhotite and disseminated pyrite, pyrrhotite, galena, and sphalerite.

Figure 13. MAP SHOWING SAMPLE SITES WITHIN THE WOODWORTH GLACIER AND SCHWAN GLACIER WATERSHEDS

Tabulation for figure 13

SAMPLE SITE	SEDIMENT ANOMALIES	CONCENTRATE ANOMALIES
782	Mg(5), Ca(5), Ni, (Cr, Cu, V)	Mg, V, (Ca, Mo).
527	---	Fe, Bi, Co(300), Cu(2,000), Ni, (Nb, Y).
528	(Cd)	Fe, Au, Bi, Co(300), Cu, (Ag, Ni).
530	(Cu)	Bi(700), Ni, (Fe, Co, Ni, V).
531	---	Ag, As(50), Bi, Pb, W.
532	---	Ag, Au.
533	---	Ag(50), Au(200).
534	Au(.20)	Ag(50), As(200), Bi, Nb, (Y, Y).
535	(Ca, Cu)	Fe(50), Ag(100), Au(300), B(1,000), Bi(50), Co(2,000), Cu, Ni(300).
536	---	Bi, Co(1,500), Cu, Ni(300), (Fe).
537	---	Fe, Ca, Ag, Bi, Co(500), Cu(1,500), Ni, Pb(1,000).
538	(Cu)	Fe, Bi, Cu(500), Cu(10,000), Ni, (Nb, Pb).
542	---	(Ca, V).
543	Cu(300), (Fe, Co, Cd)	---
547	Cu(200), Ni, Zn(250), Cd(.04), (Fe, Co)	Pb, (Bi, Cu). Cu(2,000).
548	---	Ag(200), Au(700), (Co, Nb).
744	(Pb)	(Bi).
745	---	Sn, (Ag).
746	---	Sn, (Bi).
747	Ag, (Pb)	Cu(300).
748	---	---
749	---	---
750	---	Insufficient sample.
751	Ag, Pb, Cd(.5), (Ba, As)	Ag, Au, Co(300), (Sn, Th).
752	---	(Sn).
753	(Ca)	---
755	Ca(5), (Mg, Co, Cr, Cu)	Ba(1,500).
756	Cd, (Pb)	Cu, Mo(10), (Sn).
757	(Cd)	Cu(1,500), Sn, (Bi).
758	(Pb)	(Cu).
759	(Cd)	---
760	(Co)	Au, Sn, (Ag, Nb).
761	Ca(5), Sc, (Cr)	Co(300), (Bi, Cu).
762	Ca(5), Co, Sc, (Co)	Co(500), Cu(1,500), (Mg).
763	Ca(200), (Ca)	Cu, (As).
764	Ca(5), Cr(300), (Cu)	Sc, (Mg, B, Cr).
765	---	Sn.
767	Ag, (Pb)	---
768	---	Sn.
769	Ag, (Pb)	Ag(100), Au(250), (B, Co, Pb).
770	(Ca, Cr)	Mg, Cr.
771	(Ba)	Cu(5,000), Sc, (Ba, Sn).
772	---	Co(500), Ni, (Fe).
773	Ca	Bi(1,000).
774	(Ba, Cu, Pb)	Sn.

KNOWN MINERAL OCCURRENCES (Jansons and others, 1984)

C13 Quartz-chalcopyrite veinlets in greenstone.

EXPLANATION

Qu	**Surficial deposits**
Ty	**Yakataga Formation**
Tr	**Redwood Formation**
Tp	**Poul Creek Formation**
Tt	**Tokun Formation**
Tk	**Kulthieth Formation**
Tsu	**Stillwater Formation**
Tos	**Orca Group**—Sedimentary rocks undivided
Tov	**Orca Group**—Volcanic rocks undivided
Tovs	**Orca Group**—Interbedded sedimentary and volcanic rocks
Tots	**Orca Group**—Tuffaceous sedimentary rocks
Tg	**Granite and granodiorite**
Td	**Dacite**
Kvg	**Valdez Group**—Paragneiss
Kvs	**Valdez Group**—Sedimentary rocks undivided
Kvv	**Valdez Group**—Volcanic rocks undivided
Kvvs	**Valdez Group**—Interbedded sedimentary and volcanic rocks
Kvu	**Ultramafic rocks**
C-34	**Mine or prospect**—Number refers to description in Jansons and others (1984)
•	**Sample site (this survey)**
○	**NURE sample site**
	Contact—Dotted where concealed
	Fault—Dashed and queried where probable; dotted where concealed; U, upthrown side; D, downthrown side; arrows indicate relative lateral movement
	Lineament—Identified on aerial photograph but not on ground; possible fault

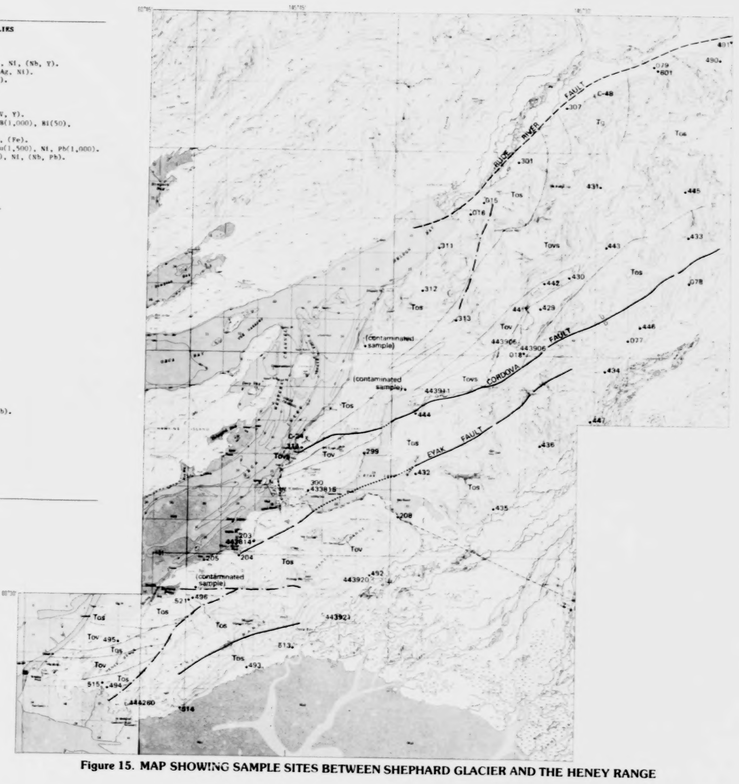

Figure 15. MAP SHOWING SAMPLE SITES BETWEEN SHEPHARD GLACIER AND THE HENEY RANGE

Tabulation for figure 15

SAMPLE SITE	SEDIMENT ANOMALIES	CONCENTRA
015	Sr, (Fe, Ca, Mn, Ni, V)	---
016	Cr(500), Ni, Sc, (Fe, Ca, Co, V)	Mg, (Cr).
016	Mn, Sc, (Fe, Ti, Ba, Co)	Sn(500),
017	(Mg, Ba, Pb)	Be(10), (Ca, Mn).
078	Sc, (Mg, Ca, Ti, Co, Cr, Cu, V)	Ce(210),
079	Mg(5), Ca(5), Co, Cr, Y(300), Cu, Sc(70), (Fe, Ti, Ni, V).	Insufficient sam
203	Fe, (Ba, Ni, V, Zn)	Mn, Sb(700), Sn,
204	Fe, Mn, Co, (Ni, Pb, V)	Mo(7,000), La, Y
205	Mn, (Co, V)	Mg(5), Bi(1,000),
208	Be(3), Sr, Zn(190), (Fe, Mn, B, Ba, Co, Ni, Pb, V).	Pb(10,000), Sn(5
299	Zn, (Mn, Co, Cu, Pb)	Ba, Pb(2,000), Sr
300	Pb, Zn(190), (Mn,Co)	Nb, Y, Th(500),
301	Fe, Mg(5), Ca(5), Co, Cr(500), Cu, Ni(150), Sc, (Mn, V).	Ce, B, Th, (Mo,
307	Co, (Fe, Ba)	Nb, Th(1,500), Y
311	Fe, Zn, (Ba, Co, Cu, Pb)	As, (Th, Pb).
312	(Fe, Ca, Ba, Co)	Nb, (Be, Sr).
313	Fe, Co, (Mg, Ca, Mn, Ba, Cu, Ni, Pb)	Bi(2,000), Sr,
314	Fe, Mn, (B, Ba, Co, Cu, Ni)	Bi(2,000), Sr, (Th).
429	Ag(.5), (Fe, Ba, Cu, Pb)	Be, (Sb).
430	Ag(.5), Cu, Pb(700), Fe, Mg, Ba, Co).	Fe, Ba, Be, Sr(1 Co, Sb).
31	Ca, Zr(500), (Fe, Mg, Co, Cu, Ni, V)	(Ca).
32	Fe, Cu, Pb, (Mg, Ba, Co, Ni, V)	Insufficient sam
33	(Co)	Cu, (Ca, Fe).
434	(B)	Ba, (Fe, Sb).
435	Pb(100), Zn, (Fe, B, Ba, Co, An)	Co, (Y).
436	(Fe, B, Ba, Co, Ni, V)	Be, Th.
441	Co, (Fe, Mn, Cu, Ni, Pb)	Ba, (Bi, Sb).
442	Fe, Co(50), Cu, Ni, Sc, (Mg, V)	Bi.
443	Fe, Ca, Cu, Pb, (Mg, Co, Ni, V)	Cd(1,500), Pb,
444	Mn, Cu, (Fe, Co, Ni, Pb, V, Zn, Cd)	Bi(2,000), Be,
445	Fe, Mg(5), Ca, Co, Cu, Ni, V)	Ce, Cu, (Be, Y)
446	Y, (Fe, Mn, Ba, Co, Ni, Pb)	Be,
447	Pb, (Fe, Mn, B, Ba, Co, Ni, As)	Be, Bi, V, (Mo,
490	(Ba)	W, Th(1,000),
491	Cu(300), (Ba)	Ba, Be, Bi, Mo(1 Sr, Th.
492	(B)	Insufficient sam
493	(Co)	Be.
494	(Cd)	(Y).
495	(Co)	Ag, Ba.
496	---	(Ba).
513	Cu, Ni, Zn(190), (Fe, Co)	---
514	(Fe, Co, Cu, Ni)	Ba, Zn, (Be).
515	Mo(5,000), Co, (Fe, B, Cu, Ni)	Cr(1,000), (Sn,
521	Zn(220), Cd, (Pb)	---
601	Fe, Ca(5), Ni(100), Sc, (Mg, Co, Cu)	Ce, Cu, Ni, (Mo,
648	Fe, Mg(5), Ca(5), Co, La, Ni, Sc, Pb, (Mn, Ba, Cr, Cu, V, Zn).	Mo(7), Ce, Cr(1,

NURE SEDIMENT ANOMALIES

443814	Al(88,250), Ce(4.5), Fe, Y(22,640), Mn(92), V, Zn(54
443815	Ce(32), Mo(2,521), Zn(211)
443905	Cu, Pb(30), Ce(31), Ca, Mn, Zn.
443906	Ce(43), (Ni), Pb(50), Co, Mn, Zn.
443911	As(.4), Ce(5.0), Eu(1.0).
443920	Rb, Zn.
443921	Ni, Yb, Zn(2223.
446260	Al, Ce(1,674), K(22,720), Mg(19,050), Na(17,050), V.

KNOWN MINERAL OCCURRENCES (Jansons and others, 1984)

C36 Chalcocite, chalcopyrite, pyrrhotite, malachite, and ma epidote veins in shear zones.

NOTE

Elements in parentheses show concentrations at the 90th level; all other elements listed exceed the 90th percentile. A centrations exceed the 95th percentile (all values in ppm ex Ca and Mg which are given in percent). Leader [ ] no data

SCALE 1:125,000
2 0 2 4 6 8 10 MILES
2 0 2 4 6 8 10 KILOMETERS
CONTOUR INTERVAL 100 FEET
NATIONAL GEODETIC VERTICAL DATUM OF 1929

MAPS AND TABULATIONS OF AREAS WITH GEOCHEMICALLY ANOMALOUS SAMPLES (FIGURES 1(CORDOVA AND MIDDLETON ISLAND 1° × 3° QUADRANGLES , ALASKA

I 19.3

best copy available

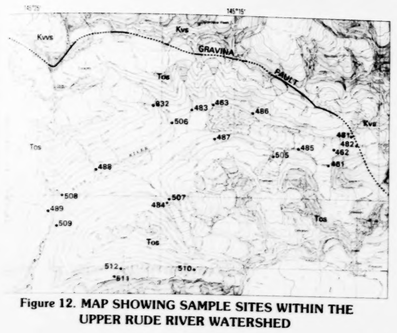
GRAVINA FAULT
Kvs
Kvs
Tos
Kvs
Tos
Tos
Tos
Tos
Tos
Kvs
Kvs
Kvv
Tos
Tos
Tos
Tos
Tos

1865

DEPARTMENT OF THE INTERIOR
U.S. GEOLOGICAL SURVEY

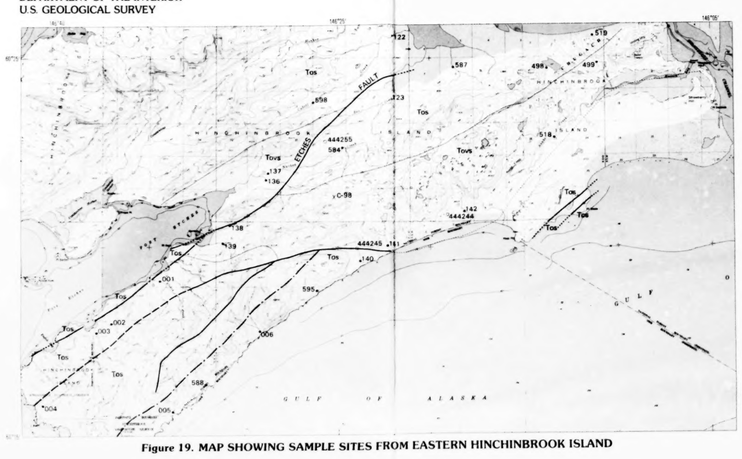

Figure 19. MAP SHOWING SAMPLE SITES FROM EASTERN HINCHINBROOK ISLAND

Tabulation for figure 19

SAMPLE SITE	SEDIMENT ANOMALIES	CONCENTRATE ANOMALIES
001	(Ti, Ba)	Ba, La(1,000).
002	(Ni)	Ba, Zn(1,500), (Ni).
003	--	Insufficient sample.
004	(Fe, Ti, Ba, Ni)	--
005	(Ti, Ba)	(Co).
006	(Fe, Ti, Ba)	(Ni).
122	--	Insufficient sample.
123	Ti(1), Sc, (Fe, Mg, Co, Cr, Ni, V)	(Mn).
136	Sc, (Ba, Ti)	Mg, Mn(3,000), (V).
137	Sc (Ba, Cr)	Mg(3), Ba,
138	--	Mg, (Mn, V, Zn).
139	(Ba)	Mg, (Cr, Co, V).
140	(Ca)	Mg, Mn, (V).
141	Sc, Y, (Mg, Ti, Mn, Co)	(Mg, Cr, V).
142	Ca, Sc, (Mg, Ti, Cr, Ni)	Mg(5).
499	(Zn)	--
499	--	--
518	(Fe)	Ba, Th, (Be, Bi).
519	Mn, Co, Cu, Zn, (Fe, Mg, Ni, Cd)	Fe, Ba, Bi, Ni(300), Zn(700), (Co).
584	Fe(20), Mg(5), Ca, Co(100), Cr(1,000), Cu, Ni(200), V(500), Y, Sc (Mn, B).	B(2,000), Ba, (Ca).
587	Fe, B(150), Ni, (Ba, Co, Cr, Cu, Ni, Pb, Zr)	Insufficient sample.
588	(Ba, Ni)	--
595	Ba, (Fe, B)	Ba, (Be, Bi, Cu, Ni).
598	Ba, (Fe, Mn, B, Co)	Ba, Mo(100), Sr(3,000), Th, (Bi).

NURE SEDIMENT ANOMALIES

444244 U(6.1, Ni(159), Sn(19), As(49), Zr(1,369), Ce(56,470), Ce(179), Co(54), Cr(552), Dy(13), Fe(223,300), Yf(51), La(160), Lu(1.2), Mg(32,730), Mo(1,737), Sc(42), Sm(20), Ta(.), Th(26), Ti(13,550), V(983), Yb(11).
444245 Ca(67,240), Cs(189), Co(48), Cr(327), Dy(10), Eu(2.0), Fe(117,800), La(85), Lu(.6), Mg(47,280), Mn(2,590), Sc(46), Sm(13), Th(21), Ti(15,930), V(402), Yb(6.1).
444255 As, Fe(139,600), Ti (14,000).

KNOWN MINERAL OCCURRENCES (Jansons and others, 1984)

C98 Manganese-rich rock.

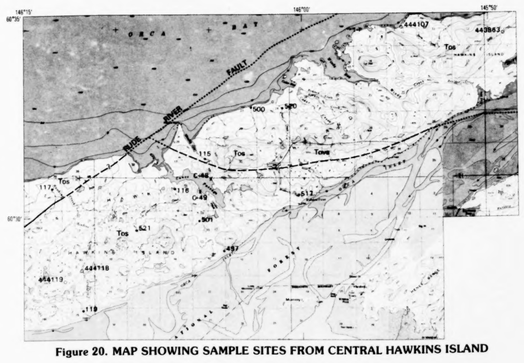

Figure 20. MAP SHOWING SAMPLE SITES FROM CENTRAL HAWKINS ISLAND

Tabulation for figure 20

SAMPLE SITE	SEDIMENT ANOMALIES	CONCENTRATE ANOMALIES
115	Fe, Mn(>5,000), Co, Sc, Y, (Cr, Ni, V)	Insufficient sample.
116	Zn, (Mn, Pb)	Insufficient sample.
117	(Ba)	Insufficient sample.
119	(Mg, Ba, Pb)	Insufficient sample.
497	(Mg)	Pb(1,000), Sn(500).
500	--	--
501	Mn, Zn(180), Cd	--
517	Mg, Mn(5,000), Co, Ni, Zn(190), (Fe, B, Ba, Cu, V)	Insufficient sample.
520	Mn	--
521	Zn(220), Cd, (Pb)	--

NURE SEDIMENT ANOMALIES

443863 Co, Pb(14), Co, Fe, Mn, Zn(20).
444107 As, Co, Ca(6.0), Fe, Mn(2,984), Rb(124), Zn(211).
444118 Zn.
444119 Co(103), Mn(20,600), Zn.

KNOWN MINERAL OCCURRENCES (Jansons and others, 1984)

C48 Pyrrhotite disseminated in greenstone.
C49 Shear zone in slate with reported anomalous copper values.

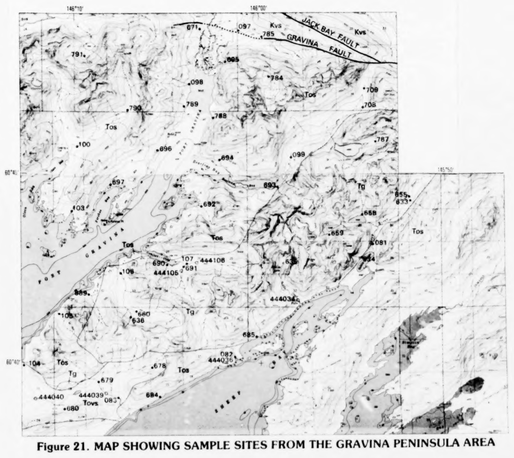

Figure 21. MAP SHOWING SAMPLE SITES FROM THE GRAVINA PENINSULA AREA

Tabulation for figure 21

SAMPLE SITE	SEDIMENT ANOMALIES	CONCENTRATE ANOMALIES
081	La(200), (Ba)	Be(10), (Ca).
082	Ca, Ag, Cr(300), Sc, (Mg, Co, Cu, Ni, V).	(Ca).
083	La, Mo(7), Y, (Mn, Co)	Insufficient sample.
097	(Ba)	--
098	(Mg, Ba, Pb)	Insufficient sample.
099	(Ba)	Be(10), (Ca, V).
100	(Ba)	Mn, La, (Mg, V).
103	Mo(5,000), Cr(300)	Insufficient sample.
104	Mn, Zn, (Ca, Co, Ni)	(Ca).
105	As(200), Mo(5), (Pb)	Insufficient sample.
106	As(500), La, Mo(7), W(50), (Pb)	Insufficient sample.
107	(Pb)	Insufficient sample.
633	(Fe, Ba, Co, Pb, Zr)	La, Y, (Ca).
634	(Fe, Ca, Ba, Co, Pb)	Ca, Th, (V).
635	(Ba, Pb, Zr)	Ca, (V).
636	Be(7), La, Pb(100), Y(100)	La(1,500), Mo(50), Nb, W, Y(2,000), (Mn). Th(>2,000).
655	Fe, Ca, Ti(1), Mn, Ba, La(200), Y(100), Zr(1,000), (Co, Cu).	Ca, V(700).
658	Be(3), La, Zr(500), As(50), (Ca, Ba)	Ca, Mn, La, (Mg,V,Y).
659	Ba, La, (Fe, Ca, Co, Cu, Zr)	Ca, B, La(1,500), Th, (Mn, V, Y).
660	Be(3), La(200), Mo(5), Y, As(90), (Ba, Zr).	Bi(300), La(2,000), Nb, Sn(>2,000), W, (Ca, V), Y, Th(2,000).
671	Zn	W.
678	Zn, (Mn, Co, Cd)	--
679	Cr(300), As, (Ni)	--
680	Mn(5,000), Sb(<1), Cd(.7)	Ag, As, Pb(1,000), Sn(70), (Bi, Th).
684	--	Insufficient sample.
685	As	B, (Th).
689	Be(3), Y, As(190), Cd	Sn(700), Th.
690	La(150)	Sn, Th.
691	La(150), As(35)	As(10,000), Sn, Th(700), (La, Pb).
692	--	(Sn).
693	As(75), (Pb)	Sn, (Th).
694	Ag, (Cd, As)	Mo, Pb, (Sn).
695	Zn, Cd(.5), As(50)	Sn(70).
696	(Cd)	--
697	Zn, Sb(2), Cd, As	--
708	--	Sn, Th.
709	Mo, As, (Zn)	(B, Be).
784	Ag, Ba, Sr	Insufficient sample.
785	Ba(2,000), Sr, (Mn)	Be(>5,000).
787	Be, La(100), Zr(700)	Cd, Sc(100), (Y, Th), Yf(1,500).
788	Ag, Ba(2,000), (Fe, Ti, Mn, Co, Cr, Ni, Pb, Y).	Insufficient sample.
789	Ag, Ba(2,000), Sb(2), As, (Ti, Mn, Bi).	Insufficient sample.
790	Ag, Ba(2,000), As, (Ti, Mn, B, Co, Cr).	Insufficient sample.
791	Ba(2,000), Sr(1,900), As(40)	Mo, W(1,500).

NURE SEDIMENT ANOMALIES

444034 U(6,5), Ni(7), W(20), Hf, Sc, Sm(8.1), Th.
444036 U(11.0), Sn(11), As(50), Hf, Sm, Th.
444039 U(18.2), Bi(5), Pb(13), As, Ce(102), Dy(12), K(24,350), La(54), Luf.8), Rb(147), Sm(12.2), Th, Th(23.4), Yb(6.8).
444040 U(7.4, Asf57).
444105 U(3.6), As(308), Ce(159), Dy(8), Eu(101,100), Laf74), Luf.8), Sm(16), Th(23), Yb(5.5).
444108 U(29.0), Ba(1,185), Ce(151), Cs(6.9), Dy(8), K(25,940), Laf46), Lu, Sm(11), Th(29), Yb(5.8), Zn.

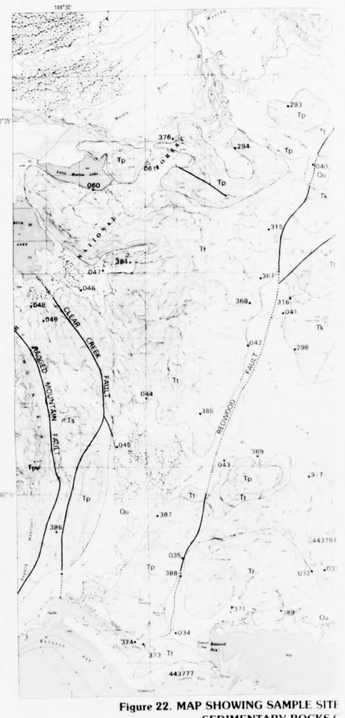

Figure 22. MAP SHOWING SAMPLE SITE
SEDIMENTARY ROCKS (

Tabulation for

SAMPLE SITE	SEDIMENT ANOMALIES	CONCENTRATE ANOMALIES
030	Ba(2,000), (Ti, Ni)	Insufficient sample.
031	Sc, (Fe, Ti, B, Mn, Ba, Co)	Insufficient sample.
032	Ag(.7), Ba(2,000), Cr(300), Mo(10), Ni, Sc, (Mg, Ti, B).	Ba, Cr(1,000), Yf(10,000).
033	Mo(5), Ni, (Fe, Ti, B, Ba, Co, V)	Insufficient sample.
034	Zn(200), (Fe, B, Ba, Ni, V)	Insufficient sample.
035	Sc, Zn(200), (Fe, Ti, B, Ba, Co, Ni, V).	Ba, Cr, Mo(5), (Ni), Sn(100), Yf(7,000), Zr(7,000).
036	Zr(500), (Ti)	La, Sc, Sr(1,500), Yf(1,500), (Y).
037	(Cd)	La, Sc, Sr(1,500), Yf(1,000), (Sb, V).
038	(Ti)	La, Y, (Sb, Sr, V).
039	(Fe, Ti, Ba)	Ba, La(1,000), Sr(2,000), Yf(7,000), (Sb, V).
040	(Fe)	La(1,000), Nb(1,000), Yf(7,000), Yf(1,000).
041	Fe, (Ti, B, Ni, V)	Zr(7,000), (Ba, Ni).
042	(Fe)	(Cd).
043	(Fe, Ti, Ba)	Insufficient sample.
044	(Fe, Ti, B)	Mo(1,000), Ba, Sb, Sc(100), Y, (Ca, Cr).
045	Ti(1), (Fe, Ba, V)	Insufficient sample.
046	Fe, (Fe, Ti, Ni, V)	Insufficient sample.
047	(Fe, Ti, Ni)	Insufficient sample.
048	Ti(1), Sc, V(500), (Fe, Co, Cu)	Ca, Ba, (Mg, V).
049	Fe, Ti(1), (Ni, V)	Insufficient sample.
060	(Fe, Ti, B, Ni)	Insufficient sample.
061	Sc, (Fe, Ti, B, Ni, V)	La, Y, (V).
062	(B, Co, Cu, Ni, Pb)	Insufficient sample.
063	Sc, (Fe, Ti, B, Ni, V)	La, Sc, (Ni, Sr, Y, V).
264	(Ba, Ni, Zr)	Ba, Sc, V, (Fe, La, Ni, Sr).
265	(Zr)	(Fe, Ni, Sr).
266	(Ni)	Nb, Sc(70), Y, (Th).
267	(B, Ni, Pb)	Ba, Ni, (Fe, Nb).
268	--	Ba, Cr, La, Sc(50), V, Th, (Nb, Sr, Y).

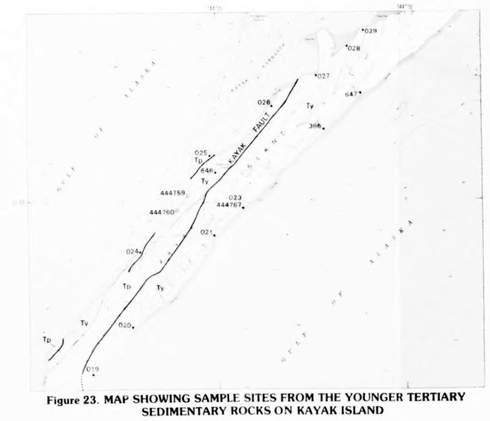

Figure 23. MAP SHOWING SAMPLE SITES FROM THE YOUNGER TERTIARY SEDIMENTARY ROCKS ON KAYAK ISLAND

Tabulation for figure 23

SAMPLE SITE	SEDIMENT ANOMALIES	CONCENTRATE ANOMALIES
019	(Fe, Ti, B, Ba, Ni)	Ba, Cd(150), Mo(10), Zn(20,000).
020	Ti(1), Ni, Zn, (Fe, B, Ba, Co)	Ba, Cd(100), Mo(10), Sr(5,000), Zn(20,000).
021	Ag(.5), Bi(150), Be(5,000), Co, Cu, Mo(20), Ni(150), Sc, Zn, (Fe, Ti, Cr).	Ba, Sn, Sr(10,000), Zn(2,000).
023	Ba, Mo(5), Ni, (Ti, B, Cu)	Ba, Mo(20), Sr(10,000), Zn(10,000).
024	Ba, Mg, Ni, Zn(1600), (Fe, Ti, B, Cu).	Ba, Cd(100), Mo(15), Sr(10,000), Zn(2,000), (Mn).
025	Zn(1900), (Fe, Ti, B, Ba, Cu)	Mn, Ba, Be(20), Cd(700), Sr(3,000), Yf(20,000), (B).
026	Ti(1), Sc, Zn, (B, Ba, Cu, Ni, V)	Ba, Sr(5,000).
027	(Ca, Zn)	Ba, Cr(500), (Nb, Sr).
028	Cr(500), Ni(150), Sc, (Fe, Ti, Ba, Co).	Ba, Cr, Sr(2,000), Zn(5,000).
029	(Fe, Ti, Ni)	Ba, Ni(1,000), Sn, (Ca, Sr).
366	(Fe, B, Co, Cr, Cu, Ni, Pb, Zr)	Fe(50), Mn, Ag, Ba, Cd(70), Cu, Mo(70), Ni(700), Sr(2,000), Zn(10,000), (Pb).
646	(Fe, B, Ba, Co, Cu, Ni, Pb, V, Cd)	(Ca, Mn, V).
647	Bi(50), Ni, Ba(2,000), Cu, Mo(5), Zn, Cd, (Fe, Co, Pb).	Ba, Mo(100), Ni(300), Sr(7,000), Zn(7,000), (Fe, Mn).

NURE SEDIMENT ANOMALIES

444759 Ag(6), Cd(5), W(15), As, Zr(493), Ba(9,134), Ce(133), Cr(319), Dy(8), Fe(68,800), Hf(24), La(81), Lu(1.2), Mn(2,842), Sc(31), Sm(8.1), Th(20), Yb(11).
444760 Ba(5,115).
444767 Ni(68), Ba(1,667), Zn(277).

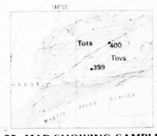

Figure 25. MAP SHOWING SAMPLE SITES
NORTH OF MARTIN RIVER GLACIER

Tabulation for figure 25

SAMPLE SITE	SEDIMENT ANOMALIES	CONCENTRATE ANOMALIES
399	Cu, Y, (Fe, Ti, B, Ba, Co, Cr, Ni, Pb).	(Zn).
400	Cu, Ni, (Fe, Cs, Ti, B, Co)	Co(500), Ni(500), Zn, (Fe, Ba, Bi).

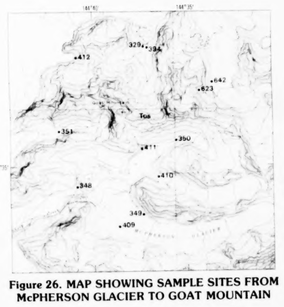

Figure 26. MAP SHOWING SAMPLE SITES FROM
McPHERSON GLACIER TO GOAT MOUNTAIN

Tabulation for figure 26

SAMPLE SITE	SEDIMENT ANOMALIES	CONCENTRATE ANOMALIES
329	La, (Ca, Ba)	Th.
348	Ni, Zn, (Fe, Ca, Ba, Cd, Co, Cu, V)	Be, (Ca).
349	(Ca, Ba, Zr)	As, Sn(100), W(2,000), (Nb).
350	(Ca, Ba, Zr)	As, Cr(500), (Ca, W).
351	Fe, (Ca, Ba, Pb, Zr)	--
394	Ba, Be(3), Cr(500), Sr, Cd, (Ca, Pb).	(Ca, B).
409	(Fe, Ba, Cu, Pb)	B, W, (Ca, Mn, Re).
410	La, (Ba)	As, (Be).
411	(Y, Ca, Sa, Pb)	(Ca, Be, Nb, V).
412	(Fe, Ca, Ba, Pb)	As, Be, W(2,000), (Ca).
623	La, (Ca, Ba, Pb)	(As).
642	(B, Ba, Co, Cu, Ni, Pb)	Ca, Mn, V, W(2,000).

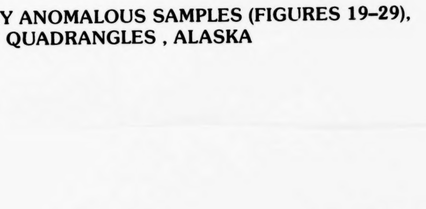

Figure 24. MAP SHOWING SAMPLE SITES FROM THE
VAN CLEVE GLACIER AREA

Tabulation for figure 24

SAMPLE SITE	SEDIMENT ANOMALIES	CONCENTRATE ANOMALIES
379	Ca, (Ba, Pb)	Ca, W, (Co).
380	(Ba)	As, Bi(50), W.
604	Ca, (Fe, Ba, Pb, Zn)	--
605	Bi(150), (Fe, Ca, Ba, Pb)	B, Cu(2,000).
606	La, (Ca, Ba, Pb, Zr)	--
607	Ca(5), Sr, Zr(700), (Ba, Pb)	B, (Ca).
612	(Ca, B, Ba, Pb, Zr)	(La).
613	La, (Ca, Ba, Pb, Zr)	Ca(20), (Y).
614	Ca, (Zr)	Th(700).
615	Fe, Ca(5), Cu(200), (Mg, Ba, Co, Ni, Pb).	Cu(1,000), Th, (Ca).
616	(Ca)	--
617	Ca, (Zr)	B(2,000), Cu(1,500), Th(1,000), (Ca).
618	La, Zr(500), (Ca)	(Be).
637	Zr(500), (Ca, Ti, Pb)	As, Co(500), Ni(300), Sc(100), (La, W, Y).

NOTE

Elements in parentheses show concentrations at the 90th percentile level; all other elements listed exceed the 90th percentile. All listed concentrations exceed the 95th percentile (all values in ppm except for Fe, Ca, and Mg which are given in percent). Leader (--), no anomalous data

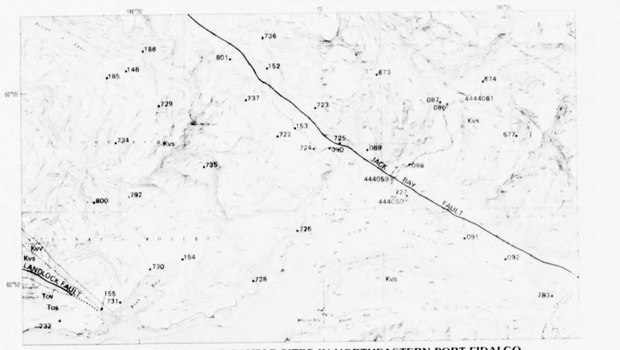

Figure 27. MAP SHOWING SAMPLE SITES IN NORTHEASTERN PORT FIDALGO

Tabulation for figure 27

SAMPLE SITE	SEDIMENT ANOMALIES	CONCENTRATE ANOMALIES
086	(Ti, Cr, Ni)	Mg, Cr(500), Nb, (Ni).
087	--	As, La, Nb(200), Sc, V, Y(1,500), Th(700).
088	Cr(300)	Mg, Cr(2,000), Sb, (Mn, As, Ni, V).
089	(Ba)	Insufficient sample.
090	(Ba)	Nb, (Y).
091	(Ba)	Insufficient sample.
092	(Ba)	Insufficient sample.
146	Ag, (Ti, Ba, Zr)	Mn, Cr(1,000), La, Sc(70).
152	Ag, (Ba)	Sc.
153	(Ba)	Sc.
154	(Ba, Pb)	--
155	Sc, (Mn, Ba, Cr, Ni, Pb)	(Mn, Cu).
185	La, (Ca, Ba, Ni, Pb, Zr, As)	As, La(2,000), Nb, Sn(70), W(1,500), (Y, Y).
186	(Ca, Ba, Ni, Pb, As)	(Nb, W).
673	(As)	B.
674	--	As(20,000), Au, Co(500), Ni(500), W, Th, (Bi, Pb).
677	--	As(20,000), Bi(70), W, Th.
722	--	Au, Cr, Mo, Sn, (Ag, Bi, Th).
723	Cd(.5), As(45)	Ag(36), As, Au(50), Cr(2,000), Pb(1,000), (Th).
724	(Cd)	Cr, Mo(10), Sn(50), Th.
725	W(50), (As)	Cr(500).
726	--	Bi, Cr(700), Sn, (Pb, Th).
727	Cr(500)	Cr(10,000), Sn, (Th).
728	--	Cr(3,000), Sn, (Th).
729	Au(.5)	As, Cr(2,000), (Bi, Pb, Sn, Th).
730	--	Cr(10,000), (Th).
731	As, (Mn)	Ag(100), As, Au(70), Bi, Cr(2,000), Sn, (Pb,Th).
732	As, (Mn, Cd)	Sn(500), (As, Cr, Th).
734	Ag, As(60)	Mo.
735	(Cd)	Sn(70).
736	--	Ag(200), Au(200), Pb, Sn(50), (As,Bi).
737	Bi	Pb, Sn, (Th).
783	Mo(5,000), Co(100), (Fe)	Sn(>2,000), (Mn,Cr).
792	As, (Mn, Co)	Insufficient sample.
800	Sb(2), As, (B, Ba)	Insufficient sample.
801	Ba	As, Cd, (Sn, Y).

NURE SEDIMENT ANOMALIES

444059 Cr(261).
444086 Cr(264).
444081 Ni(57), Cr(341), Ta(2).

Figure 28. MAP SHOWING SAMPLE SITES WITHIN
THE BREMNER RIVER WATERSHED

Tabulation for figure 28

SAMPLE SITE	SEDIMENT ANOMALIES	CONCENTRATE ANOMALIES
444197	U(.9,Ni), Cu(185), Ni(57), W(33), As(52), Zr(1,478), Au(.46), Ce(503), Dy(53), Eu(28), Hf(110), Laf264), La(4.6), Mo(4,629), Sm(50), Th(71, Th(88.9), Yb(45).	
444200	U(23.8), Zr(1,969), Au(.51), Ce(185), Dy(11), Eu(2.7), Hf(41), Laf183), Luf.5), Sm(27), Th(42), Yb(11).	
444201	U(12.6), Zr(1,195), Ce(163), Dy(9), Hf(52), Laf76), Luf.4), Sm(17), Th(28), Yb(6.4).	
444202	U(5.9), Zr(556), Hf(19).	

EXPLANATIO

Qu	Surficial deposits
Ty	Yakataga Formation
Tr	Redwood Formation
Tp	Poul Creek Formation
Tt	Tokun Formation
Tk	Kulthieth Formation
Tsu	Stillwater Formation
Tos	Orca Group—Sedimentary rocks undivided
Tov	Orca Group—Volcanic rocks undivided
Tovs	Orca Group—Interbedded sedimentary and volcanic rocks
Tots	Orca Group—Tuffaceous sedimentary rocks
Tg	Granite and granodiorite
Td	Dacite

MAPS AND TABULATIONS OF AREAS WITH GEOCHEMICALLY ANOMALOUS SAMPLES (FIGURES 19–29), CORDOVA AND MIDDLETON ISLAND 1° × 3° QUADRANGLES , ALASKA

I 19.3:

Reproduced from poor document

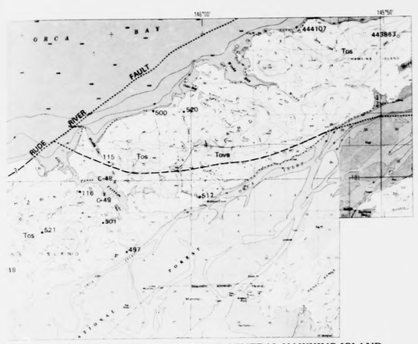

). MAP SHOWING SAMPLE SITES FROM CENTRAL HAWKINS ISLAND

Tabulation for figure 20

SEDIMENT ANOMALIES	CONCENTRATE ANOMALIES
Fe, Mo(>5,000), Co, Sc, Y, (Cr, Ni, V)	Insufficient sample.
Ca, (Mn, Pb)	Insufficient sample.
(Ba)	Insufficient sample.
(Mg, Ba, Pb)	Insufficient sample.
(Mg)	Pb(1,000), Sn(500).
Mn, Zn(100), Cd	---
Mg, Mn(5,000), Co, Ni, Zn(190), (Fe, B, Ba, Co, V)	Insufficient sample.
Mn	---
Cu(250), Cd, (Pb)	---

EDIMENT ANOMALIES

Co, Pb(14), Cd, Fe, Mn, Zn(201).
Ba, Co, Ca(6.0), Fe, Mo(2,964), Rb(124), Zn(211).
Co
Cu(131), Mo(20,600), Zn.

MINERAL OCCURRENCES (Jansons and others, 1984)

Arsenopyrite disseminated in greenstone.
Quartz vein in slate with reported anomalous copper values.

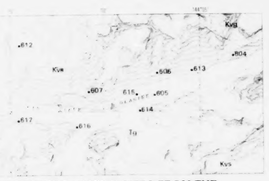

24. MAP SHOWING SAMPLE SITES FROM THE VAN CLEVE GLACIER AREA

Tabulation for figure 24

T ANOMALIES	CONCENTRATE ANOMALIES
	Ca, W, (Co).
	As, Bi(50), W.
Pb, Zn)	---
Ca, Ba, Pb)	B, Co(2,000).
Pb, Zn)	---
(Co), (Ba, Pb)	B, (Ca).
Mg, Fe)	(La).
Pb, Zn)	Ca(20), (Y).
	Th(700).
Mn(>5,000),	Cu(1,000), Th, (Ca).
Y, Ni, Pb).	---
	Bi(2,000), Cu(1,500), Th(1,000), (Ca).
(Ca).	(Be).
Ti, Pb)	As, Co(500), Ni(300), Sc(100), (La, W, Y).

Tabulation for figure 25

NOMALIES	CONCENTRATE ANOMALIES
b, Ba,	(Zn).
Ti, B, Ca)	Co(500), Ni(500), Zn, (Fe, Ba, Bi).

Tabulation for figure 26

SEDIMENT ANOMALIES	CONCENTRATE ANOMALIES
, (Ca, Ba)	Th.
Zn, (Fe, Ca, Ba, Cd, Co, Cu, V)	Be, (Ca).
, Ba, Zr)	As, Sn(100), W(2,000), (Nb).
, Ba, Zr)	As, Cr(500), (Ca, W).
, (Co, Ba, Pb, Zr)	---
, Be(1), Cr(500), Sr,	(Ca, B).
Cd, (Co, Pb),	
, Ba, Co, Pb)	B, W, (Ca, Mn, Be).
(Ba)	As, (Be).
, Ca, Ba, Pb)	(Co, Be, Sb, V).
, Ca, Ba, Pb)	As, Be, W(2,000), (Ca).
(Co, Ba, Pb)	(As).
, Ba, Co, Cu, Ni, Pb)	Ca, Mn, V, W(2,000).

NOTE

Elements in parentheses show concentrations at the 90th percentile level; all other elements listed exceed the 90th percentile. All listed concentrations exceed the 95th percentile (all values in ppm except for Fe, Ca, and Mg which are given in percent). Leader (---), no anomalous data

US SAMPLES (FIGURES 19–29), LES , ALASKA

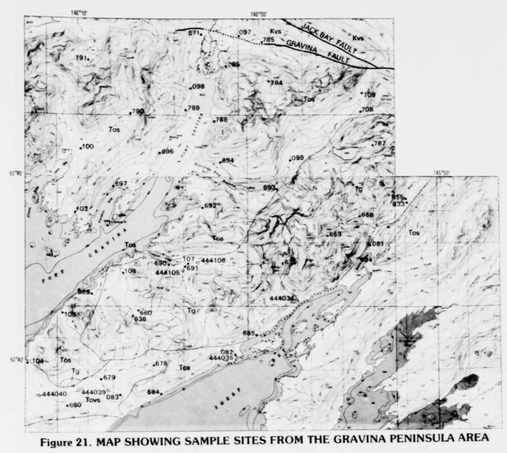

Figure 21. MAP SHOWING SAMPLE SITES FROM THE GRAVINA PENINSULA AREA

Tabulation for figure 21

SAMPLE SITE	SEDIMENT ANOMALIES	CONCENTRATE ANOMALIES
081	La(200), (Ba)	Be(10), (Ca).
082	Ca, Ag, Cr(300), Sc, (Mg, Co, Cu, Ni, V).	(Ca).
083	La, Mo(7), Y, (Mn, Co)	Insufficient sample.
097	(Ba)	---
098	(Mg, Ba, Pb)	Insufficient sample.
099	(Ba)	Be(10), (Ca, V).
100	(Ba)	Mn, La, (Mg, V).
103	Mo(5,000), Cr(300)	Insufficient sample.
104	Mn, Zn, (Ca, Co, Ni)	(Ca).
105	As(200), Mo(5), (Pb)	Insufficient sample.
106	As(500), La, Mo(7), W(50), (Pb)	Insufficient sample.
107	(Pb)	Insufficient sample.
633	(Fe, Ba, Co, Pb, Zr)	La, Y, (Ca).
634	(Fe, Ca, Ba, Co, Pb)	Ca, Th, (Y).
635	(Ba, Pb, Zr)	Ca, (V).
636	Be(7), La, Pb(100), Y(100	La(1,500), Mo(50), Nb, W, Y(2,000), (Mn), Th(>2,000).
655	Fe, Ca, Ti(1), Mn, Ba, La(200), Y(100), Zr(1,000), (Co, Cu).	Ca, Y(700).
658	Be(3), La, Zr(500), As(50), (Ca, Ba)	Ca, Mn, La, (Mg,Y,V).
659	Ba, La, (Fe, Ca, Co, Cu, Zr)	Ca, B, La(1,500), Th, (Mn, Y, Y).
660	Be(3), La(200), Mo(5), Y, As(90), (Ba, Zr).	Bi(300), La(2,000), Sb, Sm(>2,000), W, (Ca, V), Y, Th(1,000).
671	Zn	W.
678	Zn, (Mn, Co, Cd)	---
679	Cr(300), As, (Ni)	---
680	Mo(5,000), Sn(<), Cd(.7)	Ag, As, Pb(1,000), Sn(70), (Bi, Th).
684	---	Insufficient sample.
685	As	B, (Th).
689	Be(5), Y, As(190), Cd	Sn(700), Th.
690	La(150)	Sn, Th.
691	La(150), As(35)	As(10,000), Sn, Th(700), (La, Pb).
692	---	(Sn).
693	As(75), (Pb)	Sn, (Th).
694	Ag, (Cd, As)	Mo, Pb, (Sn).
695	Zn, Cd(.5), As(50)	Sn(70).
696	(Cd)	---
697	Zn, Sb(2), Cd, As	---
708	---	Sn, Th.
709	Mo, As, (Zn)	(B, Be).
784	Ag, Ba, Sr	Insufficient sample.
785	Ba(2,000), Sr, (Mn)	B(>5,000).
787	Ba, La(100), Zr(700)	Cd, Sc(100), (V, Th), Y(1,500).
788	Ag, Ba(2,000), (Fe, Ti, Mn, Co, Cr, Ni, Pb, V).	Insufficient sample.
789	Ag, Ba(2,000), Sb(2), As, (Ti, Mn, B).	Insufficient sample.
790	Ag, Ba(2,000), As, (Ti, Mn, B, Co, Cr).	Insufficient sample.
791	Ba(2,000), Sr(1,000), As(40)	Mn, Bi(1,500).

NURE SEDIMENT ANOMALIES

444034	U(6.5), Bi(7), W(20), Hf, Sc, Sm(8.1), Th.
444036	U(11.0), Sm(11), As(50), Hf, Sm, Th.
444039	U(18.2), Bi(5), Pb(13), As, Ce(102), Dy(12), K(24,350), La(54), Lu(.8), Rb(147), Sm(12.2), Tb, Th(23.4), Yb(6.8).
444040	U(7.6), As(57),
444105	U(35.6), As(308), Ce(159), Dy(8), Fe(101,100), La(74), Lu(.8), Sm(16), Th(21), Yb(5.5),
444108	U(9.0), Ba(1,185), Ce(151), Co(6.9), Dy(8), K(25,960), La(86), Lu, Sm(11), Th(29), Yb(5.6), Zn.

Figure 22. MAP SHOWING SAMPLE SITES FROM THE YOUNGER TERTIARY SEDIMENTARY ROCKS ON THE MAINLAND

Tabulation for figure 22

SAMPLE SITE	SEDIMENT ANOMALIES	CONCENTRATE ANOMALIES
030	Ba(2,000), (Ti, Ni)	Insufficient sample.
031	Sc, (Fe, Ti, B, Mn, Ba, Co)	Insufficient sample.
032	Ag(.7), Ba(2,000), Cr(500), Mo(10), Ni, Sc, (Mg, Ti, B).	Ba, Cr(1,000), Sr(10,000).
033	Mo(3), Ni, (Fe, Ti, B, Ba, Co, V)	Insufficient sample.
034	Zn(220), (Fe, B, Ba, Ni, V)	Insufficient sample.
035	Sc, Zn(200), (Fe, Ti, B, Ba, Co, Ni, V).	Ba, Cr, Mo(15), (Ni), Sm(100), Sr(2,000), Zn(2,000).
036	Zr(500), (Ti)	La, Sc, Sr(1,500), Y(1,500), (V).
037	(Zr)	La, Sc, Sr(1,500), Y(1,000), (Nb, V).
038	(Ti)	La, Y, (Nb, Sr, V).
039	(Fe, Ti, Ba)	Ba, La(1,000), Sr(2,000), Y(1,000), (Nb, V).
040	(Fe)	La(1,000), Nb(1,000), V(700), Y(1,000).
041	Fe, (Ti, B, Ni, V)	Zn(7,000), (Ba, Ni).
042	(Fe)	(Cr).
043	(Fe, Ti, Ba)	Insufficient sample.
044	(Fe, Ti, V)	Mn(5,000), Ba, Nb, Sc(100), Y, (Ca, Sr).
045	Ti(1), (Fe, Ni, V)	Insufficient sample.
046	Fe, (Ti, B, Ni, V)	Sn.
047	(Fe, Ti, Ni)	Insufficient sample.
048	Ti(1), Sc, V(500), (Fe, Co, Cu)	Ca, Ba, (Mg, Y).
049	Fe, Ti(1), (Ni, V)	Insufficient sample.
060	(Fe, Ti, B, Ni)	Insufficient sample.
061	Sc, (Fe, Ti, B, Ni, V)	Be, Mo(70), Ni(200), Zn(700), (Fe).
062	Mn, Sc, Zn, (Fe, Ti, B, Co, Ni)	Mg, Ca, Be, (Mn, Ni).
273	Ni, (Ti)	Insufficient sample.
274	Ni, Cd(.6), (Ti, Ba)	Insufficient sample.
275	(Ni)	Ba, Cr(500), La, Nb, Sc, V, Y, Zn(1,000), (Sr).
276	(Co, Ni, Pb)	Ba, Y, Dy, (Cu, Nb, Yb.
277	(Ni)	Nb(200), Sc, V, Zn, (Ca, La, Y).
278	Mo(10), (B, Co, Ni)	Insufficient sample.
279	---	---
280	(B, Co, Cu, Ni, Pb)	Insufficient sample.
281	(B, Ni, Zr)	La, Y, (Y).
282	(B, Co, Cu, Ni, Pb)	Insufficient sample.
283	Cr(300), (B, Zr)	La, Sc, (Nb, Ni, Sr, V, Y).
284	(Ba, Ni, Zr)	Ba, Sc, V, (Fe, La, Ni, Sr).
285	(Zr)	(Fe, Ni, Sr).
286	(Ni)	Nb, Sc(70), V, (Th).
287	(B, Ni, Pb)	Ba, Ni, (Fe, Sb).
288	---	Ba, Cr, La, Sc(150), V, Th, (Sb, Cr, Y).
289	(Ba, Ni, Pb, Zr)	Sb, Sc(100), Y, Sr.
290	Zr(700), (Ni)	Sc(500), V, Y, (Ni).
291	(Ni, Pb)	Sc, (Co, Ni).
292	(Co, Ni, Pb)	Sb, Sc, V, (Ca).
293	(Co, Ni, Pb, Zn)	(Ca).
294	Co, Ni, Zn(170), (B, Cu, Pb)	Ba, Sr(2,000), (Ni).
295	(Ni, Pb)	Ba, Sb, (Ni).
296	Zr(500)	Sc, V, (Y).
297	Zr(500)	La, Nb(200), Sc, V, (Y).
298	Zr(500), (Ce)	La, Nb, Sc, V, Y.
315	Fe, Bi(50), Zn, (Ba, Co, Ni, Pb)	Fe, Ba, Cd(50), Ni(500), Pb, Sr(1,500), (Bi, Co, Nb).
316	Fe, Ni, Pb, Zn, (B, Co, Cu, V)	Nb.
317	Ni, (Fe, B, Co)	Ba, (Bi).
367	(Fe, B, Co, Cr, Cu, Ni, Pb)	Ba, Cd(200), Mo(10), Ni(500), Sr(2,000), (Fe, Bi, Pb), Zn(20,000).
368	(Fe, B, Co, Ni, Pb)	Ba, Cd(500), La, Ni(700), Sr(2,000), (Be, Bi, Y, Y), Zn(>20,000).
369	(B, Cr, Ni, Pb)	Fe, Ba, Mo(10), Nb(200), Sr(700), (Be, Bi, Y).
370	Ca(7), (B, Cr, Ni, Pb)	Sr(2,000), Zn(2,000).
371	(B, Co, Cr, Ni, Pb)	Ba, Mo, Nb(200), V, (Y), Zn(2,000).
372	(Fe, B, Co, Cr, Cu, Ni, Pb)	Mo, Be, Nb(200), V, (Be, Bi, Y).
373	(Fe, B, Co, Cr, Cu, Ni, Pb)	Ba, Nb, Ni, Sr(3,000), V, (Y).
374	Zn(>W), (Fe, B, Ba, Cr, Ni, Pb, Cd)	Ba, Cd(300), Mo(20), Ni, Sr(3,000), Zn(>20,000).
375	Zn, (B, Co)	Insufficient sample.
384	(Fe, B)	Insufficient sample.
385	(B, Cr, Ni, Pb)	Zn(1,000).
386	(Fe, B, Ba, Cu, Ni)	Fe, Ag, Ba, Ni(500), Zn(2,000), (Bi, Cu).
387	(B, Ba, Pb)	Insufficient sample.
388	(Fe, B, Ba, Co, Cu, Ni, Pb)	Zn(1,000).
389	Fe, Co, (Mo, Ti, B, Ba, Co, Cr, Cu, Ni, Pb).	Insufficient sample.
390	---	V, Zn(1,000), (Sb,Y).
391	Fe, (B, Ba, Co, Ni)	Ba, (Sb, Zn).

NURE SEDIMENT ANOMALIES

443777	U(21.1), Ni(452), W(27), Zr(5,503), Ca(4,010), Cr(348), Cr(1,004), Dy(14), Eu(4.6), Hf(256), La(255), Lu(1.8), Mo(4,823), Eu(87,040), Sc(53), Sm(26), Tb(3), Th(51), Yb(50), Ta(20,810), Y(134), Yb(24).
443786	U(21.7), Ba(1,466), Ce(145), Cr(143), Dy, Eu(2.4), Eu(49,100), La, Mo(38,200), Sm(8.1), Ta(3), Tl(0.25), Zn(520).

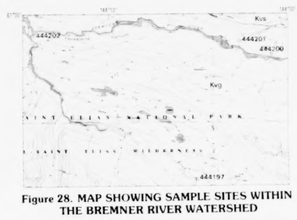

Figure 28. MAP SHOWING SAMPLE SITES WITHIN THE BREMNER RIVER WATERSHED

Tabulation for figure 28

SAMPLE SITE	SEDIMENT ANOMALIES	CONCENTRATE ANOMALIES
444197	U(30.0), Cu(185), Ni(57), W(33), As(52), Zr(1,478), Anf.84), Ce(501), Dy(53), Eu(28), Hf(110), La(254), Lu(4.6), Mo(4,479), Sm(50), Th(71), Th(84.9), Yb(44), Sm(22), Th(42), Yb(13).	
444208	U(25.6), Zr(1,989), Au(.51), Ce(236), Dy(11), Eu(2.7), Hf(81), La(131), Lu(1.5), Th(9.4).	
444201	U(12.6), Zr(1,195), Ce(163), Dy(9), Hf(52), La(76), Lu(.8), Sm(17), Th(28).	
444202	U(5.9), Zr(556), Hf(19).	

Figure 29. MAP SHOWING SAMPLE SITES IN THE McKINLEY LAKE REGION

Tabulation for figure 29

SAMPLE SITE	SEDIMENT ANOMALIES	CONCENTRATE ANOMALIES
079	Ag, Ba, (Ti, Co, Cr, Ni, Pb)	Insufficient sample.
071	(Ba)	Ba, Be(7).
072	Mo(5), (Ba)	Insufficient sample.
073	Co, Mo(5), Au(.1)	Insufficient sample.
428	Pb	(Bi).
429	Pb, Cr, As(35), (Fe, Ba, Cu, Ni)	Insufficient sample.
440	Ag(.5), Pb, (Fe, Ba, Co, Cu, Ni)	Insufficient sample.
069	(Ba)	Nb(200), (Mo, V).
466	(Pb)	Be, Th, (Bi, Sb).
467	(Pb, As)	(Be, Bi).
439	(Co)	Be(7), (W).
468	Ag(7), As(400), Au(9), Pb(300), (Fe, B, Ba).	Ag(1,500), As(>20,000), Au(3,000), Bi, Sr, Pd(1,500), Sb(700), (Fe, Th).

NURE SEDIMENT ANOMALIES

443810	Pb(13), As(453), Au(4,064), Co, Cs(6.3), K, Mn(2,265).
443986	Al(>2,900), Ba, Co, Cr, Cs(5.6), Fe, K(21,700), Mg, Rb(88), Sb(3), V, Zr(217).
444150	Bi(3), Pb(13), As(491), Au(1.71), Co(34), Cs(6.7), Mn(2,715).
444151	Cu, (Ni), Pb(13), As(92), Cs, Rb(124), Zn(231).

EXPLANATION

Qu	**Surficial deposits**
Ty	**Yakataga Formation**
Tr	**Redwood Formation**
Tp	**Poul Creek Formation**
Tt	**Tokun Formation**
Tk	**Kultheith Formation**
Tsu	**Stillwater Formation**
Tos	**Orca Group**—Sedimentary rocks undivided
Tov	**Orca Group**—Volcanic rocks undivided
Tovs	**Orca Group**—Interbedded sedimentary and volcanic rocks
Tots	**Orca Group**—Tuffaceous sedimentary rocks
Tg	**Granite and granodiorite**
Td	**Dacite**
Kvg	**Valdez Group**—Paragneiss
Kvs	**Valdez Group**—Sedimentary rocks undivided
Kvv	**Valdez Group**—Volcanic rocks undivided
Kvvs	**Valdez Group**—Interbedded sedimentary and volcanic rocks
Kvu	**Ultramafic rocks**
x	**Mine or prospect**—Number refers to description in Jansons and others (1984)
•	**Sample site (this survey)**
	NURE sample site
	Contact—Dotted where concealed
U D	**Fault**—Dashed and queried where probable; dotted where concealed; U, upthrown side; D, downthrown side; arrows indicate relative lateral movement
	Lineament—Identified on aerial photograph but not on ground; possible fault

Geology modified from Winkler and Plafker (1981) and Nelson and others (1985)

Figure 27. MAP SHOWING SAMPLE SITES IN NORTHEASTERN PORT FIDALGO

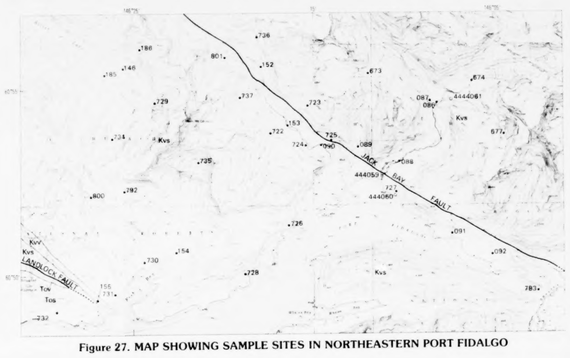

Tabulation for figure 27

SAMPLE SITE	SEDIMENT ANOMALIES	CONCENTRATE ANOMALIES
086	(Ti, Cr, Ni)	Mg, Cr(500), Nb, (Ni).
087	---	As, La, Nb(200), Rb, V, Y(1,500), Th(700).
088	Cr(300)	Mg, Cr(2,000), Nb, (Mn, As, Ni, V).
089	(Ba)	Insufficient sample.
090	(Ba)	Nb, (Y).
091	(Ba)	Insufficient sample.
092	(Ba)	Insufficient sample.
146	Ag, (Ti, Ba, Zr)	Mn, Cr(1,000), La, Sc(70).
152	Ag, (Ba)	Sc.
153	(Ba)	Sc.
154	(Ba, Pb)	---
155	Sc, (Mn, Ba, Cr, Ni, Pb)	(Mn, Cu).
185	La, (Ca, Ba, Ni, Pb, Zr, As)	As, La(2,000), Nb, Sn(70), W(1,500), (V, Y).
186	(Ca, Ba, Ni, Pb, As)	(Nb, W).
671	(As)	B.
674	---	As(20,000), Au, Co(500), Ni(500), W, Th, (Bi, Pb).
677	---	As(20,000), Bi(70), W, Th.
722	---	Au, Cr, Mo, Sn, (Ag, Bi, Th).
723	Cd(.5), As(45)	Ag(36), As, Au(50), Cr(2,000), Pb(1,000), (Th).
724	(Cd)	Cr, Mo(10), Sn(50), Th.
725	W(50), (Au)	Cr(500).
726	---	Bi, Cr(700), Sn, (Pb, Th).
727	Cr(500)	Cr(10,000), Sn, (Th).
728	---	Cr(1,000), Sn, (Th).
729	Au(.5)	As, Cr(7,000), (Bi, Pb, Sn, Th).
730	---	Cr(10,000), (Th).
731	As, (Mn)	Ag(100), As, Au(70), Bi, Cr(2,000), Sn, (Pb,Th).
732	As, (Mn, Cd)	Sn(500), (As, Cr, Th).
734	Ag, As(60)	Mn.
735	(Cd)	Sn(70).
736	---	Ag(200), Au(200), Pb, Sn(50), (As,Bi).
737	Bi	Pb, Sn, (Th).
741	Mn(>5,000), Co(100), (Fe)	Sn(>2,000), (Mn,Cr).
742	As, (Mn, Co)	Insufficient sample.
800	Sb(2), As, (B, Ba)	Insufficient sample.
801	Ba	As, Cd, (Sn, Y).

NURE SEDIMENT ANOMALIES

444059	Cr(261).
444060	Cr(264).
444061	Ni(37), Cr(341), Ta(2).

Reproduced from poor document.